May 2017

Gene Expression Profiling in the Larval Fat Body of Desiccation Selected Drosophila melanogaster

Adriana Michelle Charles
University of Nevada, Las Vegas, adrianacharles@yahoo.com

GENE EXPRESSION PROFILING IN THE LARVAL FAT BODY OF DESICCATION SELECTED *DROSOPHILA MELANOGASTER*

By

Adriana Michelle Charles

Bachelor of Science- Biological Sciences
University of Nevada Reno
2014

A thesis submitted in partial fulfillment
of the requirements for the

Master of Science- Biological Sciences

School of Life Sciences
College of Sciences
The Graduate College

University of Nevada Las Vegas
May 2017

UNLV | GRADUATE COLLEGE

Thesis Approval

The Graduate College
The University of Nevada, Las Vegas

May 30, 2017

This thesis prepared by

Adriana Michelle Charles

entitled

Gene Expression Profiling in the Larval Fat Body of Desiccation Selected *Drosophila melanogaster*

is approved in partial fulfillment of the requirements for the degree of

Master of Science- Biological Sciences
School of Life Sciences

Philippos Tsourkas, Ph.D.
Examination Committee Chair

Kathryn Hausbeck Korgan, Ph.D.
Graduate College Interim Dean

Allen Gibbs, Ph.D.
Examination Committee Member

Mira Han, Ph.D.
Examination Committee Member

Kaushik Ghosh, Ph.D.
Graduate College Faculty Representative

Abstract

Drosophila melanogaster selected for resistance to desiccation (no food or water) display slower development and a higher body mass compared to fed controls due to an extended third larval instar. I hypothesize that desiccation selected *D. melanogaster* larvae will have a different gene expression profile compared to fed controls. Separate populations of *D. melanogaster* were subjected to desiccation (no food or water), starvation (no food) until 80-85% mortality, for 75 generations. mRNA from the larval fat body was collected at 88 hours, 96 hours, 112 hours and 120 hours post-hatching. Four replicate samples were used for each condition and time point. Gene expression was measured using two color cDNA microarrays. I analyzed the microarray data using a two-way factorial design ANOVA implemented in R using a significance level of 0.05 with FDR correction. The FDR adjusted results showed 43 genes differentially expressed for selection condition, 4590 genes for time, and 122 for selection by time (interaction). I then used DAVID 6.7 to explore which biological pathways are over-represented for these genes. One biological process was shown to be over-represented for the selection genes, 67 for time, and 10 for interaction. These over-represented processes suggest desiccation selected and control populations are indeed developing differently.

Table of Contents

List of Tables

List of Figures

List of Equations

Chapter 1

Introduction

Climate change is placing land across the globe at risk for degradation and desertification due to increased aridity, warming, and human activity. By the end of the 21st century, drylands are predicted to begin dominating the global land surface, with drier areas covering large parts of North America, Eurasia, and Africa (Huang et al. 2015). As the environment experiences enhanced warming and extended droughts due to climate change, organisms living in those areas will be subject to increased stress, such as starvation and desiccation. The geographical distribution of terrestrial organisms is largely influenced by water availability and temperature. It is important to understand how organisms will respond to these environmental changes, not only at the physiological or ecological level, but also at the genomic level. To study organismal response to climate change, I studied desiccation selection in *Drosophila melanogaster*.

Laboratory selection for desiccation resistance in *Drosophila melanogaster* has resulted in a reduction in water loss rates, an increase in both water and carbohydrate contents, and an overall increase in survival under stress (Hoffmann and Harshman 1999; Gibbs and Gefen 2009). The increased accumulation of water and carbohydrates by larvae in the third instar contributes to adult stress resistance (Gefen et al. 2006). During development, carbohydrates, proteins, and lipids are stored inside an organ known as the fat body. The fat body serves major metabolic, endocrine, and immune functions in *Drosophila*. It is the main sensor for nutrient levels, produces factors to regulate insulin signaling, and responds to the physiological needs of the organism during different developmental stages and environmental conditions (Colombani et al. 2003). It is a crucial organ involved in the systemic control of insect growth and serves as a physical link to carry nutrients to the adult.

Selection for adult desiccation resistance has been shown to affect larval development physiology by extending the third larval instar in desiccation selected flies compared to controls, although larvae are not directly exposed to desiccation stress. The change in development is suggested to be caused by a shift in the critical weight associated with commitment of the larva to pupate (Gefen et al. 2006). Among

natural populations of *Drosophila*, considerable genetic variation in mean critical weight has been previously reported (de Moed et al. 1999). This variation is likely to allow shifts in timing if larval resource accumulation affects adult fitness, leading us to hypothesize that selection for desiccation resistance will delay and shift the temporal expression pattern of genes associated with key developmental stages, such as the cessation of feeding and the commitment to metamorphosis in the fat body of *Drosophila melanogaster*. I also hypothesize that the number of differentially expressed genes will be higher at the end of the third larval instar between desiccation selected, starvation selected, and fed control populations as compared to the early third larval instar.

Methods

Selection of Flies

Selection of flies and generation of the raw data sets were carried out by other researchers (Gefen E., Marlon A.J., and Gibbs A.). Separate populations of *D. melanogaster* were subjected to 3 different selection regimes: desiccation, starvation, and fed (unstressed). For each selection regime, there were 3 replicate populations (A, B, C), which were treated identically, yielding a total of 9 fly populations. The desiccation selected populations were matched with the starvation selected lines. The starvation selected lines were then matched with the fed control populations to control for the effects of starvation stress. Each population of adult files, of every selection and control line, was put into a selection cage. After 1-4 hours, desiccation selected flies were deprived of food and water. Silica gel was placed inside the desiccation selection cages to maintain low humidity. Starvation selected flies were also deprived of food, during the time desiccation selected lines were deprived of food and water, but were given 2 plates of non-nutritious agar, as a water source. Selection continued until ~1000 survivors remained from each population (Figure 1). Not shown in Figure 1 is the unstressed fed control lines. Fed flies were also transferred to selection cages for the duration of selection, but were given both fresh food and water each time the other lines were deprived of food and/or water, to keep all populations in sync. Survivors were given new food and water to allow for recovery for several days before egg collection. Starved and fed control flies were given fresh food and water. The next generation of flies were then subjected to the same

selection the previous generation underwent. Selection continued for 75 generations and fly populations were taken off selection for at least one generation to control for parent- of- origin effects. Additional details for fly selection can be found in Gefen et al 2006.

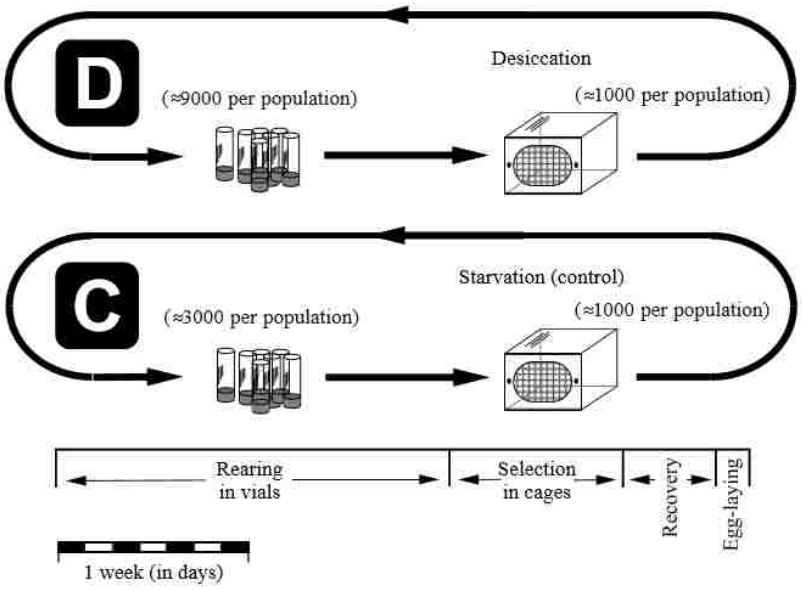

Figure 1: Schematic illustration of desiccation and starvation selection experienced by *Drosophila melanogaster* populations. "D" represents the desiccation selected populations and "C" represents the starvation selected populations, which serve as a control treatment for starvation and desiccation selection experienced by the desiccation selected populations. Figure taken from Gibbs et al, 1997. Not shown are the unstressed fed control populations.

Fat Body Sampling

Two replicate populations (A and B) from the 3 total replicate populations were used for microarray experiments. From each population, 4-7 day old flies were placed in 175mL plastic bottles. They were provided fresh food and yeast paste to induce egg production and minimize egg retention. After 24 hours, the flies were placed in identical empty bottles covered with 35x10mm petri dishes. Grape agar was used as a substrate for egg laying and the bottles were placed upside down in an incubator. After an hour, the agar plates were removed and time of egg lay was determined (±0.5hr). Using a dissection

microscope, the plates were inspected and 75 eggs were transferred into vials with 10mL of cornmeal. Vials were placed inside the incubator at 24.5^{o}C and exposed to constant light.

Larvae were collected from the vials, submerged in 1x PBS to prevent tissue disintegration, and dissected under a dissecting microscope. Samples were taken from the fat body of third instar larvae from replicate populations A and B for each selection regime at 4 different time points: 88 hr AEL (after egg lay), 96 hr AEL, 112 hr AEL, and 120 hr AEL. These time points were chosen based on a study that showed significant differences in rates of commitment to pupation 90 hours AEL and reflect hours after the midpoint of the 1 hour egg laying interval resulting in a total time resolution of ±1 hour (Gefen et al. 2006). Time points span the early third instar to the early wandering stage and cessation of feeding, covering the developmental time points where physiological differences in rates of commitment to pupation between desiccation selected and control fly populations were observed. For each time point, there were 4 replicate samples, 2 coming from each replicate population, yielding a total of 48 gene expression profiles (Figure 2).

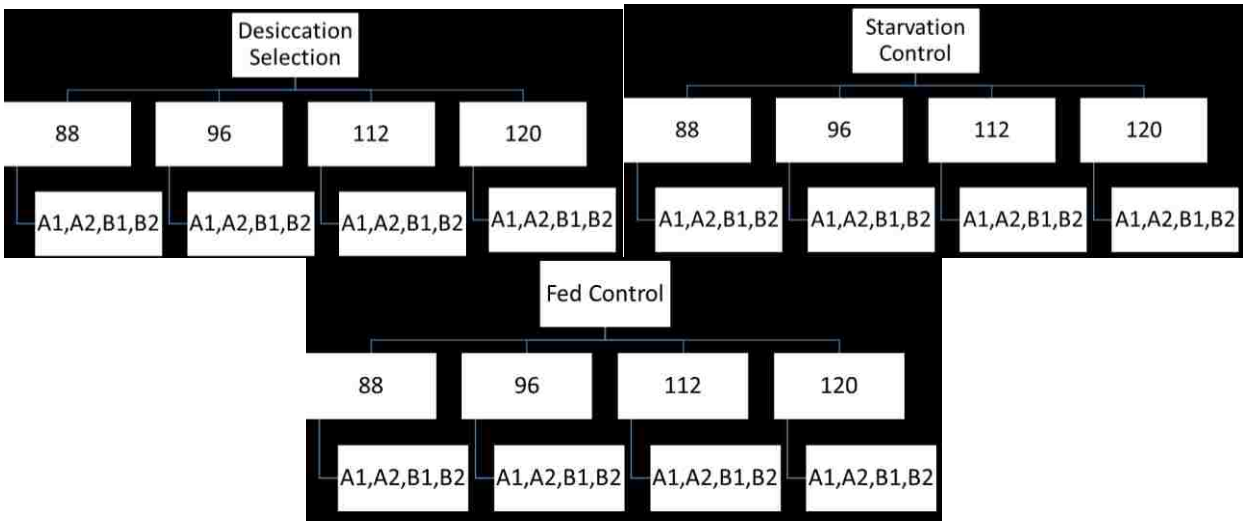

Figure 2: 48 gene expression profiles generated from 3 selection conditions, 4 time points, and 4 replicates per time point.

mRNA extraction and microarray experiments

Extracted fat bodies were placed in 1ml RNAlater® (#AM7020, Ambion) and stored at -20^{o}C until RNA purification. Fat body RNA was purified using RNeasy Mini Kit[3] (Qiagen; # 74104) and stored at -80^{o}C. Because of the varying quantities of purified RNA samples and low yields for 88 and 96h old larvae, the amino allyl MessageAmp^{TM} II aRNA amplification kit (#AM1753, Ambion) was used to amplify similar amounts of original RNA to obtain 8-10µg amplified RNA (aRNA) recommended for dye coupling. The amino allyl modified aRNA samples were then labelled using Amersham CyDye Post-Labeling Reactive Dye Packs (#RPN5661, GE Healthcare). Samples of 3µg dyed aRNA samples were then fragmented (RNA fragmentation reagents; #AM8740, Ambion) in a total volume of 11µl. The hybridization mix (total volume 60µl) consisted of two 11µl samples, 13µl nuclease-free water and 25µl formamide buffer (#AM9342, Ambion). The hybridization mix was gently vortexed and briefly spun, followed by 10-minute incubation at 80^{o}C and then kept at 55^{o}C until loading on the pre-hybridized slides.

The slides were pre-hybridized for 1 hour at 55^{o}C in 50ml pre-hybridization buffer (5x SSC, 0.1% SDS, 1% I-block in water), then washed for 1 minute in a 50ml water-filled tube, and centrifuged at 500rcf for two minutes to dry. Sample loading was carried out immediately after drying the pre-hybridized slides to maximize hybridization efficiency (Hedge et al. 2000). After sample loading the slides were placed in the hybridization chambers and 20µl water were added to the wells on each side. The chambers were then sealed, and placed in sealed plastic bags. Air was removed from bags prior to sealing, and submerged in a pre-heated water bath overnight at 42^{o}C. Following hybridization, the cover slip was removed by immersing the slide in a beaker filled with 2x SSC/0.2% SDS at 55^{o}C. The slide was then incubated in 2x SSC/0.2% SDS at 65^{o}C for 15 minutes, followed by two 15 minute washes at room temperature in 2x SSC and 0.2x SSC respectively. The slide was then centrifuged at 500rcf for 2 minutes to dry. Slides were scanned using a Gene Pix 4000B scanner and Gene Pix Pro 6.0.1.26 software. Experimental design of microarrays can be found in Table 1.

Table 1: Experimental design of pairwise comparisons used in microarray experiment. Cy5 and Cy3 represent fluorescent dye used to label sample. 1 represents fat body mRNA from flies in generation 76 (one generation off selection) and 2 represents fat body mRNA from generation 77 (two generations off selection). D represents desiccation selected populations, S represents starvation selected populations, and F represents fed control populations. A and B indicate the replicate population used. 88, 96, 112, 120 denote the hours AEL each mRNA sample was collected.

Cy5	Cy3
2DA120	2FA120
2FB120	2SB120
2SB112	2DA112
2DB112	2FB112
2DA96	2FA96
2FB96	2SA96
1DB96	1DA88
1DA112	1 DA96

Cy5	Cy3
1DA120	1DB112
1DB88	1DB120
1SB120	1SA112
1SA88	1SA120
1SA96	1SB88
1SB112	1SB96
1FB96	1FA88
1FA112	1FA96

Cy5	Cy3
1FA120	1FB112
1FB88	1FB120
2SA88	2DA88
2SB96	2DB96
2FA88	2SB88
2SA120	2DB120
2FA112	2SA112
2DB88	1FB88

Normalization and Statistical Analysis of Microarray Data

Log transformation was used to normalized the raw microarray data, collected by other researches. Log transformation is often used because it provides values that are more easily interpreted, eliminates misleading disproportions between relative changes, decouples the variance and mean intensities so that fold changes happening around small intensity values will be comparable to similar fold changes happening around large intensity values, and log transformation makes the distribution symmetrical and almost normal (Draghici 2012). For background correction, I subtracted the background intensity from the median gene intensity. This difference was transformed using Log Base 2. A two-factorial design ANOVA was used since the microarray data could be grouped into 2 factors, selection and time, as modeled by (Equation 1):

$$X_{ijk}=\mu + S_i + T_j + I_{ijSxT} + E_{ijk} \quad (1)$$

where μ_{ij} is the global mean, S_i is the effect of selection, T_j is effect of time, I_{SxT} is the interaction between selection and time, and E_{ijk} is the experimental error. Subscript "i", ranging from 1-3, represents selection (desiccation selection, starvation selection, and unstressed fed controls). Subscript "j", ranging from 1-4, represent each time point (88, 96, 112, and 120 hours AEL), and subscript "k" ranging from 1-4,

represents the replicates (A1, A2, B1, B2). FDR was used to remove false positives as included in code (Pavlidis, 2003). False positives were removed using false discovery rate (FDR) as modeled by (Equation 2):

$$P_k < \frac{k}{R}\ \alpha_e \tag{2}$$

where P is the p-value of a gene, k is the position of the gene in the ordered list, R is the total number of genes in the list, and α_e is the experimental significance level. I also performed an additional one-way ANOVA to find the number of differentially expressed genes across populations at each time point to assess changes between the early third instar and the late third instar as modeled by (Equation 3):

$$X_{ik}=\mu + S_i + E_{ik} \tag{3}$$

where μ is the global mean, S_i is the effect of selection, and E_{ik} is the experimental error. Any variance between replicate populations is assumed to be less than the variance due to selection and time. I used Short Time-series Expression Miner (STEM) to cluster, compare, and visualize the gene expression data to identify significant temporal expression profiles and gene associated with the profiles (Ernst and Bar-Joseph 2006). The genes generated from the STEM software program were compared to the list generated by the two-way factorial design ANOVA.

Gene enrichment was analyzed using DAVID 6.7 (Huang et al. 2009; Huang et al. 2009). GOTERM_BP_FAT was used to find clusters of genes that participate in the same biological processes and pathways. Because gene ontology is hierarchical in nature, GO-Module was used to remove any false positives in the GOTerms (Yang et al. 2011). A significance cut off level of α=0.05 was used for ANOVA, FDR, and DAVID 6.7, so as to not exclude any potential interesting results. WEB-based Gene Set Analysis Toolkit (WEBGestalt) overrepresentation enrichment analysis was also used to find enrichment in various biological processes using the list of genes generated by the two-way factorial design ANOVA (Wang et al. 2013). The GO terms generated in DAVID 6.7 and WEB Gestalt were then compared.

Results

Differential Gene Expression

Our two-way factorial design ANOVA included 2 main effects, selection and time, and one interaction effect. A cut off value of α=0.05 was used for the p-value and for the FDR. Over 4000 genes were differentially expressed with respect to time, while 43 were differentially expressed with respect to selection, and 122 genes were differentially expressed with respect to interaction (Table 2). For selection and interaction, a full list of differentially expressed genes and their p- values can be found in Supplemental Table 1. After a comparison to the list of genes generated in STEM, 1877 genes were found to overlap (Sup. Table 2). All overlapped genes could be found in the list of differentially expressed genes generated for time, with the exception of CG14153, which was found in the list for interaction and has no known molecular function or biological process.

Table 2: Summary of gene expression differences generated from two-way factorial design ANOVA.

Factors	Number of statistically significant differences FDR<0.05
Selection (S)	43
Time (T)	4590
Interaction- Selection by Time (S x T)	122

The most strongly differentially expressed genes with respect to selection are shown in Table 3A. This list of genes also included genes like Sap130, suggested to be involved in mitotic division based on the mutant phenotype, and CG7560, which is suggested to have methylenetetrahydrofolate reductase activity based on sequence similarity, as well as play a role in single carbon metabolism. CG7560 was

expressed at higher levels in the desiccation selected lines as compared to the fed controls, while Sap130 was expressed at lower levels.

Pertaining to time, the most strongly differentially expressed genes showed 3 genes from the Tetraspanin family with unknown function and biological process (Table 3B). Other genes included Fat Body Protein 1 and Shroud. Fat Body Protein 1 is induced by ecdysone and expressed during the late third larval instar. The protein product is a receptor that allows for storage proteins to be taken into the fat body, which later serve to provide energy and an amino acid pool during metamorphosis. Shroud is part of a gene family known as the Halloween genes. These genes are all cytochrome P450 enzymes which make up the pathway to synthesize ecdysone from cholesterol. When analyzing the pattern of expression over time, 14 out of the 15 of the most strongly differentially expressed genes increase in expression over time (Figure 3). Odorant-binding protein 83cd, which is involved in sensory perception of chemical stimulus, was shown to decrease in expression over time.

The most strongly differentially expressed genes in interaction between selection and time showed 2 genes with unknown biological processes, 1 with an unknown function, and 1 with both unknown function and unknown biological process (Table 3C). Fat Body Protein 1 is included on this list. Other genes include Sgf29 involved in chromatin remodeling, Fuzzy, responsible for establishing cell polarity, Hand, which takes part in several developmental processes, including dendrite morphogenesis, and embryonic heart tube development, and CG42588, which has no known function, but thought to be involved in neurogenesis.

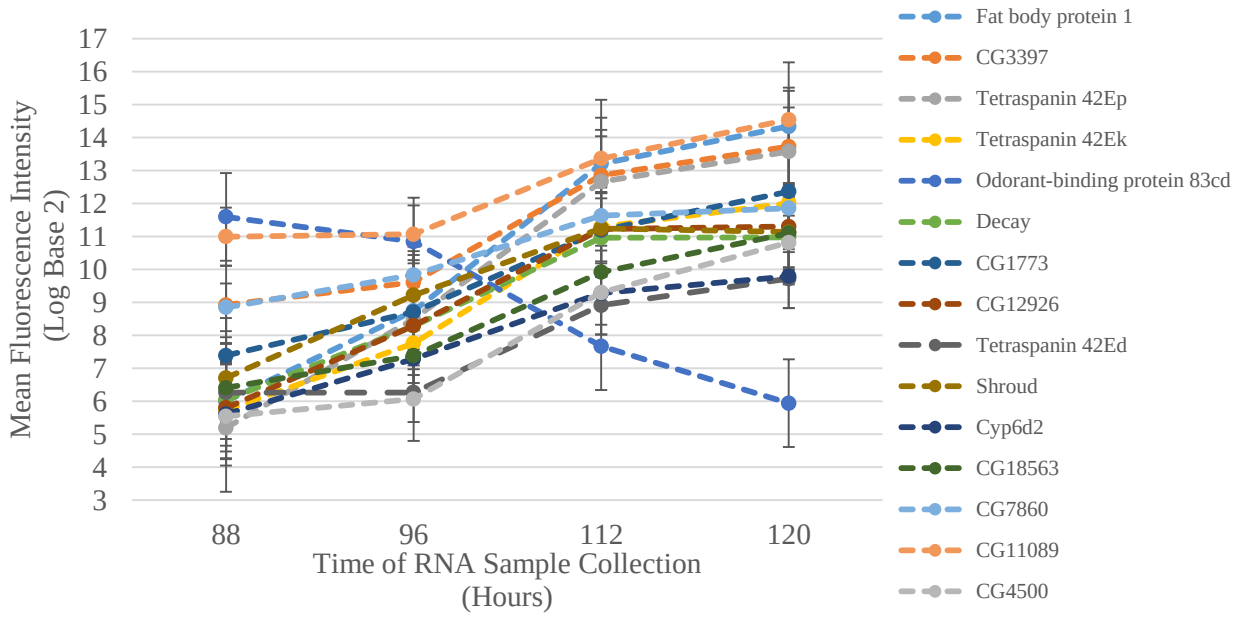

Figure 3: Mean fluorescence intensities of the 15 most differentially expressed genes with respect to to time, resulting from the two-way factorial design ANOVA. Intensity increases over time, except for Odorant-binding protein 83cd.

Table 3: 15 most differentially expressed genes for selection (A), time (B), and interaction (C) resulting from the two-way factorial design ANOVA.

A

Gene	P- value	Function	Biological Process
CG11236	2.39E-10	D-aspartate oxidase activity; FAD binding	Oxidation-reduction process; D-amino acid metabolic process
Cytochrome P450-9b2	3.65E-09	Electron carrier activity; Heme binding; Monooxygenase activity	Oxidation-reduction process
CG5715	4.68E-09	Metalloendopeptidase activity; Zinc ion binding	Phagocytosis; Proteolysis
Sap130	5.13E-09	N/A	Mitotic spindle organization
CG2837	8.32E-09	N/A	N/A
α-Esterase-4	8.71E-09	Carboxylic ester hydrolase activity	N/A
Seven in absentia	7.13E-08	Protein binding; Ubiquitin-protein transferase activity; Zinc ion binding	Sensory organ development; Proteasomal protein catabolic process; Proteolysis; Regulation of R7 cell differentiation
CG4709	1.54E-07	Metal ion binding; Nucleic acid binding	N/A
CG31337	2.10E-07	N/A	N/A
CG13077	4.02E-07	N/A	N/A
Metallothionein D	1.73E-06	Metal ion binding	Response to copper ion
Photorepair	3.16E-06	Deoxyribodipyrimidine photo-lyase activity	DNA repair
CG14567	3.24E-06	N/A	N/A
CG4306	5.01E-06	Gamma-glutamylcyclotransferase activity	Hemolymph coagulation; Glutathione biosynthetic process
CG7560	5.72E-06	Methylenetetrahydrofolate reductase (NAD(P)H) activity	Methionine metabolic process; Oxidation-reduction process

B

Gene	P- value	Function	Biological Process
Fat body protein 1	2.39E-26	Protein transporter activity	Storage protein import into fat body
CG3397	2.03E-24	Oxidoreductase activity	Oxidation-reduction process; potassium ion transport
Tetraspanin 42Ep	1.45E-23	N/A	N/A
Tetraspanin 42Ek	7.04E-23	N/A	N/A
Odorant-binding protein 83cd	1.46E-22	Odorant binding	Sensory perception of chemical stimulus
Decay	4.40E-22	Cysteine-type endopeptidase activity	Apoptotic process; Larval midgut histolysis
CG1773	1.02E-21	Serine-type endopeptidase activity	Proteolysis
CG12926	1.03E-21	Transporter activity; Vitamin E binding	Transport
Tetraspanin 42Ed	2.70E-21	N/A	N/A
Shroud	1.73E-20	3-hydroxybutyrate dehydrogenase activity	Ecdysone biosynthetic process
Cyp6d2	2.05E-20	Electron carrier activity; Heme binding; oxidoreductase activity	Oxidation-reduction process; response to camptothecin
CG18563	5.41E-20	Serine-type endopeptidase activity	Proteolysis
CG7860	7.18E-20	Asparaginase activity	Autophagic cell death; Asparagine catabolic process
CG11089	7.98E-20	IMP cyclohydrolase activity; Phosphoribosylaminoimidazolecarbox-amide formyltransferase activity	Wound healing; Purine nucleotide biosynthetic process
CG4500	1.22E-19	Long-chain fatty acid-CoA ligase activity	Mesoderm development; Long-chain fatty acid metabolic process

C

Gene	P-value	Function	Biological Processes
ZC3H3	0.001146	Metal ion binding	mRNA polyadenylation; Nuclear export
Fat body protein 1	0.001182	Protein transporter activity	Storage protein import into fat body
CG6418	0.001279	ATP binding; ATP-dependent RNA helicase activity	N/A
CG42588	0.001528	N/A	Neurogenesis
Galactosyl-transferase II	0.001999	Galactosyltransferase activity	Glycosaminoglycan biosynthetic process; Heparan sulfate proteoglycan biosynthetic process
CG11381	0.002293	N/A	N/A
Fuzzy	0.002321	N/A	Establishment or maintenance of cell polarity
Ccp84Ab	0.00414	Structural constituent of chitin-based cuticle	Chitin-based cuticle development
Stretchin-Mlck	0.004616	Calmodulin-dependent protein kinase activity; ATP binding	Protein phosphorylation
α-Esterase-4	0.004873	Carboxylic ester hydrolase activity	N/A
Hand	0.005111	Sequence-specific DNA binding transcription factor activity	Dendrite morphogenesis; Embryonic heart tube development; Positive regulation of transcription elongation
Sgf29	0.0053	Histone acetyltransferase activity; Methylated histone binding	Chromatin remodeling; Histone H3 acetylation
CG6678	0.005495	N/A	N/A
CG7378	0.005651	protein tyrosine/serine/threonine phosphatase activity	protein dephosphorylation
CG4573	0.006348	ATP binding; tRNA binding	glutamyl-tRNA aminoacylation

Functional Analysis

DAVID 6.7 restricts genes lists larger than 3000 genes. After removal of false positives with GO Module, there was a total of 78 GO terms with a P-value <0.05 that were denoted as true positive p-values for the local minimum (K terms). A detailed summary of GO Module results showing true positive p-values for local minimum (K), significant hierarchical descendants of local minimum (T), and false positively enriched GO terms (F) can be found in Supplemental Table 3. For selection, oxidation-reduction was enriched with 6 genes from the ANOVA list of 43 (Table 4A). For time, a list of 67 GO terms was found (Table 5, Appendix A). These terms mainly consist of a variety of metabolic and catabolic processes, such as ribonucleotide metabolic process, coenzyme metabolic process, cellular lipid catabolic process. Other terms include GO terms such as DNA replication and programmed cell death. For interaction, a list of 10 GO terms was found, which showed terms for neurogenesis and heart development (Table 4B).

When using the overrepresentation enrichment analysis (ORA) by WEBGestalt, 10 GO terms were found to be overrepresented for selection, time, and interaction, yielding a total of 30 GO terms (Sup. Table 4A). With respect to selection, one GO term, oxidation reduction, overlapped with that of DAVID 6.7 after GO module was used to remove false positives. With respect to time, 2 GO terms overlapped: oxidation reduction and carboxylic acid catabolic process. Pertaining to interaction, 2 GO terms overlapped between WEBGestalt and DAVID 6.7: cell projection organization and neuron differentiation (Sup. Table 4B). Analyzing genes that were found in overlapping GO terms, with respect to selection, showed 5 genes in common for oxidation reduction. For time, there were 14 genes in common for oxidation reduction, and 3 genes in common for carboxylic acid catabolic process. Pertaining to interaction, selection by time, 8 genes were found in common for cell projection organization, and 6 genes were found in common for neuron differentiation (Sup. Table 4C).

Table 4: GO terms shown for selection (A) and interaction (B). GO terms were generated from DAVID 6.7 and false positives removed with GO Module. P-values and FDR included in the table

A

Biological Process	P-value	FDR	Genes
Oxidation Reduction	0.008026727	9.622716016	Cytochrome P450-9b2
			Glutathione S transferase O3
			CG7560
			CG11236
			CG9527
			Thioredoxin-2

C

Biological Process	P Value	FDR	Number of genes
Cellular component morphogenesis	0.000602	0.878775	12
Cell projection organization	0.000706	1.028696	10
Axonogenesis	0.00213	3.075852	7
Axon guidance	0.002213	3.194036	6
Heart development	0.011368	15.42301	4
Cell morphogenesis involved in neuron differentiation	0.012965	17.40311	7
Movement of cell or subcellular component	0.016802	21.98411	7
Neuron differentiation	0.020007	25.62888	8
Neuron development	0.029516	35.52929	7
Regulation of cell morphogenesis	0.046909	50.53566	4

Delay in Expression

Out of 122 genes found to be differentially expressed in interaction, 22 of those genes could potentially show delayed expression. Delayed expression is shown if the expression of the desiccation selected line is shifted over to overlap with that of the unstressed fed control line. Perfect overlap between desiccation selected lines and fed control lines was not observed. Genes shown in Figure 4 are those which have overlap of the error bars in at least one time point or where expression is similar between desiccation selected populations and fed controls. Examples shown include CG8734, also known as Galactosyltransferase II, which is involved in the synthesis of a common linkage tetrasaccharide structure of heparan and chondroitin sulfates, and CG5864, which has protein transporter activity, and based on the mutant phenotype, is thought to be involved in axon guidance and compound eye photoreceptor development. Fy, also known as Fuzzy, is involved in the establishment or maintenance of cell polarity and establishment of imaginal disc-derived wing hair orientation, CG31704, inferred from expression patter, is involved in multicellular organism reproduction, Fas1 is involved in cell-cell adhesion via plasma membrane cell adhesion molecules, and Zfh1 has transcription factor activity and thought to be involved in developmental processes, such as hemocyte, lymph gland, mesoderm, and nervous system development. Other genes that could have potential delayed expression can be found in Supplementary Figure 2. The plotted mean fluorescence intensity of all genes found with respect to interaction can be found in Supplemental Figure 3.

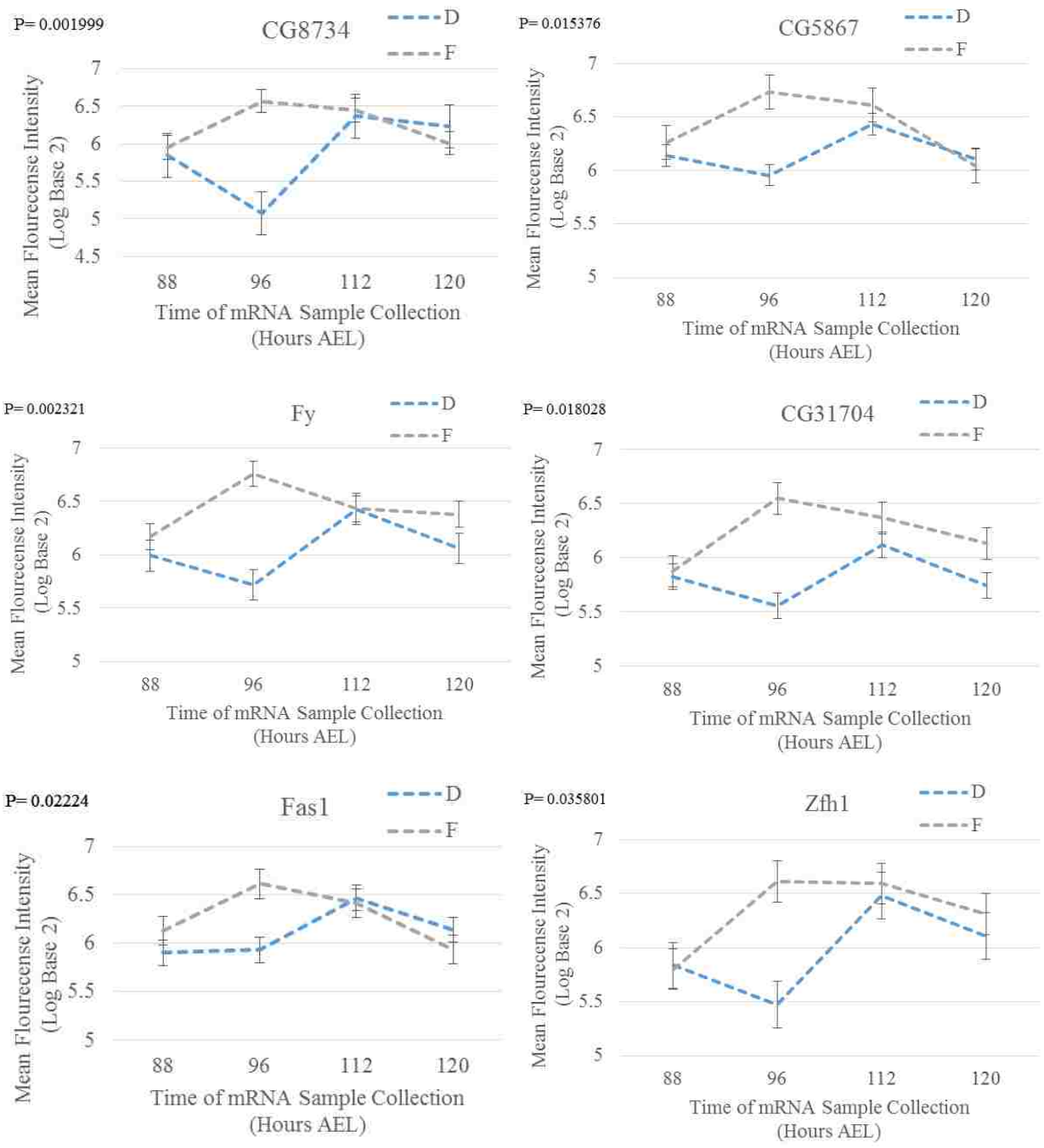

Figure 4: Potential delayed expression in desiccation selected populations vs fed controls shown for 6 genes found differentially expressed with respect to interaction from the two-way factorial design ANOVA. Dotted lines have been included to better visualize trends over time, although linear connection between points cannot be assumed. To emphasize the expression of the unstressed fed control and the desiccation selected lines, gene expression of starvation selected controls have been removed. P- value of each gene shown in the top left corner.

Discussion

After running the ANOVA and FDR, 43 genes were shown to be differentially expressed for selection, 4590 for time, and 122 for interaction. This suggests there are in fact differences in gene expression levels between selection conditions. There are several genes which could potentially be significant in the physiological differences seen between desiccation selected *Drosophila melanogaster* and the controls. For example, Sap130, inferred from the mutant phenotype, is suggested to be involved in mitotic division, and CG7560 is a metabolic gene, based on sequence similarity, and it is predicted to have methylenetetrahydrofolate reductase activity, which plays a role in processing amino acids by taking part in a multistep process to create methionine. It is also important in single carbon metabolism. Its known there is a significant amount of cell division and amino acid processing occurring during the third larval instar, so these two genes could be important in developmental differences. In addition, with respect to interaction, two genes found in the top most strongly differentially genes, Hand and CG42588, are thought to be involved in development processes, such as neurogenesis and embryonic heart tube formation. These could potentially be genes and biological pathways of significance.

Analysis of the list of differentially expressed genes using DAVID 6.7 showed enrichment of several biological processes. Pertaining to interaction between selection and time, biologically processes such neuron differentiation and heart development, were differentially expressed, suggesting the desiccation selected populations compared to the starvation selected control populations and fed control populations are developing differently. Because there were genes involved in neurogenesis and heart development found in the two-way factorial design ANOVA, and these were biological processes found as differentially expressed, they could possibly account for the differences in development, as well provide tissues worth looking at in the future, such as the brain and heart. Biologically processes, such as the commitment to metamorphosis and the cessation of feeding, as I hypothesized, were not found in the functional analysis component of my research.

Plotting the mean fluorescence intensities of genes found differentially expressed in interaction showed potential delayed expression in 22 genes. Based on the results, it is not possible to confirm there is in fact delayed expression, and it cannot be confirmed that there is no delayed expression. Instead, a list of 22 potentially delayed genes have been generated and need further attention in future studies. I also ran an addition one-way design ANOVA comparing selection conditions per each time point hypothesizing the number of differentially expressed genes would increase over time because the physiological difference between desiccation selected flies and fed controls become more pronounced over time, but yielded no results. In this study, a few number of differentially expressed genes have been found, with respect to selection and interaction, in the two-way factorial design and no gene were found to be differentially expressed using the one-way ANOVA. I have attributed these results to analyzing mRNA expression hours after egg lay. Although eggs are laid at the same time, there are differences in hatching times. The difference in hatching times could account for the low number of differentially expressed genes found due to the introduction of biological noise into the data that cannot be taken out in the normalization of the raw microarray data file. In future studies, biological noise can be reduced by considering the hatching times of larvae and taking samples after hatching rather than after egg lay. The effects of desiccation on gene expression will further be assessed using different tissues, such as the heart and brain, and analyzed using next generation sequencing.

Appendix A

Table 5: GO terms shown for time. GO terms were generated from DAVID 6.7 and false positives removed with GO Module. P values and FDR included in the table

Biological Process	P-value	FDR	Number of genes
oxidation-reduction process	4.04E-22	7.27E-19	283
generation of precursor metabolites and energy	3.69E-13	6.64E-10	112
cellular nitrogen compound biosynthetic process	4.93E-11	8.87E-08	113
ribonucleotide metabolic process	3.28E-08	5.90E-05	60
ribonucleoprotein complex biogenesis	2.45E-07	4.41E-04	51
coenzyme metabolic process	4.79E-07	8.62E-04	48
mitochondrial ATP synthesis coupled electron transport	8.2E-07	0.001475234	39
protein folding	5.17E-06	0.009293976	56
establishment of protein localization	7.7E-06	0.013856388	115
ncRNA metabolic process	8.8E-06	0.015838781	62
fatty acid metabolic process	1.24E-05	0.022339946	31
monosaccharide metabolic process	1.61E-05	0.028892023	48
carboxylic acid catabolic process	2.88E-05	0.051881016	27
ribonucleoside monophosphate biosynthetic process	4.71E-05	0.084711384	16
alcohol catabolic process	5.14E-05	0.092430305	29
acetyl-CoA metabolic process	7.95E-05	0.142910217	22
intracellular transport	0.000194	0.347560636	118
tricarboxylic acid cycle	0.000212	0.380197309	20
ribonucleoside triphosphate metabolic process	0.000377	0.67650345	41
cellular lipid catabolic process	0.000382	0.68475771	17
cellular carbohydrate catabolic process	0.00046	0.823923877	27
amine catabolic process	0.000492	0.882121482	21
transmembrane transport	0.000559	1.000885119	49
mitochondrial transport	0.000976	1.74054303	27
cellular biogenic amine metabolic process	0.000994	1.773415069	20

Biological Process	P-value	FDR	Number of genes
carboxylic acid biosynthetic process	0.001064	1.897607807	31
pyridine nucleotide metabolic process	0.002471	4.353169467	10
indole-containing compound metabolic process	0.002742	4.82010267	9
purine nucleobase metabolic process	0.00286	5.022130943	8
cellular macromolecular complex assembly	0.003108	5.446991614	64
glutamine family amino acid metabolic process	0.003145	5.508637418	17
dicarboxylic acid metabolic process	0.004288	7.440514967	11
pyruvate metabolic process	0.005195	8.944985561	10
hydrogen transport	0.005306	9.127295824	29
nicotinamide metabolic process	0.006199	10.58403569	9
cortical actin cytoskeleton organization	0.006199	10.58403569	9
membrane invagination	0.006799	11.55072711	92
Endocytosis	0.006799	11.55072711	92
transition metal ion transport	0.007807	13.15097211	11
regulation of dephosphorylation	0.008022	13.48938637	7
aromatic compound catabolic process	0.008022	13.48938637	7
cellular modified amino acid catabolic process	0.008108	13.6246114	6
nucleoside diphosphate metabolic process	0.008108	13.6246114	6
peroxisome organization	0.009766	16.18464742	10
macromolecular complex subunit organization	0.010447	17.21623385	98
aspartate family amino acid metabolic process	0.012164	19.7625379	9
transcription from RNA polymerase III promoter	0.01504	23.86236116	8
secondary metabolic process	0.017423	27.10922439	30
cellular carbohydrate biosynthetic process	0.019031	29.22591992	13
small GTPase mediated signal transduction	0.019711	30.1033819	42
programmed cell death	0.020857	31.55967431	56
aromatic amino acid family metabolic process	0.020913	31.63004098	11
RNA modification	0.02109	31.8519522	18

Biological Process	P-value	FDR	Number of genes
serine family amino acid biosynthetic process	0.021788	32.71999722	6
regulation of protein modification process	0.023021	34.22937737	20
L-serine metabolic process	0.024318	35.78301764	5
cell redox homeostasis	0.024835	36.3922581	23
pteridine-containing compound metabolic process	0.026934	38.81100399	10
phagocytosis, engulfment	0.02739	39.32539452	66
alcohol biosynthetic process	0.027416	39.35466314	8
lipid transport	0.029887	42.06660731	14
sulfur compound metabolic process	0.034939	47.26125363	17
cellular modified amino acid metabolic process	0.038384	50.54771306	25
nucleoside metabolic process	0.043901	55.4099297	16
negative regulation of mitotic cell cycle	0.04473	56.10115136	6
DNA replication	0.046599	57.62076708	36
obsolete death	0.047523	58.35338567	57

Appendix B

Equation 1: Commented code for two-way factorial design ANOVA to generate a list of differentially expressed genes for selection, time, and selection by time (interaction).

```
ANOVAdata=read.csv("FOR ANOVA.csv",header=T,row.names=1)
        #Read data into variable ANOVA
Selection<- gl(3,16,48, label=c("D","S","F"))
Time<- gl(4,4,48, label=c("88","96","112","120"))
        #Define factors selection and time
aof<-function(x){
   m=data.frame(Selection,Time,x);
   anova(aov(x~Selection+Time+Selection*Time,m));
}
        #Model formula equivalent to Eq.1 for data set
ANOVAresults=apply(ANOVAdata,1,aof)
ANOVAresults
        # Results of ANOVA
pvalues=data.frame(lapply(ANOVAresults, function(x){x["Pr(>F)"][1:3,]}))
pvalues
write.table(t(pvalues), file="anova-results.txt",quote=F,sep='\t')
        #All p-values placed in one tab-delimited table
regionp=sort(t(pvalues[1,]))
region
        #Sort p-values in ascending order
bh <- function(x, fdr) {
  thresh <- F;
  crit<-0;
  len<-length(x)
  answer <- array(len);
  first <- T;
  for(i in c(len:0)) {
```

```
   crit<-fdr*i/len;
   if (x[i] < crit || thresh == T) {
     answer[i]<-T
     thresh <- T
     if (first) {
       cat(i ,"genes selected at FDR =", fdr ,"\n")
       first = F;
     }
   } else {
     answer[i]<-F
   }
 }
          # Code for function bh can be found in Appendix A of Pavlidis 2003
          #x, list of p-values; fdr, desired FDR
 answer
}
fdr.results=bh(regionp,0.05)
fdr.results
bhthresh <- cbind(regionp, fdr.results)
bhthresh
          #Algorithm given in Benjamini et al. 1995
          #Find p-value threshold that maintains FDR at a given level
write.table(bhthresh, "bhthresh.txt", sep='\t', quote=F)
          #Text file with p-value in first column
          #FDR indicator in second column; 1= FDR criterion met, 0= FDR criterion not met
```

Equation 2: Commented code for FDR

```
keeps=data.frame()
out=vector()
k=1
for(i in 1:nrow(pvaluessorted)){
   out[i]=((i)/nrow(pvaluessorted))*(SL)
   if(pvaluessorted[i,1]<out[i]){
      keeps[k,1]=pvaluessorted[i,1]
      k=k+1
   }
}
         #FDR based on positions of gene in ordered p-value list
keeps
         #P-values, which met FDR criterion
write.table(keeps, "keeps88.txt", sep='\t', quote=F)
write.table(keeps, "keeps96.txt", sep='\t', quote=F)
write.table(keeps, "keeps112.txt", sep='\t', quote=F)
write.table(keeps, "keeps120.txt", sep='\t', quote=F)
         #Table of p-values, which met FDR criterion
```

Equation 3: Commented code for ANOVA generating a list of differentially expressed genes across populations per time point to assess changes between the early and late third larval instar.

```
SL=0.05
        #P-value cutoff
ANOVAdata=read.csv("FOR ANOVA.csv",header=T,row.names=1)
        #Read data into variable ANOVAdata
total88_D=ANOVAdata[,1:4]
total88_S= ANOVAdata[,17:20]
total88_F=ANOVAdata[,33:36]
total88= cbind(total88_D, total88_S, total88_F)
        #Gathering all time points for 88 hours AEL
total96_D=ANOVAdata[,5:8]
total96_S= ANOVAdata[,21:24]
total96_F=ANOVAdata[,37:40]
total96=cbind(total96_D,total96_S, total96_F)
        #Gathering all time points for 96 hours AEL
total112_D=ANOVAdata[,9:12]
total112_S= ANOVAdata[,25:28]
total112_F=ANOVAdata[,41:44]
total112= cbind(total112_D,total112_S, total112_F)
        #Gathering all time points for 112 hours AEL
total120_D=ANOVAdata[,13:16]
total120_S= ANOVAdata[,29:32]
total120_F=ANOVAdata[,45:48]
total120= cbind(total120_D,total120_S, total120_F)
        #Gathering all time points for 120 hours AEL
Selection<- gl(3,4,12, label=c("D","S","F"))
        #Defining Selection
aof<-function(x){
    m=data.frame(Selection,x);
```

```
    anova(aov(x~Selection,m));
}
        #Model formula equivalent to Eq.2 for data set
ANOVAresults=apply(total88,1,aof)
ANOVAresults
        #ANOVA results only for 88 hours AEL
ANOVAresults=apply(total96,1,aof)
ANOVAresults
        #ANOVA results only for 96 hours AEL
ANOVAresults=apply(total112,1,aof)
ANOVAresults
        #ANOVA results only for 112 hours AEL
ANOVAresults=apply(total120,1,aof)
ANOVAresults
        #ANOVA results only for 120 hours AEL
pvalues=data.frame(lapply(ANOVAresults, function(x){x["Pr(>F)"][1,]}))
pvalues
        #P-values shown
pvaluessorted=sort(pvalues)
        #Sort p-values in ascending order
pvaluessorted=t(pvaluessorted)
        #Transfer rows and columns
```

Appendix C

Supplemental Table 1: List of genes using their corresponding FlyBase ID and p- values resulting from ANOVA for selection (A) and interaction (B)

A

FlyBase ID	P- value	FlyBase ID	P- value	FlyBase ID	P- value
FBgn0031860	2.39E-10	FBgn0015573	6.92E-06	FBgn0033240	8.30E-05
FBgn0015039	3.65E-09	FBgn0051324	9.48E-06	FBgn0033821	8.80E-05
FBgn0039180	4.68E-09	FBgn0040887	1.22E-05	FBgn0032197	9.11E-05
FBgn0027534	5.13E-09	FBgn0028519	1.36E-05	FBgn0010053	9.96E-05
FBgn0031646	8.32E-09	FBgn0039099	1.65E-05	FBgn0015396	0.0001
FBgn0015572	8.71E-09	FBgn0069056	2.21E-05	FBgn0039319	0.000101
FBgn0003410	7.13E-08	FBgn0036094	2.44E-05	FBgn0035904	0.000104
FBgn0032169	1.54E-07	FBgn0028394	3.61E-05	FBgn0002869	0.000121
FBgn0051337	2.10E-07	FBgn0015773	3.71E-05	FBgn0015011	0.000121
FBgn0032810	4.02E-07	FBgn0031813	3.72E-05	FBgn0030246	0.000124
FBgn0053192	1.73E-06	FBgn0040070	3.74E-05	FBgn0051288	0.000124
FBgn0003082	3.16E-06	FBgn0016797	4.06E-05	FBgn0027843	0.000141
FBgn0037126	3.24E-06	FBgn0038020	4.18E-05	FBgn0035734	0.000144
FBgn0036787	5.01E-06	FBgn0039149	6.33E-05		
FBgn0036157	5.72E-06	FBgn0034736	8.22E-05		

B

FlyBase ID	P- value	FlyBase ID	P- value	FlyBase ID	P- value
FBgn0035900	0.001146	FBgn0051704	0.018028	FBgn0032694	0.034728
FBgn0000639	0.001182	FBgn0011673	0.018284	FBgn0051782	0.034767
FBgn0036104	0.001279	FBgn0034987	0.018408	FBgn0036492	0.035369
FBgn0052108	0.001528	FBgn0033204	0.018949	FBgn0032481	0.03563
FBgn0033315	0.001999	FBgn0034837	0.01906	FBgn0004606	0.035801
FBgn0029568	0.002293	FBgn0023129	0.019537	FBgn0034470	0.036068
FBgn0001084	0.002321	FBgn0024806	0.019878	FBgn0052656	0.036383
FBgn0004782	0.00414	FBgn0039831	0.019995	FBgn0038588	0.036748
FBgn0013988	0.004616	FBgn0037850	0.020098	FBgn0030691	0.037479
FBgn0015572	0.004873	FBgn0023023	0.020848	FBgn0037573	0.037788
FBgn0032209	0.005111	FBgn0026375	0.021168	FBgn0030539	0.038667
FBgn0050390	0.0053	FBgn0033701	0.021188	FBgn0034643	0.039374
FBgn0038917	0.005495	FBgn0037144	0.021409	FBgn0000667	0.039481
FBgn0030976	0.005651	FBgn0033793	0.021447	FBgn0030530	0.039717
FBgn0036629	0.006348	FBgn0036187	0.021688	FBgn0040366	0.039911
FBgn0033182	0.006455	FBgn0000634	0.02224	FBgn0000228	0.040515
FBgn0002781	0.006724	FBgn0032130	0.024264	FBgn0040104	0.041161
FBgn0037502	0.007434	FBgn0030813	0.024377	FBgn0033729	0.042033

FlyBase ID	P- value	FlyBase ID	P- value	FlyBase ID	P- value
FBgn0037290	0.007478	FBgn0003970	0.02439	FBgn0021800	0.042151
FBgn0053225	0.009879	FBgn0026326	0.024765	FBgn0034411	0.042182
FBgn0002565	0.01006	FBgn0032473	0.024986	FBgn0035253	0.042192
FBgn0029896	0.010829	FBgn0004556	0.025091	FBgn0032705	0.042593
FBgn0035523	0.011261	FBgn0039449	0.025272	FBgn0014024	0.042896
FBgn0033609	0.011327	FBgn0035235	0.02621	FBgn0032413	0.043204
FBgn0031074	0.011757	FBgn0037486	0.027263	FBgn0053056	0.043651
FBgn0052547	0.012538	FBgn0051320	0.028042	FBgn0052209	0.043889
FBgn0036365	0.012721	FBgn0000524	0.028224	FBgn0038916	0.044192
FBgn0032283	0.013437	FBgn0003013	0.028241	FBgn0004921	0.044469
FBgn0025388	0.013807	FBgn0026085	0.029552	FBgn0034075	0.0446
FBgn0000464	0.014982	FBgn0002891	0.029764	FBgn0039544	0.044666
FBgn0031242	0.015033	FBgn0033128	0.02977	FBgn0004009	0.044855
FBgn0027586	0.015376	FBgn0004876	0.030984	FBgn0005630	0.045241
FBgn0036491	0.015467	FBgn0030687	0.031007	FBgn0025740	0.045767
FBgn0034819	0.015534	FBgn0051643	0.031334	FBgn0001206	0.046074
FBgn0050021	0.015545	FBgn0000095	0.031482	FBgn0051759	0.046916
FBgn0035145	0.015565	FBgn0026315	0.031919	FBgn0033960	0.047256
FBgn0030780	0.016118	FBgn0030563	0.032293	FBgn0005630	0.047339
FBgn0026148	0.01617	FBgn0015038	0.032519	FBgn0010215	0.048312
FBgn0000479	0.016387	FBgn0034491	0.032545	FBgn0051005	0.048922
FBgn0032019	0.016902	FBgn0002562	0.033404	FBgn0011296	0.049024
FBgn0027542	0.01702	FBgn0052275	0.033604	FBgn0010830	0.049512

Appendix D

Supplemental Figure 1: STEM profiles ordered based on the p-value significance of number of genes assigned versus expected number of genes. The colored profiles are representative of statistically significant temporal expression profiles.

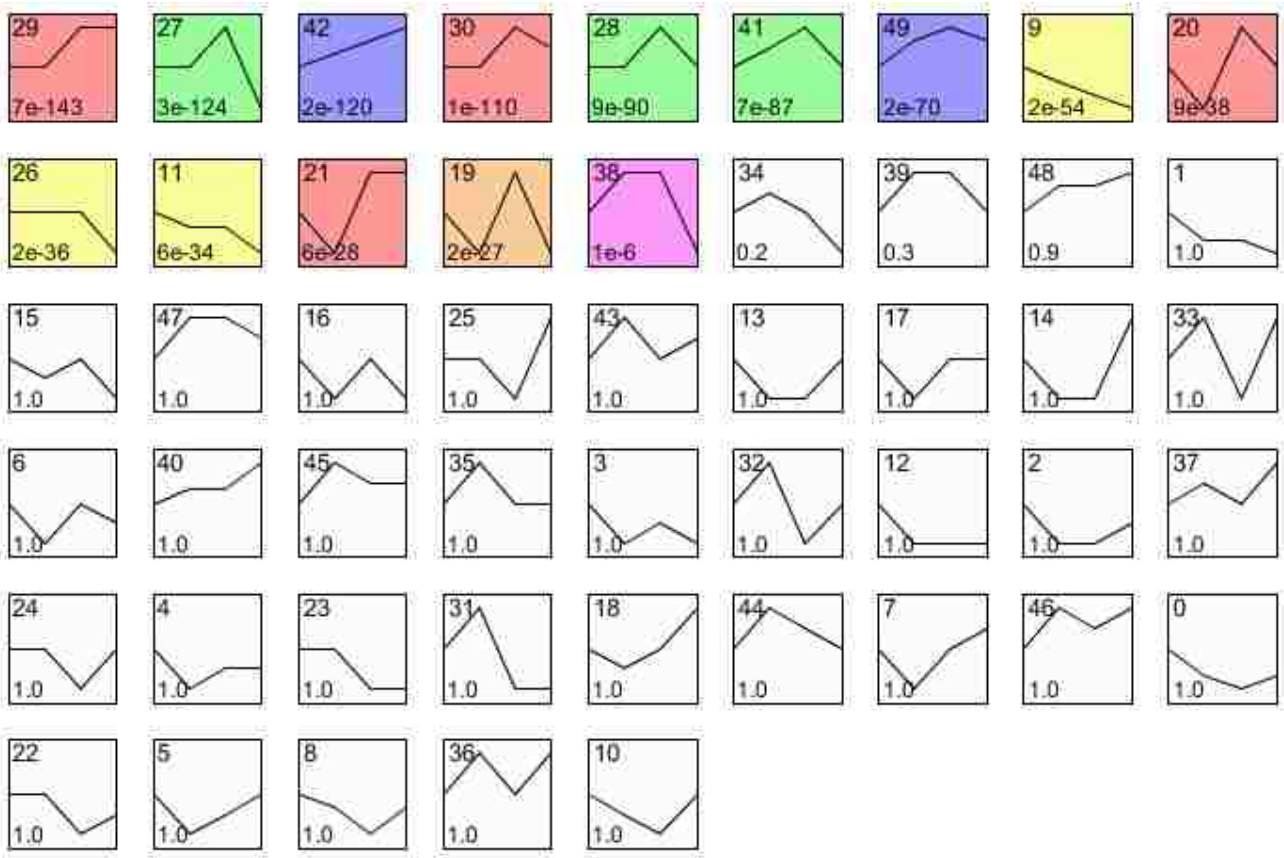

Supplemental Table 2: List of genes which show overlap between differentially expressed genes from two-way factorial design ANOVA and STEM. Flybase IDs shown.

FlyBase ID					
FBgn0036094	FBgn0038519	FBgn0050273	FBgn0040994	FBgn0032072	FBgn0032675
FBgn0000639	FBgn0020640	FBgn0038373	FBgn0005670	FBgn0039145	FBgn0038596
FBgn0037975	FBgn0015754	FBgn0039404	FBgn0033247	FBgn0050158	FBgn0030964
FBgn0033137	FBgn0031307	FBgn0033421	FBgn0040649	FBgn0022708	FBgn0041150
FBgn0033133	FBgn0024183	FBgn0033868	FBgn0037777	FBgn0038210	FBgn0023167
FBgn0046878	FBgn0035412	FBgn0037898	FBgn0034134	FBgn0034184	FBgn0039737
FBgn0028381	FBgn0050345	FBgn0032726	FBgn0037213	FBgn0013951	FBgn0038798
FBgn0033439	FBgn0033205	FBgn0032727	FBgn0035028	FBgn0027657	FBgn0035742
FBgn0033437	FBgn0039135	FBgn0037283	FBgn0031099	FBgn0034651	FBgn0032010
FBgn0029507	FBgn0017567	FBgn0050349	FBgn0037939	FBgn0036162	FBgn0038356
FBgn0034756	FBgn0011770	FBgn0004107	FBgn0033734	FBgn0036101	FBgn0025578
FBgn0032639	FBgn0034786	FBgn0025741	FBgn0038346	FBgn0004101	FBgn0032227
FBgn0030653	FBgn0028411	FBgn0050185	FBgn0015038	FBgn0052057	FBgn0032350
FBgn0039241	FBgn0039183	FBgn0030322	FBgn0031656	FBgn0037101	FBgn0013745
FBgn0028519	FBgn0036449	FBgn0037553	FBgn0010213	FBgn0033741	FBgn0031624
FBgn0051075	FBgn0031764	FBgn0024360	FBgn0003969	FBgn0019947	FBgn0003079
FBgn0037971	FBgn0003178	FBgn0036928	FBgn0050291	FBgn0038084	FBgn0034712
FBgn0035811	FBgn0038110	FBgn0034365	FBgn0003308	FBgn0013749	FBgn0035193
FBgn0041710	FBgn0040899	FBgn0026872	FBgn0051802	FBgn0052371	FBgn0037114
FBgn0031471	FBgn0038307	FBgn0034082	FBgn0051093	FBgn0031298	FBgn0052984
FBgn0033170	FBgn0023549	FBgn0051800	FBgn0037709	FBgn0029718	FBgn0032775
FBgn0027601	FBgn0051380	FBgn0040942	FBgn0050075	FBgn0041712	FBgn0051935
FBgn0032900	FBgn0050414	FBgn0051788	FBgn0035952	FBgn0033367	FBgn0033729
FBgn0034443	FBgn0011704	FBgn0037566	FBgn0051949	FBgn0028402	FBgn0038038
FBgn0002567	FBgn0038961	FBgn0032236	FBgn0037724	FBgn0017424	FBgn0035689
FBgn0032620	FBgn0011227	FBgn0031639	FBgn0015766	FBgn0035786	FBgn0036862
FBgn0052758	FBgn0052687	FBgn0037518	FBgn0004174	FBgn0025140	FBgn0038649
FBgn0031515	FBgn0040732	FBgn0034919	FBgn0040996	FBgn0015808	FBgn0036602
FBgn0032720	FBgn0030735	FBgn0050080	FBgn0031505	FBgn0039850	FBgn0015381
FBgn0052626	FBgn0037167	FBgn0011013	FBgn0033138	FBgn0003075	FBgn0029643
FBgn0033221	FBgn0034727	FBgn0032824	FBgn0051050	FBgn0032346	FBgn0017482
FBgn0031362	FBgn0028325	FBgn0053510	FBgn0039836	FBgn0023023	FBgn0037765
FBgn0031907	FBgn0034418	FBgn0037468	FBgn0037987	FBgn0031367	FBgn0052690
FBgn0038474	FBgn0052448	FBgn0029942	FBgn0036740	FBgn0033542	FBgn0027092
FBgn0052736	FBgn0022073	FBgn0011296	FBgn0038979	FBgn0043535	FBgn0053191
FBgn0036622	FBgn0034422	FBgn0032202	FBgn0036922	FBgn0037513	FBgn0037435
FBgn0032945	FBgn0029996	FBgn0004175	FBgn0034882	FBgn0011725	FBgn0033702
FBgn0024740	FBgn0033904	FBgn0034161	FBgn0003651	FBgn0030191	FBgn0032713
FBgn0033132	FBgn0039829	FBgn0010391	FBgn0034840	FBgn0039668	FBgn0029769
FBgn0051778	FBgn0030572	FBgn0010041	FBgn0031830	FBgn0030966	FBgn0034540
FBgn0022355	FBgn0022288	FBgn0024188	FBgn0050487	FBgn0033495	FBgn0000171
FBgn0038964	FBgn0030986	FBgn0039190	FBgn0036288	FBgn0032291	FBgn0036890
FBgn0028396	FBgn0036988	FBgn0032487	FBgn0051294	FBgn0033065	FBgn0036416
FBgn0026878	FBgn0026261	FBgn0003943	FBgn0031146	FBgn0040389	FBgn0052462
FBgn0038903	FBgn0029672	FBgn0051955	FBgn0030283	FBgn0032464	FBgn0026392
FBgn0044812	FBgn0039218	FBgn0030029	FBgn0037010	FBgn0039207	FBgn0043792
FBgn0031971	FBgn0032285	FBgn0033466	FBgn0037248	FBgn0039812	FBgn0034564

FlyBase ID					
FBgn0036921	FBgn0038585	FBgn0039049	FBgn0038052	FBgn0030441	FBgn0028408
FBgn0015393	FBgn0051779	FBgn0031059	FBgn0040827	FBgn0046793	FBgn0015772
FBgn0005655	FBgn0034997	FBgn0035393	FBgn0000024	FBgn0020616	FBgn0038523
FBgn0051076	FBgn0036030	FBgn0032421	FBgn0034266	FBgn0034744	FBgn0033130
FBgn0050288	FBgn0050269	FBgn0026089	FBgn0037265	FBgn0041102	FBgn0034732
FBgn0025456	FBgn0035552	FBgn0051323	FBgn0051407	FBgn0028515	FBgn0039915
FBgn0015039	FBgn0032668	FBgn0040963	FBgn0005322	FBgn0036386	FBgn0039304
FBgn0020303	FBgn0052672	FBgn0037009	FBgn0035704	FBgn0036125	FBgn0038980
FBgn0037897	FBgn0020513	FBgn0034761	FBgn0000181	FBgn0037202	FBgn0025352
FBgn0037007	FBgn0014011	FBgn0011241	FBgn0051644	FBgn0037087	FBgn0032553
FBgn0022160	FBgn0040777	FBgn0037073	FBgn0037890	FBgn0051230	FBgn0020509
FBgn0010438	FBgn0016126	FBgn0035204	FBgn0021875	FBgn0027087	FBgn0000137
FBgn0026196	FBgn0050196	FBgn0032111	FBgn0029755	FBgn0030763	FBgn0029878
FBgn0031500	FBgn0013349	FBgn0000043	FBgn0016076	FBgn0003748	FBgn0010425
FBgn0003411	FBgn0035473	FBgn0052409	FBgn0026576	FBgn0035147	FBgn0032554
FBgn0040666	FBgn0029765	FBgn0031244	FBgn0030519	FBgn0040299	FBgn0036832
FBgn0052803	FBgn0038473	FBgn0030502	FBgn0032913	FBgn0038102	FBgn0052334
FBgn0032222	FBgn0038271	FBgn0030552	FBgn0032444	FBgn0031282	FBgn0037766
FBgn0013269	FBgn0002772	FBgn0036601	FBgn0042641	FBgn0036782	FBgn0035768
FBgn0031534	FBgn0051344	FBgn0040534	FBgn0033121	FBgn0003275	FBgn0003892
FBgn0031417	FBgn0034221	FBgn0053198	FBgn0038811	FBgn0039912	FBgn0051090
FBgn0044047	FBgn0040091	FBgn0034940	FBgn0030615	FBgn0062517	FBgn0035685
FBgn0039681	FBgn0036813	FBgn0032190	FBgn0063485	FBgn0052459	FBgn0039819
FBgn0031389	FBgn0038601	FBgn0036126	FBgn0029764	FBgn0037019	FBgn0024222
FBgn0036058	FBgn0031651	FBgn0001281	FBgn0000083	FBgn0030691	FBgn0020224
FBgn0051288	FBgn0036157	FBgn0037901	FBgn0037552	FBgn0023542	FBgn0037964
FBgn0029002	FBgn0040321	FBgn0014163	FBgn0039796	FBgn0015527	FBgn0028491
FBgn0034259	FBgn0032264	FBgn0040346	FBgn0052299	FBgn0011640	FBgn0053515
FBgn0028955	FBgn0037978	FBgn0036529	FBgn0037579	FBgn0037994	FBgn0034228
FBgn0039319	FBgn0052284	FBgn0033624	FBgn0030607	FBgn0033853	FBgn0029644
FBgn0036353	FBgn0033584	FBgn0019938	FBgn0034214	FBgn0037916	FBgn0030805
FBgn0010043	FBgn0034366	FBgn0034512	FBgn0036334	FBgn0034243	FBgn0029911
FBgn0015572	FBgn0034726	FBgn0037350	FBgn0036348	FBgn0011592	FBgn0035598
FBgn0040064	FBgn0039627	FBgn0032170	FBgn0029667	FBgn0027084	FBgn0032901
FBgn0027932	FBgn0045823	FBgn0051528	FBgn0051546	FBgn0038498	FBgn0036367
FBgn0033548	FBgn0035122	FBgn0001332	FBgn0034198	FBgn0051842	FBgn0003189
FBgn0037330	FBgn0010222	FBgn0004240	FBgn0037749	FBgn0039577	FBgn0051627
FBgn0011638	FBgn0035805	FBgn0053308	FBgn0033112	FBgn0039344	FBgn0034864
FBgn0063493	FBgn0037684	FBgn0011570	FBgn0024491	FBgn0036448	FBgn0030420
FBgn0025682	FBgn0037730	FBgn0037440	FBgn0036837	FBgn0037339	FBgn0036697
FBgn0032762	FBgn0040717	FBgn0039564	FBgn0030218	FBgn0039553	FBgn0035734
FBgn0035542	FBgn0003205	FBgn0052141	FBgn0015278	FBgn0000165	FBgn0038266
FBgn0031972	FBgn0028572	FBgn0004172	FBgn0015924	FBgn0038118	FBgn0024943
FBgn0031285	FBgn0010415	FBgn0033286	FBgn0035298	FBgn0033190	FBgn0032827
FBgn0031912	FBgn0033304	FBgn0031008	FBgn0038054	FBgn0031178	FBgn0052461
FBgn0033134	FBgn0002741	FBgn0040286	FBgn0032161	FBgn0032385	FBgn0039617
FBgn0039574	FBgn0033079	FBgn0039639	FBgn0032871	FBgn0033701	FBgn0038099
FBgn0037151	FBgn0016917	FBgn0022359	FBgn0034461	FBgn0031816	FBgn0029939
FBgn0038234	FBgn0035438	FBgn0039537	FBgn0037471	FBgn0034721	FBgn0015477
FBgn0036760	FBgn0030611	FBgn0031559	FBgn0037061	FBgn0032938	FBgn0035708

FlyBase ID					
FBgn0040104	FBgn0000055	FBgn0053293	FBgn0004171	FBgn0047178	FBgn0033517
FBgn0032801	FBgn0037230	FBgn0032976	FBgn0039613	FBgn0052425	FBgn0036784
FBgn0040850	FBgn0038419	FBgn0036871	FBgn0030277	FBgn0010051	FBgn0038847
FBgn0036056	FBgn0003067	FBgn0051548	FBgn0031469	FBgn0032269	FBgn0052476
FBgn0032297	FBgn0033907	FBgn0035272	FBgn0016687	FBgn0037059	FBgn0037563
FBgn0038194	FBgn0000473	FBgn0019624	FBgn0031103	FBgn0034869	FBgn0038124
FBgn0037819	FBgn0033571	FBgn0046297	FBgn0037582	FBgn0035584	FBgn0039801
FBgn0038020	FBgn0038290	FBgn0036218	FBgn0032217	FBgn0035679	FBgn0030319
FBgn0039130	FBgn0039098	FBgn0051820	FBgn0010620	FBgn0046769	FBgn0032878
FBgn0032005	FBgn0015610	FBgn0036759	FBgn0051141	FBgn0051370	FBgn0003498
FBgn0033808	FBgn0036942	FBgn0031702	FBgn0039349	FBgn0034560	FBgn0038983
FBgn0051636	FBgn0038869	FBgn0034362	FBgn0038598	FBgn0026252	FBgn0051304
FBgn0037833	FBgn0039068	FBgn0022029	FBgn0003687	FBgn0003034	FBgn0029645
FBgn0034398	FBgn0029512	FBgn0033287	FBgn0033453	FBgn0038957	FBgn0051099
FBgn0040503	FBgn0031968	FBgn0035032	FBgn0038347	FBgn0036439	FBgn0052158
FBgn0035534	FBgn0047338	FBgn0037051	FBgn0034573	FBgn0020643	FBgn0000273
FBgn0010238	FBgn0050052	FBgn0032642	FBgn0010295	FBgn0031626	FBgn0031722
FBgn0040532	FBgn0034361	FBgn0031436	FBgn0031241	FBgn0025683	FBgn0034776
FBgn0050091	FBgn0032787	FBgn0010340	FBgn0028858	FBgn0035251	FBgn0030150
FBgn0027793	FBgn0036846	FBgn0025574	FBgn0002865	FBgn0023477	FBgn0030843
FBgn0030480	FBgn0039115	FBgn0031558	FBgn0032755	FBgn0000567	FBgn0013988
FBgn0052418	FBgn0031295	FBgn0029094	FBgn0034261	FBgn0038989	FBgn0033663
FBgn0044030	FBgn0034791	FBgn0033504	FBgn0001989	FBgn0036159	FBgn0030776
FBgn0029093	FBgn0038400	FBgn0033604	FBgn0030726	FBgn0028544	FBgn0014027
FBgn0032329	FBgn0000308	FBgn0004901	FBgn0034097	FBgn0027945	FBgn0034979
FBgn0011787	FBgn0037817	FBgn0030745	FBgn0024556	FBgn0039694	FBgn0051163
FBgn0067779	FBgn0033092	FBgn0025336	FBgn0032018	FBgn0036301	FBgn0031142
FBgn0003890	FBgn0037492	FBgn0034454	FBgn0002174	FBgn0034312	FBgn0035760
FBgn0001967	FBgn0037244	FBgn0037035	FBgn0030520	FBgn0037829	FBgn0030331
FBgn0003141	FBgn0038463	FBgn0032549	FBgn0026263	FBgn0029865	FBgn0038512
FBgn0031489	FBgn0031689	FBgn0037358	FBgn0036316	FBgn0011672	FBgn0017581
FBgn0000409	FBgn0025186	FBgn0034802	FBgn0038200	FBgn0038219	FBgn0032492
FBgn0034688	FBgn0034528	FBgn0033875	FBgn0037391	FBgn0029866	FBgn0028871
FBgn0051450	FBgn0038053	FBgn0039765	FBgn0038805	FBgn0052354	FBgn0037547
FBgn0052115	FBgn0027561	FBgn0038078	FBgn0003360	FBgn0039799	FBgn0052087
FBgn0033507	FBgn0036297	FBgn0003889	FBgn0034741	FBgn0035068	FBgn0038458
FBgn0025885	FBgn0031538	FBgn0031939	FBgn0004811	FBgn0039358	FBgn0051038
FBgn0033085	FBgn0030593	FBgn0040491	FBgn0038276	FBgn0002525	FBgn0034660
FBgn0039735	FBgn0034436	FBgn0031851	FBgn0034094	FBgn0053054	FBgn0003425
FBgn0039678	FBgn0036441	FBgn0038539	FBgn0038673	FBgn0030695	FBgn0037483
FBgn0031381	FBgn0031405	FBgn0034245	FBgn0023514	FBgn0039856	FBgn0050409
FBgn0026313	FBgn0030086	FBgn0002031	FBgn0033635	FBgn0036806	FBgn0052353
FBgn0000565	FBgn0033583	FBgn0038662	FBgn0039685	FBgn0040512	FBgn0010235
FBgn0011361	FBgn0039189	FBgn0039051	FBgn0036194	FBgn0044871	FBgn0035797
FBgn0000044	FBgn0036929	FBgn0033928	FBgn0034879	FBgn0037071	FBgn0030786
FBgn0041194	FBgn0051870	FBgn0051357	FBgn0032516	FBgn0033457	FBgn0010218
FBgn0001208	FBgn0036980	FBgn0030718	FBgn0036483	FBgn0033458	FBgn0030215
FBgn0030876	FBgn0025839	FBgn0053217	FBgn0034158	FBgn0030802	FBgn0035001
FBgn0042206	FBgn0032538	FBgn0024958	FBgn0037543	FBgn0035496	FBgn0031721
FBgn0030187	FBgn0051229	FBgn0035469	FBgn0035782	FBgn0051882	FBgn0005666

FlyBase ID					
FBgn0031813	FBgn0036571	FBgn0036437	FBgn0030053	FBgn0004366	FBgn0046302
FBgn0036853	FBgn0030060	FBgn0043806	FBgn0040706	FBgn0028936	FBgn0053172
FBgn0039274	FBgn0032881	FBgn0022344	FBgn0038175	FBgn0037354	FBgn0052486
FBgn0032400	FBgn0029857	FBgn0001186	FBgn0035915	FBgn0038359	FBgn0035929
FBgn0051126	FBgn0050217	FBgn0031263	FBgn0038516	FBgn0015571	FBgn0052250
FBgn0032885	FBgn0036613	FBgn0033812	FBgn0050356	FBgn0042133	FBgn0039792
FBgn0031148	FBgn0039881	FBgn0027836	FBgn0052708	FBgn0037592	FBgn0035857
FBgn0032679	FBgn0036876	FBgn0039687	FBgn0031531	FBgn0001104	FBgn0033141
FBgn0038074	FBgn0033754	FBgn0038978	FBgn0053284	FBgn0037373	FBgn0032430
FBgn0031092	FBgn0030791	FBgn0037235	FBgn0022774	FBgn0015287	FBgn0014861
FBgn0035063	FBgn0033631	FBgn0041183	FBgn0039083	FBgn0027602	FBgn0038120
FBgn0039798	FBgn0036462	FBgn0033243	FBgn0034505	FBgn0039778	FBgn0036843
FBgn0002778	FBgn0027360	FBgn0029704	FBgn0027086	FBgn0037899	FBgn0029830
FBgn0033035	FBgn0032849	FBgn0031831	FBgn0038853	FBgn0037928	FBgn0031987
FBgn0034488	FBgn0038243	FBgn0046322	FBgn0038716	FBgn0040816	FBgn0031069
FBgn0042120	FBgn0036272	FBgn0033989	FBgn0032644	FBgn0032180	FBgn0034229
FBgn0022338	FBgn0038183	FBgn0039113	FBgn0051363	FBgn0040764	FBgn0030578
FBgn0042118	FBgn0010040	FBgn0031751	FBgn0039438	FBgn0004919	FBgn0032207
FBgn0037969	FBgn0032408	FBgn0050039	FBgn0033452	FBgn0053513	FBgn0033828
FBgn0050154	FBgn0004654	FBgn0052267	FBgn0039642	FBgn0015268	FBgn0030746
FBgn0016685	FBgn0036035	FBgn0037962	FBgn0027598	FBgn0039867	FBgn0035360
FBgn0034140	FBgn0033269	FBgn0023527	FBgn0052308	FBgn0039777	FBgn0040092
FBgn0038925	FBgn0004173	FBgn0026315	FBgn0039453	FBgn0024753	FBgn0003162
FBgn0033544	FBgn0030326	FBgn0038787	FBgn0032262	FBgn0010292	FBgn0039727
FBgn0050359	FBgn0038746	FBgn0033476	FBgn0015585	FBgn0020909	FBgn0038166
FBgn0035065	FBgn0032370	FBgn0027501	FBgn0000259	FBgn0035916	FBgn0036395
FBgn0031717	FBgn0019972	FBgn0036696	FBgn0064912	FBgn0035165	FBgn0052814
FBgn0053056	FBgn0032244	FBgn0039767	FBgn0028424	FBgn0036808	FBgn0052204
FBgn0030040	FBgn0032746	FBgn0037883	FBgn0030484	FBgn0035380	FBgn0027330
FBgn0040099	FBgn0035726	FBgn0002527	FBgn0033981	FBgn0036533	FBgn0052161
FBgn0015714	FBgn0035524	FBgn0037842	FBgn0039002	FBgn0033323	FBgn0030947
FBgn0034390	FBgn0033945	FBgn0042198	FBgn0030999	FBgn0033872	FBgn0036607
FBgn0037370	FBgn0002528	FBgn0045827	FBgn0032382	FBgn0035439	FBgn0028915
FBgn0028648	FBgn0033772	FBgn0031270	FBgn0040309	FBgn0024973	FBgn0051755
FBgn0033451	FBgn0026562	FBgn0038225	FBgn0032919	FBgn0052298	FBgn0035192
FBgn0037834	FBgn0024364	FBgn0037612	FBgn0052295	FBgn0045770	FBgn0031872
FBgn0035444	FBgn0029079	FBgn0039360	FBgn0035161	FBgn0050324	FBgn0030586
FBgn0039741	FBgn0025629	FBgn0033483	FBgn0038552	FBgn0029894	FBgn0030587
FBgn0036488	FBgn0052407	FBgn0015035	FBgn0035047	FBgn0051244	FBgn0039771
FBgn0033373	FBgn0031395	FBgn0032168	FBgn0052649	FBgn0036705	FBgn0032471
FBgn0034579	FBgn0030753	FBgn0037652	FBgn0050093	FBgn0032206	FBgn0030631
FBgn0039929	FBgn0010039	FBgn0004057	FBgn0015338	FBgn0063667	FBgn0030969
FBgn0038923	FBgn0051313	FBgn0038410	FBgn0034851	FBgn0051286	FBgn0051921
FBgn0051534	FBgn0052344	FBgn0032530	FBgn0028913	FBgn0033273	FBgn0011576
FBgn0063494	FBgn0001612	FBgn0039023	FBgn0033543	FBgn0028646	FBgn0050072
FBgn0034199	FBgn0019960	FBgn0038313	FBgn0034510	FBgn0035978	FBgn0030537
FBgn0038306	FBgn0032282	FBgn0044511	FBgn0052440	FBgn0052192	FBgn0033189
FBgn0039835	FBgn0034065	FBgn0039341	FBgn0032191	FBgn0035138	FBgn0052946
FBgn0029092	FBgn0038796	FBgn0031723	FBgn0034915	FBgn0028471	FBgn0030077
FBgn0035422	FBgn0035312	FBgn0050365	FBgn0031292	FBgn0051851	FBgn0030377

FlyBase ID					
FBgn0030485	FBgn0035600	FBgn0031695	FBgn0042189	FBgn0040291	FBgn0000064
FBgn0011455	FBgn0039157	FBgn0038806	FBgn0041174	FBgn0039109	FBgn0053265
FBgn0036341	FBgn0038387	FBgn0037102	FBgn0036093	FBgn0032702	FBgn0000277
FBgn0035202	FBgn0050360	FBgn0051174	FBgn0039235	FBgn0031256	FBgn0052274
FBgn0031801	FBgn0030270	FBgn0035585	FBgn0036064	FBgn0021953	FBgn0034876
FBgn0003257	FBgn0036557	FBgn0038388	FBgn0040798	FBgn0034126	FBgn0050373
FBgn0044020	FBgn0035850	FBgn0040814	FBgn0031476	FBgn0053061	FBgn0051308
FBgn0024558	FBgn0035541	FBgn0028582	FBgn0025803	FBgn0033540	FBgn0052570
FBgn0053093	FBgn0033857	FBgn0039152	FBgn0004896	FBgn0028436	FBgn0025874
FBgn0039112	FBgn0030183	FBgn0051226	FBgn0033968	FBgn0051735	FBgn0037366
FBgn0038275	FBgn0036774	FBgn0019828	FBgn0036188	FBgn0015801	FBgn0003089
FBgn0038146	FBgn0020305	FBgn0050499	FBgn0031485	FBgn0003600	FBgn0037307
FBgn0026084	FBgn0034628	FBgn0034270	FBgn0035491	FBgn0032021	FBgn0037040
FBgn0050148	FBgn0034399	FBgn0040493	FBgn0037172	FBgn0000337	FBgn0052628
FBgn0030511	FBgn0038129	FBgn0032358	FBgn0019948	FBgn0039672	FBgn0040993
FBgn0030765	FBgn0051909	FBgn0024332	FBgn0010220	FBgn0041180	FBgn0039371
FBgn0030668	FBgn0037504	FBgn0043575	FBgn0003691	FBgn0035776	FBgn0051008
FBgn0015033	FBgn0011270	FBgn0034595	FBgn0038107	FBgn0031228	FBgn0033306
FBgn0037680	FBgn0050423	FBgn0036373	FBgn0035592	FBgn0043456	FBgn0028855
FBgn0039543	FBgn0037892	FBgn0000286	FBgn0036516	FBgn0028700	FBgn0026015
FBgn0053126	FBgn0034299	FBgn0051100	FBgn0027654	FBgn0035588	FBgn0026056
FBgn0001187	FBgn0031494	FBgn0011577	FBgn0032715	FBgn0036426	FBgn0030899
FBgn0010741	FBgn0052698	FBgn0039538	FBgn0032646	FBgn0039807	FBgn0035711
FBgn0020638	FBgn0037933	FBgn0053095	FBgn0003545	FBgn0039827	FBgn0026369
FBgn0036410	FBgn0039745	FBgn0036932	FBgn0035152	FBgn0035529	FBgn0045759
FBgn0035374	FBgn0039356	FBgn0036221	FBgn0053523	FBgn0034909	FBgn0016694
FBgn0038017	FBgn0032429	FBgn0051523	FBgn0051542	FBgn0053092	FBgn0031757
FBgn0035854	FBgn0036891	FBgn0029161	FBgn0035802	FBgn0031940	FBgn0053474
FBgn0033059	FBgn0035582	FBgn0067628	FBgn0004363	FBgn0002945	FBgn0038042
FBgn0030481	FBgn0020389	FBgn0033307	FBgn0040755	FBgn0032836	FBgn0015584
FBgn0014469	FBgn0015245	FBgn0037936	FBgn0034282	FBgn0037718	FBgn0031514
FBgn0023184	FBgn0033777	FBgn0033522	FBgn0034087	FBgn0030007	FBgn0039503
FBgn0038009	FBgn0051337	FBgn0033513	FBgn0010083	FBgn0037915	FBgn0031633
FBgn0053503	FBgn0036381	FBgn0027363	FBgn0033268	FBgn0033076	FBgn0040977
FBgn0035160	FBgn0016032	FBgn0034826	FBgn0029539	FBgn0052495	FBgn0040362
FBgn0037714	FBgn0037146	FBgn0021750	FBgn0052137	FBgn0001220	FBgn0034774
FBgn0030521	FBgn0010226	FBgn0031591	FBgn0023000	FBgn0028496	FBgn0000659
FBgn0039233	FBgn0035710	FBgn0033802	FBgn0038377	FBgn0037175	FBgn0020372
FBgn0030105	FBgn0036990	FBgn0030278	FBgn0032280	FBgn0031737	FBgn0031325
FBgn0053099	FBgn0033292	FBgn0033978	FBgn0035285	FBgn0033067	FBgn0033494
FBgn0036650	FBgn0033724	FBgn0032703	FBgn0051787	FBgn0051295	FBgn0010241
FBgn0019982	FBgn0010042	FBgn0037484	FBgn0030431	FBgn0039927	FBgn0053521
FBgn0011824	FBgn0031231	FBgn0053123	FBgn0032622	FBgn0046214	FBgn0036369
FBgn0001995	FBgn0037121	FBgn0026741	FBgn0033235	FBgn0025592	FBgn0034356
FBgn0032785	FBgn0030447	FBgn0032205	FBgn0013432	FBgn0039036	FBgn0020620
FBgn0031657	FBgn0039159	FBgn0037828	FBgn0036588	FBgn0033093	FBgn0015608
FBgn0040918	FBgn0015286	FBgn0000239	FBgn0033100	FBgn0042086	FBgn0051798
FBgn0039868	FBgn0053225	FBgn0032298	FBgn0035146	FBgn0014143	FBgn0032440
FBgn0031117	FBgn0033820	FBgn0029737	FBgn0053460	FBgn0050472	FBgn0030390
FBgn0031040	FBgn0029148	FBgn0037955	FBgn0032519	FBgn0014851	FBgn0028924

FlyBase ID					
FBgn0016041	FBgn0027571	FBgn0031020	FBgn0031598	FBgn0038237	FBgn0037772
FBgn0027493	FBgn0030733	FBgn0029903	FBgn0027291	FBgn0010339	FBgn0038316
FBgn0035039	FBgn0027655	FBgn0038127	FBgn0033089	FBgn0026403	FBgn0029976
FBgn0001224	FBgn0035675	FBgn0051029	FBgn0010198	FBgn0034291	FBgn0053543
FBgn0035806	FBgn0038437	FBgn0032022	FBgn0038567	FBgn0034368	FBgn0033153
FBgn0031357	FBgn0004868	FBgn0040747	FBgn0039635	FBgn0051281	FBgn0029848
FBgn0031432	FBgn0038966	FBgn0020642	FBgn0030106	FBgn0032664	FBgn0051697
FBgn0014028	FBgn0032638	FBgn0024811	FBgn0034455	FBgn0030594	FBgn0038095
FBgn0025814	FBgn0034931	FBgn0027610	FBgn0030395	FBgn0036884	FBgn0035402
FBgn0034059	FBgn0063261	FBgn0003961	FBgn0030878	FBgn0050296	FBgn0050432
FBgn0010591	FBgn0036663	FBgn0032166	FBgn0031661	FBgn0052564	FBgn0037161
FBgn0051248	FBgn0010551	FBgn0028683	FBgn0051765	FBgn0051698	FBgn0034137
FBgn0032420	FBgn0034986	FBgn0034478	FBgn0035046	FBgn0038854	FBgn0031957
FBgn0039357	FBgn0046873	FBgn0033477	FBgn0026439	FBgn0028904	FBgn0029931
FBgn0034232	FBgn0033816	FBgn0037723	FBgn0035124	FBgn0033248	FBgn0038390
FBgn0036460	FBgn0053193	FBgn0011509	FBgn0039345	FBgn0051053	FBgn0001145
FBgn0030737	FBgn0031182	FBgn0003660	FBgn0033518	FBgn0035048	FBgn0051713
FBgn0033188	FBgn0036623	FBgn0030067	FBgn0034710	FBgn0036642	FBgn0036800
FBgn0035085	FBgn0039417	FBgn0034275	FBgn0010278	FBgn0050464	FBgn0041581
FBgn0037607	FBgn0035348	FBgn0052351	FBgn0037759	FBgn0052686	FBgn0040813
FBgn0052579	FBgn0033083	FBgn0039890	FBgn0050366	FBgn0031684	FBgn0033862
FBgn0004432	FBgn0001197	FBgn0063497	FBgn0038610	FBgn0033214	FBgn0050037
FBgn0050172	FBgn0031227	FBgn0037815	FBgn0036214	FBgn0035273	FBgn0051867
FBgn0036875	FBgn0036886	FBgn0052030	FBgn0034011	FBgn0031414	FBgn0031606
FBgn0042092	FBgn0003996	FBgn0032588	FBgn0036945	FBgn0034493	FBgn0001977
FBgn0030610	FBgn0032770	FBgn0030851	FBgn0037750	FBgn0037894	FBgn0039006
FBgn0032053	FBgn0038319	FBgn0030955	FBgn0031599	FBgn0036992	FBgn0038063
FBgn0037181	FBgn0015777	FBgn0033285	FBgn0036089	FBgn0052081	FBgn0038764
FBgn0000084	FBgn0034230	FBgn0051206	FBgn0033596	FBgn0053468	FBgn0028866
FBgn0019957	FBgn0036490	FBgn0038655	FBgn0003231	FBgn0034351	FBgn0037690
FBgn0051974	FBgn0026778	FBgn0000426	FBgn0030014	FBgn0000047	FBgn0029914
FBgn0038426	FBgn0029990	FBgn0033742	FBgn0030882	FBgn0037200	FBgn0033949
FBgn0016715	FBgn0035321	FBgn0023519	FBgn0033737	FBgn0037757	FBgn0052670
FBgn0010609	FBgn0039632	FBgn0037219	FBgn0053462	FBgn0037514	FBgn0040719
FBgn0015570	FBgn0036271	FBgn0010611	FBgn0034893	FBgn0032709	FBgn0051205
FBgn0052266	FBgn0038312	FBgn0033600	FBgn0051816	FBgn0050108	FBgn0016792
FBgn0035335	FBgn0038865	FBgn0053459	FBgn0028430	FBgn0051923	FBgn0039451
FBgn0031766	FBgn0032511	FBgn0035517	FBgn0042174	FBgn0036394	FBgn0027593
FBgn0034162	FBgn0039118	FBgn0011211	FBgn0034405	FBgn0002534	FBgn0040775
FBgn0027615	FBgn0036415	FBgn0037191	FBgn0003313	FBgn0035722	FBgn0004888
FBgn0017558	FBgn0029665	FBgn0031504	FBgn0000546	FBgn0032935	FBgn0020385
FBgn0031470	FBgn0053276	FBgn0031937	FBgn0035876	FBgn0037850	FBgn0032894
FBgn0036262	FBgn0036998	FBgn0010038	FBgn0031062	FBgn0032502	FBgn0026394
FBgn0032896	FBgn0037873	FBgn0033562	FBgn0031012	FBgn0036141	FBgn0029697
FBgn0028940	FBgn0051414	FBgn0033209	FBgn0033755	FBgn0050083	FBgn0051115
FBgn0034870	FBgn0038809	FBgn0030853	FBgn0000210	FBgn0034606	FBgn0033798
FBgn0031250	FBgn0029828	FBgn0033953	FBgn0031808	FBgn0032863	FBgn0004854
FBgn0038651	FBgn0053002	FBgn0036438	FBgn0039661	FBgn0028336	FBgn0028487
FBgn0037489	FBgn0030740	FBgn0035981	FBgn0034276	FBgn0029964	FBgn0051121
FBgn0036787	FBgn0039239	FBgn0001226	FBgn0035945	FBgn0038161	FBgn0038423

FlyBase ID					
FBgn0040887	FBgn0037460	FBgn0028671	FBgn0040694	FBgn0021967	FBgn0034076
FBgn0011273	FBgn0016940	FBgn0047351	FBgn0040906	FBgn0021995	FBgn0030492
FBgn0032026	FBgn0037070	FBgn0051102	FBgn0015831	FBgn0001980	FBgn0029974
FBgn0037137	FBgn0031809	FBgn0028883	FBgn0043578	FBgn0011695	FBgn0023531
FBgn0033903	FBgn0052662	FBgn0041629	FBgn0031821	FBgn0030504	FBgn0029924
FBgn0036916	FBgn0030834	FBgn0032925	FBgn0031824	FBgn0035162	FBgn0037465
FBgn0032033	FBgn0034733	FBgn0015372	FBgn0030719	FBgn0037762	FBgn0039378
FBgn0037537	FBgn0034658	FBgn0014368	FBgn0035878	FBgn0050192	FBgn0034377
FBgn0030545	FBgn0030692	FBgn0038217	FBgn0039208	FBgn0029902	FBgn0035626
FBgn0034406	FBgn0035528	FBgn0042138	FBgn0050056	FBgn0040078	FBgn0015218
FBgn0036335	FBgn0028939	FBgn0013308	FBgn0058169	FBgn0031998	FBgn0034432
FBgn0033961	FBgn0033244	FBgn0026088	FBgn0039612	FBgn0036824	FBgn0040685
FBgn0053120	FBgn0052528	FBgn0034263	FBgn0051184	FBgn0037541	FBgn0037430
FBgn0039566	FBgn0035211	FBgn0037913	FBgn0030555	FBgn0038838	FBgn0030743
FBgn0028744	FBgn0004624	FBgn0051938	FBgn0034958	FBgn0033885	FBgn0050095
FBgn0036762	FBgn0031516	FBgn0035007	FBgn0035603	FBgn0000227	

Appendix E

Supplemental Table 3: GO module results for selection (A), time (B), and interaction (C) sorted by significance. K denotes positive p-values for local minimum, T denotes significant hierarchical descendants of local minimum, and F denotes false positively enriched GO terms.

A

Submitted GO IDs	Submitted p- values	Significance	GO terms	GO-Module IDs
GO:0055114	0.008027	K	oxidation-reduction process	2
GO:0030182	0.053942	K	neuron differentiation	1
GO:0044242	0.054306	K	cellular lipid catabolic process	3
GO:0016042	0.092223	F	lipid catabolic process	

B

Submitted GO IDs	Submitted p- values	Significance	GO terms	GO-Module IDs
GO:0015980	7.80E-11	T	energy derivation by oxidation of organic compounds	50;64
GO:0045333	1.28E-09	T	cellular respiration	50;64
GO:0009260	3.32E-08	T	ribonucleotide biosynthetic process	13
GO:0022900	3.86E-08	T	electron transport chain	50;64
GO:0009150	9.82E-08	T	purine ribonucleotide metabolic process	13
GO:0009152	1E-07	T	purine ribonucleotide biosynthetic process	13
GO:0034654	1.53E-07	T	nucleobase-containing compound biosynthetic process	5
GO:0034404	1.53E-07	T	nucleobase-containing small molecule biosynthetic process	5
GO:0006119	4.83E-07	T	oxidative phosphorylation	13;36;64
GO:0042254	5.96E-07	T	ribosome biogenesis	7
GO:0022904	7.11E-07	T	respiratory electron transport chain	50;64
GO:0042773	1.78E-06	T	ATP synthesis coupled electron transport	50;64
GO:0015031	1.12E-05	T	protein transport	60
GO:0009168	4.88E-05	T	purine ribonucleoside monophosphate biosynthetic process	14
GO:0009109	9.65E-05	T	coenzyme catabolic process	19
GO:0034470	0.000106	T	ncRNA processing	2
GO:0019318	0.000152	T	hexose metabolic process	23
GO:0006120	0.000173	T	mitochondrial electron transport, NADH to ubiquinone	50;64
GO:0009060	0.000173	T	aerobic respiration	50;64
GO:0046356	0.000212	T	acetyl-CoA catabolic process	10;19
GO:0009309	0.000252	T	amine biosynthetic process	5

Submitted GO IDs	Submitted p- values	Significance	GO terms	GO-Module IDs
GO:0006886	0.000351	T	intracellular protein transport	60;73
GO:0006006	0.000387	T	glucose metabolic process	23
GO:0009201	0.000439	T	ribonucleoside triphosphate biosynthetic process	36
GO:0006605	0.000539	T	protein targeting	60;73
GO:0046365	0.000613	T	monosaccharide catabolic process	23
GO:0009205	0.000625	T	purine ribonucleoside triphosphate metabolic process	36
GO:0009206	0.000732	T	purine ribonucleoside triphosphate biosynthetic process	36
GO:0006399	0.000903	T	tRNA metabolic process	2
GO:0046034	0.000913	T	ATP metabolic process	13;36
GO:0006364	0.000975	T	rRNA processing	2
GO:0009062	0.001014	T	fatty acid catabolic process	33;63
GO:0006007	0.001167	T	glucose catabolic process	23
GO:0019320	0.001167	T	hexose catabolic process	23
GO:0016072	0.001475	T	rRNA metabolic process	2
GO:0006754	0.002426	T	ATP biosynthetic process	13;14;36
GO:0006188	0.002637	T	IMP biosynthetic process	13;14
GO:0046040	0.002637	T	IMP metabolic process	13
GO:0006635	0.002742	T	fatty acid beta-oxidation	33;50;63
GO:0009063	0.003796	T	cellular amino acid catabolic process	3
GO:0008033	0.004871	T	tRNA processing	2
GO:0006733	0.004956	T	oxidoreduction coenzyme metabolic process	19
GO:0008652	0.006129	T	cellular amino acid biosynthetic process	61
GO:0046496	0.006199	T	nicotinamide nucleotide metabolic process	24
GO:0034440	0.006199	T	lipid oxidation	50
GO:0019395	0.006199	T	fatty acid oxidation	33;50
GO:0006189	0.008108	T	'de novo' IMP biosynthetic process	13;14
GO:0015992	0.008516	T	proton transport	62
GO:0034220	0.010221	T	ion transmembrane transport	22
GO:0017038	0.011332	T	protein import	60
GO:0006122	0.012164	T	mitochondrial electron transport, ubiquinol to cytochrome c	50;64
GO:0065003	0.015385	T	macromolecular complex assembly	54
GO:0006586	0.018346	T	indolalkylamine metabolic process	12;47
GO:0006626	0.018417	T	protein targeting to mitochondrion	55;60;73
GO:0042402	0.024318	T	cellular biogenic amine catabolic process	47;52
GO:0015986	0.025212	T	ATP synthesis coupled proton transport	13;14;36
GO:0043623	0.025492	T	cellular protein complex assembly	58
GO:0006909	0.028543	T	Phagocytosis	26

Submitted GO IDs	Submitted p- values	Significance	GO terms	GO-Module IDs
GO:0006536	0.035044	T	glutamate metabolic process	17;57
GO:0009108	0.036832	T	coenzyme biosynthetic process	19
GO:0042401	0.040685	T	cellular biogenic amine biosynthetic process	5;47
GO:0022618	0.043901	T	ribonucleoprotein complex assembly	58
GO:0006096	0.043901	T	glycolytic process	16;24
GO:0006098	0.04473	T	pentose-phosphate shunt	24
GO:0006825	0.04473	T	copper ion transport	43
GO:0006739	0.04473	T	NADP metabolic process	24
GO:0006458	0.045211	T	'de novo' protein folding	71
GO:0055114	4.04E-22	K	oxidation-reduction process	50
GO:0006091	3.69E-13	K	generation of precursor metabolites and energy	64
GO:0044271	4.93E-11	K	cellular nitrogen compound biosynthetic process	5
GO:0009259	3.28E-08	K	ribonucleotide metabolic process	13
GO:0022613	2.45E-07	K	ribonucleoprotein complex biogenesis	7
GO:0006732	4.79E-07	K	coenzyme metabolic process	19
GO:0042775	8.2E-07	K	mitochondrial ATP synthesis coupled electron transport	38
GO:0006457	5.17E-06	K	protein folding	71
GO:0045184	7.7E-06	K	establishment of protein localization	60
GO:0034660	8.8E-06	K	ncRNA metabolic process	2
GO:0006631	1.24E-05	K	fatty acid metabolic process	33
GO:0005996	1.61E-05	K	monosaccharide metabolic process	23
GO:0046395	2.88E-05	K	carboxylic acid catabolic process	3
GO:0009156	4.71E-05	K	ribonucleoside monophosphate biosynthetic process	14
GO:0046164	5.14E-05	K	alcohol catabolic process	28
GO:0006084	7.95E-05	K	acetyl-CoA metabolic process	10
GO:0046907	0.000194	K	intracellular transport	73
GO:0006099	0.000212	K	tricarboxylic acid cycle	39
GO:0009199	0.000377	K	ribonucleoside triphosphate metabolic process	36
GO:0044242	0.000382	K	cellular lipid catabolic process	63
GO:0044275	0.00046	K	cellular carbohydrate catabolic process	74
GO:0009310	0.000492	K	amine catabolic process	52
GO:0055085	0.000559	K	transmembrane transport	22
GO:0006839	0.000976	K	mitochondrial transport	55
GO:0006576	0.000994	K	cellular biogenic amine metabolic process	47
GO:0046394	0.001064	K	carboxylic acid biosynthetic process	61
GO:0019362	0.002471	K	pyridine nucleotide metabolic process	24
GO:0042430	0.002742	K	indole-containing compound metabolic process	12
GO:0006144	0.00286	K	purine nucleobase metabolic process	18

Submitted GO IDs	Submitted p- values	Significance	GO terms	GO-Module IDs
GO:0034622	0.003108	K	cellular macromolecular complex assembly	58
GO:0009064	0.003145	K	glutamine family amino acid metabolic process	17
GO:0043648	0.004288	K	dicarboxylic acid metabolic process	57
GO:0006090	0.005195	K	pyruvate metabolic process	16
GO:0006818	0.005306	K	hydrogen transport	62
GO:0006769	0.006199	K	nicotinamide metabolic process	72
GO:0030866	0.006199	K	cortical actin cytoskeleton organization	49
GO:0010324	0.006799	K	membrane invagination	29
GO:0006897	0.006799	K	Endocytosis	26
GO:0000041	0.007807	K	transition metal ion transport	43
GO:0035303	0.008022	K	regulation of dephosphorylation	37
GO:0019439	0.008022	K	aromatic compound catabolic process	40
GO:0042219	0.008108	K	cellular modified amino acid catabolic process	27
GO:0009132	0.008108	K	nucleoside diphosphate metabolic process	45
GO:0007031	0.009766	K	peroxisome organization	31
GO:0043933	0.010447	K	macromolecular complex subunit organization	54
GO:0009066	0.012164	K	aspartate family amino acid metabolic process	59
GO:0006383	0.01504	K	transcription from RNA polymerase III promoter	6
GO:0019748	0.017423	K	secondary metabolic process	68
GO:0034637	0.019031	K	cellular carbohydrate biosynthetic process	34
GO:0007264	0.019711	K	small GTPase mediated signal transduction	8
GO:0012501	0.020857	K	programmed cell death	53
GO:0009072	0.020913	K	aromatic amino acid family metabolic process	70
GO:0009451	0.02109	K	RNA modification	9
GO:0009070	0.021788	K	serine family amino acid biosynthetic process	44
GO:0031399	0.023021	K	regulation of protein modification process	15
GO:0006563	0.024318	K	L-serine metabolic process	67
GO:0045454	0.024835	K	cell redox homeostasis	42
GO:0042558	0.026934	K	pteridine-containing compound metabolic process	20
GO:0006911	0.02739	K	phagocytosis, engulfment	32
GO:0046165	0.027416	K	alcohol biosynthetic process	56
GO:0006869	0.029887	K	lipid transport	30
GO:0006790	0.034939	K	sulfur compound metabolic process	4
GO:0006575	0.038384	K	cellular modified amino acid metabolic process	51
GO:0009116	0.043901	K	nucleoside metabolic process	1
GO:0045930	0.04473	K	negative regulation of mitotic cell cycle	66
GO:0006260	0.046599	K	DNA replication	35
GO:0016265	0.047523	K	obsolete death	11
GO:0009165	8.89E-08	F	nucleotide biosynthetic process	

Submitted GO IDs	Submitted p- values	Significance	GO terms	GO-Module IDs
GO:0051186	1.4E-06	F	cofactor metabolic process	
GO:0006163	8.16E-06	F	purine nucleotide metabolic process	
GO:0006164	2.12E-05	F	purine nucleotide biosynthetic process	
GO:0016054	2.88E-05	F	organic acid catabolic process	
GO:0051187	4.32E-05	F	cofactor catabolic process	
GO:0009161	4.71E-05	F	ribonucleoside monophosphate metabolic process	
GO:0009127	4.88E-05	F	purine nucleoside monophosphate biosynthetic process	
GO:0009126	4.88E-05	F	purine nucleoside monophosphate metabolic process	
GO:0009167	4.88E-05	F	purine ribonucleoside monophosphate metabolic process	
GO:0016310	0.000122	F	Phosphorylation	
GO:0006793	0.000231	F	phosphorus metabolic process	
GO:0006796	0.000231	F	phosphate-containing compound metabolic process	
GO:0009142	0.000439	F	nucleoside triphosphate biosynthetic process	
GO:0009141	0.000502	F	nucleoside triphosphate metabolic process	
GO:0008104	0.000507	F	protein localization	
GO:0034613	0.000519	F	cellular protein localization	
GO:0009144	0.000625	F	purine nucleoside triphosphate metabolic process	
GO:0009145	0.000732	F	purine nucleoside triphosphate biosynthetic process	
GO:0006396	0.000973	F	RNA processing	
GO:0016053	0.001064	F	organic acid biosynthetic process	
GO:0016042	0.002482	F	lipid catabolic process	
GO:0016052	0.004105	F	carbohydrate catabolic process	
GO:0009112	0.004288	F	nucleobase metabolic process	
GO:0030865	0.006199	F	cortical cytoskeleton organization	
GO:0009820	0.006199	F	alkaloid metabolic process	
GO:0033365	0.006623	F	protein localization to organelle	
GO:0009123	0.007508	F	nucleoside monophosphate metabolic process	
GO:0043603	0.007807	F	cellular amide metabolic process	
GO:0016192	0.010133	F	vesicle-mediated transport	
GO:0009124	0.011756	F	nucleoside monophosphate biosynthetic process	
GO:0070585	0.018417	F	protein localization to mitochondrion	
GO:0018130	0.020747	F	heterocycle biosynthetic process	
GO:0006767	0.021456	F	water-soluble vitamin metabolic process	
GO:0006221	0.021456	F	pyrimidine nucleotide biosynthetic process	
GO:0061024	0.024498	F	membrane organization	

Submitted GO IDs	Submitted p- values	Significance	GO terms	GO-Module IDs
GO:0070727	0.024543	F	cellular macromolecule localization	
GO:0015985	0.025212	F	energy coupled proton transport, down electrochemical gradient	
GO:0019725	0.026906	F	cellular homeostasis	
GO:0006220	0.034816	F	pyrimidine nucleotide metabolic process	
GO:0008219	0.042523	F	cell death	

C

Submitted GO IDs	Submitted p- values	Significance	GO terms	GO-Module IDs
GO:0000902	0.000678	T	cell morphogenesis	13
GO:0048858	0.005629	T	cell projection morphogenesis	10;13
GO:0032990	0.006748	T	cell part morphogenesis	13
GO:0008045	0.00962	T	motor neuron axon guidance	8
GO:0048812	0.012559	T	neuron projection morphogenesis	10;13
GO:0031175	0.012761	T	neuron projection development	10
GO:0000904	0.016314	T	cell morphogenesis involved in differentiation	13
GO:0032989	0.000602	K	cellular component morphogenesis	13
GO:0030030	0.000706	K	cell projection organization	10
GO:0007409	0.00213	K	Axonogenesis	5
GO:0007411	0.002213	K	axon guidance	8
GO:0007507	0.011368	K	heart development	1
GO:0048667	0.012965	K	cell morphogenesis involved in neuron differentiation	7
GO:0006928	0.016802	K	movement of cell or subcellular component	9
GO:0030182	0.020007	K	neuron differentiation	6
GO:0048666	0.029516	K	neuron development	4
GO:0022604	0.046909	K	regulation of cell morphogenesis	3
GO:0048534	0.057172	K	hematopoietic or lymphoid organ development	2
GO:0002520	0.057172	K	immune system development	11
GO:0016055	0.083875	K	Wnt signaling pathway	12
GO:0006378	0.091222	K	mRNA polyadenylation	14

Appendix F

Supplemental Table 4: GO terms found by WEBGestalt using overrepresentation enrichment analysis (ORA) with their corresponding p-value (A), ORA GO term overlap with DAVID 6.7 showing GO IDs and name of biological process (B), and number of genes found in overlapping GO terms for ORA, DAVID 6.7, and number of genes overlapping between ORA and DAVID 6.7 (C).

A

Overrepresentation Enrichment Analysis (ORA)

Selection		Time		Interaction	
GO ID	**P-value**	**GO ID**	**P-value**	**GO ID**	**P-value**
GO:0006790	4.55E-05	GO:0044282	9.71E-04	GO:0031175	2.54E-04
GO:0055114	3.13E-04	GO:0055114	5.14E-05	GO:0048812	1.74E-04
GO:0006730	2.76E-05	GO:1901564	2.56E-04	GO:0030182	6.68E-05
GO:0007599	4.64E-04	GO:0016054	1.84E-04	GO:0022008	3.12E-04
GO:0006749	3.21E-04	GO:0072329	1.17E-04	GO:0007399	1.49E-04
GO:0098754	6.61E-04	GO:0007005	4.54E-06	GO:0048699	4.59E-06
GO:0050817	4.64E-04	GO:0032543	5.84E-07	GO:0032989	2.45E-04
GO:0098869	5.3E-04	GO:0009062	8.5E-04	GO:0030030	1.33E-05
GO:0006575	3.59E-05	GO:0043603	2.38E-04	GO:0048858	1.76E-04
GO:1990748	5.3E-04	GO:0046395	1.84E-04	GO:0032990	2.12E-04

B

ORA GO Term Overlap with DAVID 6.7

Selection		Time		Interaction	
GO ID	**Name**	**GO ID**	**Name**	**GO ID**	**Name**
GO:0055114	Oxidation-reduction process	GO:0055114	Oxidation-reduction process	GO:0030030	Cell projection organization
		GO:0046395	Carboxylic acid catabolic process	GO:0030182	Neuron differentiation

C

		Number of Genes		
	GO ID	**ORA**	**DAVID 6.7**	**Overlap**
Selection	GO:0055114	8	5	5
Time	GO:0055114	19	282	14
	GO:0046395	6	27	3
Interaction	GO:0030030	17	10	8
	GO:0030182	17	8	6

Appendix G

Supplemental Figure 2: Additional genes that possibly show delayed expression in desiccation selected populations versus fed controls. Dotted lines have been included to better visualize trends over time, although linear connection between points cannot be assumed. To emphasize the expression of the unstressed fed control and the desiccation selected lines, gene expression of starvation selected controls have been removed.

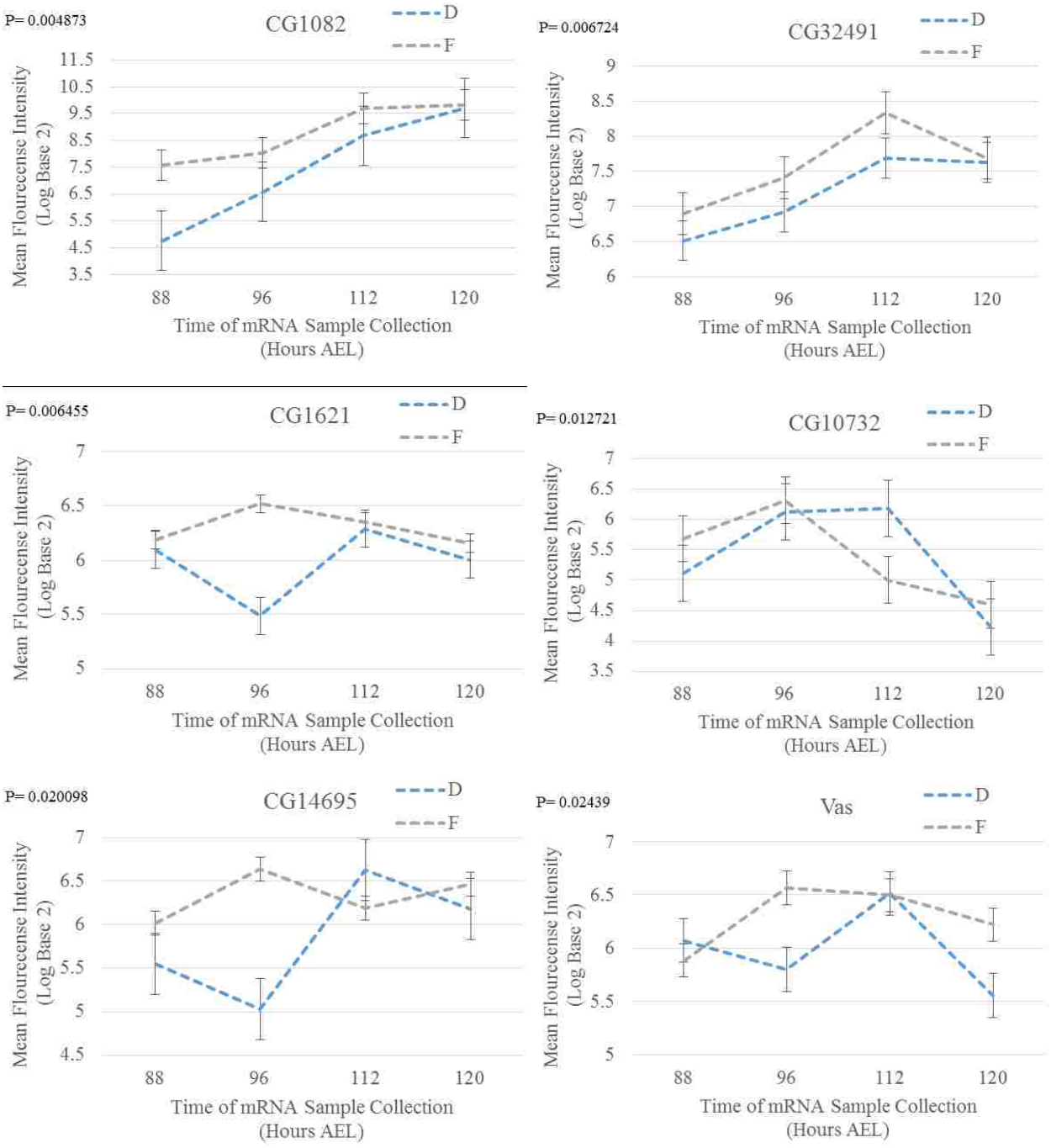

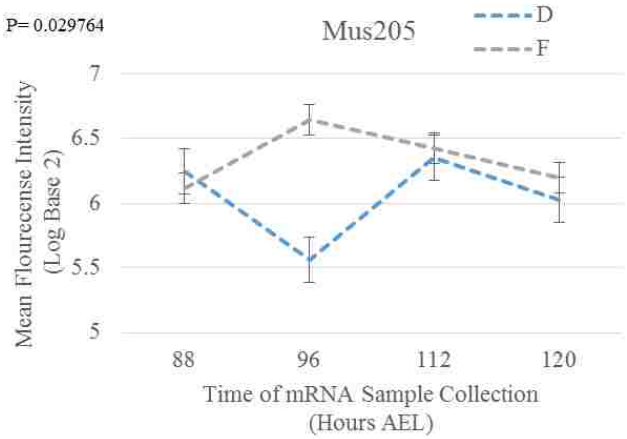
P= 0.029764
Mus205
D
F
Mean Flourecense Intensity (Log Base 2)
7
6.5
6
5.5
5
88
96
112
120
Time of mRNA Sample Collection (Hours AEL)

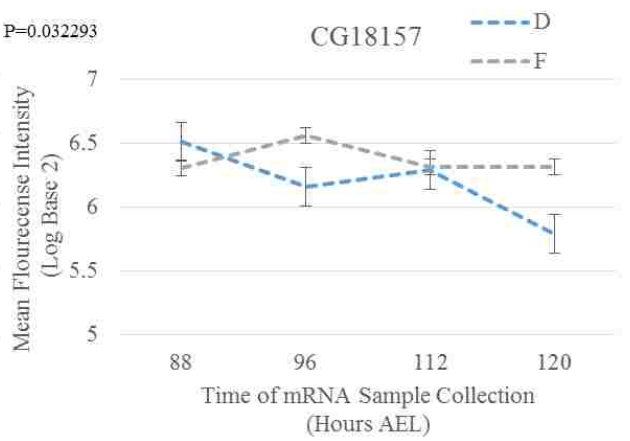
P=0.032293
CG18157
D
F
Mean Flourecense Intensity (Log Base 2)
7
6.5
6
5.5
5
88
96
112
120
Time of mRNA Sample Collection (Hours AEL)

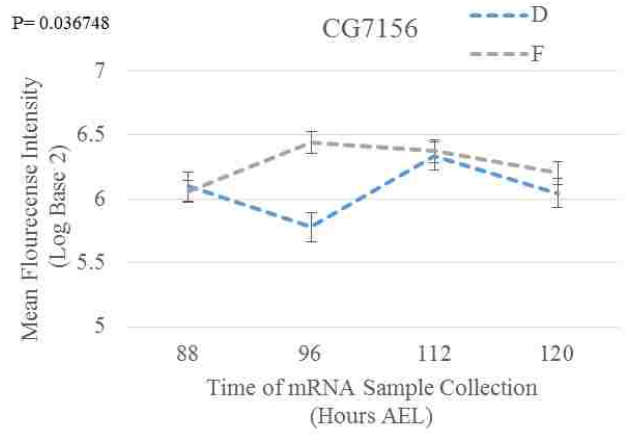
P= 0.036748
CG7156
D
F
Mean Flourecense Intensity (Log Base 2)
7
6.5
6
5.5
5
88
96
112
120
Time of mRNA Sample Collection (Hours AEL)

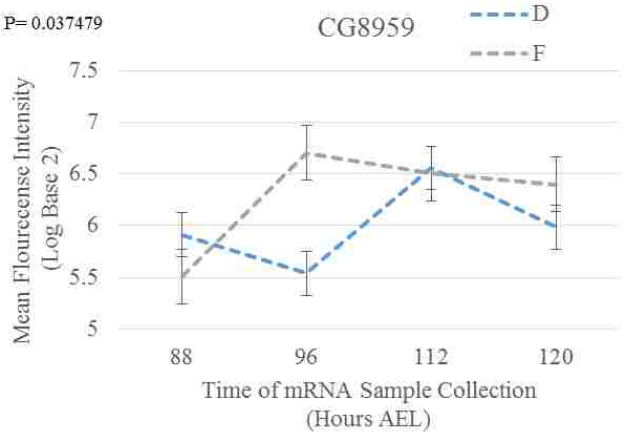
P= 0.037479
CG8959
D
F
Mean Flourecense Intensity (Log Base 2)
7.5
7
6.5
6
5.5
5
88
96
112
120
Time of mRNA Sample Collection (Hours AEL)

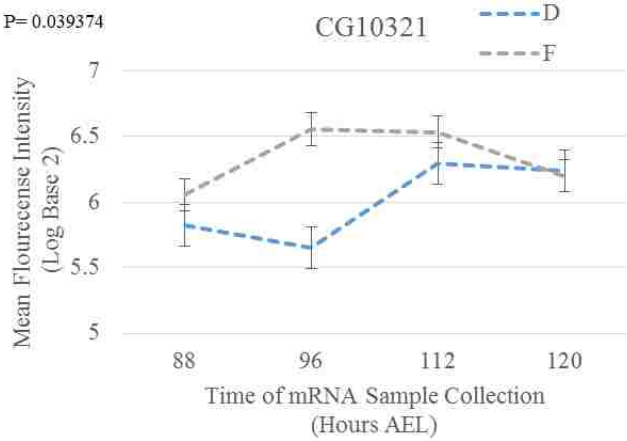
P= 0.039374
CG10321
D
F
Mean Flourecense Intensity (Log Base 2)
7
6.5
6
5.5
5
88
96
112
120
Time of mRNA Sample Collection (Hours AEL)

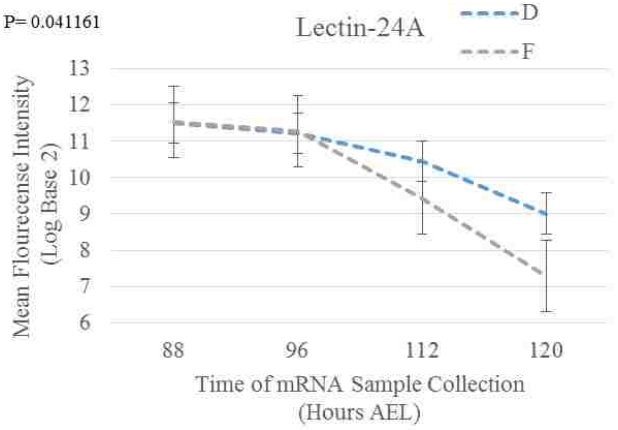
P= 0.041161
Lectin-24A
D
F
Mean Flourecense Intensity (Log Base 2)
13
12
11
10
9
8
7
6
88
96
112
120
Time of mRNA Sample Collection (Hours AEL)

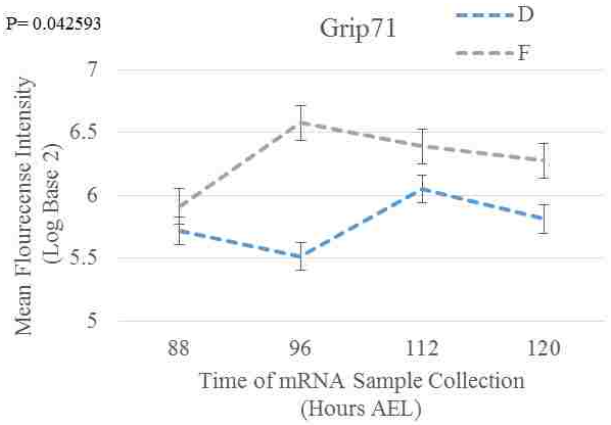
P= 0.042593
Grip71
D
F
Mean Flourecense Intensity (Log Base 2)
7
6.5
6
5.5
5
88
96
112
120
Time of mRNA Sample Collection (Hours AEL)

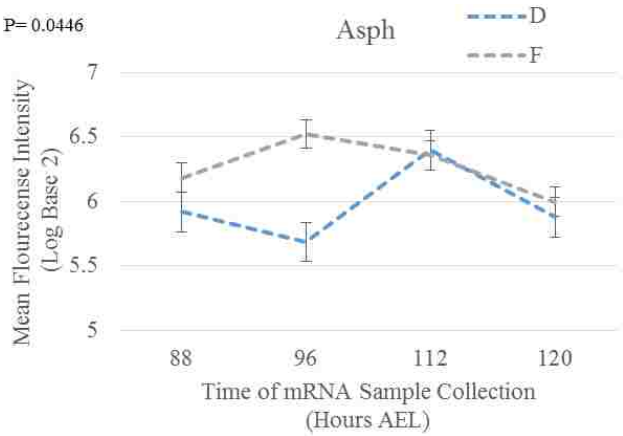
P= 0.0446
Asph
D
F
Mean Flourecense Intensity (Log Base 2)
7
6.5
6
5.5
5
88
96
112
120
Time of mRNA Sample Collection (Hours AEL)

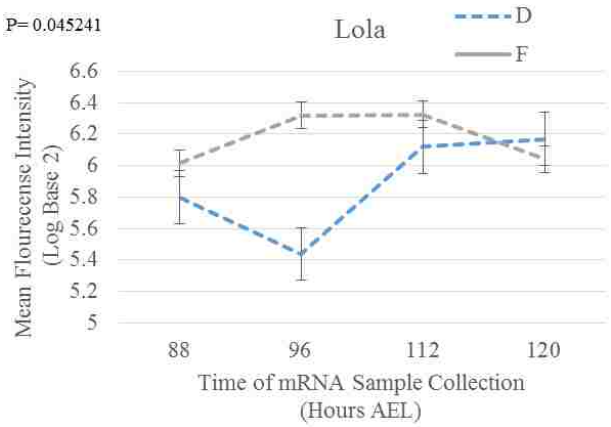
P= 0.045241
Lola
D
F
Mean Flourecense Intensity (Log Base 2)
6.6
6.4
6.2
6
5.8
5.6
5.4
5.2
5
88
96
112
120
Time of mRNA Sample Collection (Hours AEL)

Supplemental Figure 3: Plotted mean fluorescence intensity for each differentially expressed gene with respect to interaction.

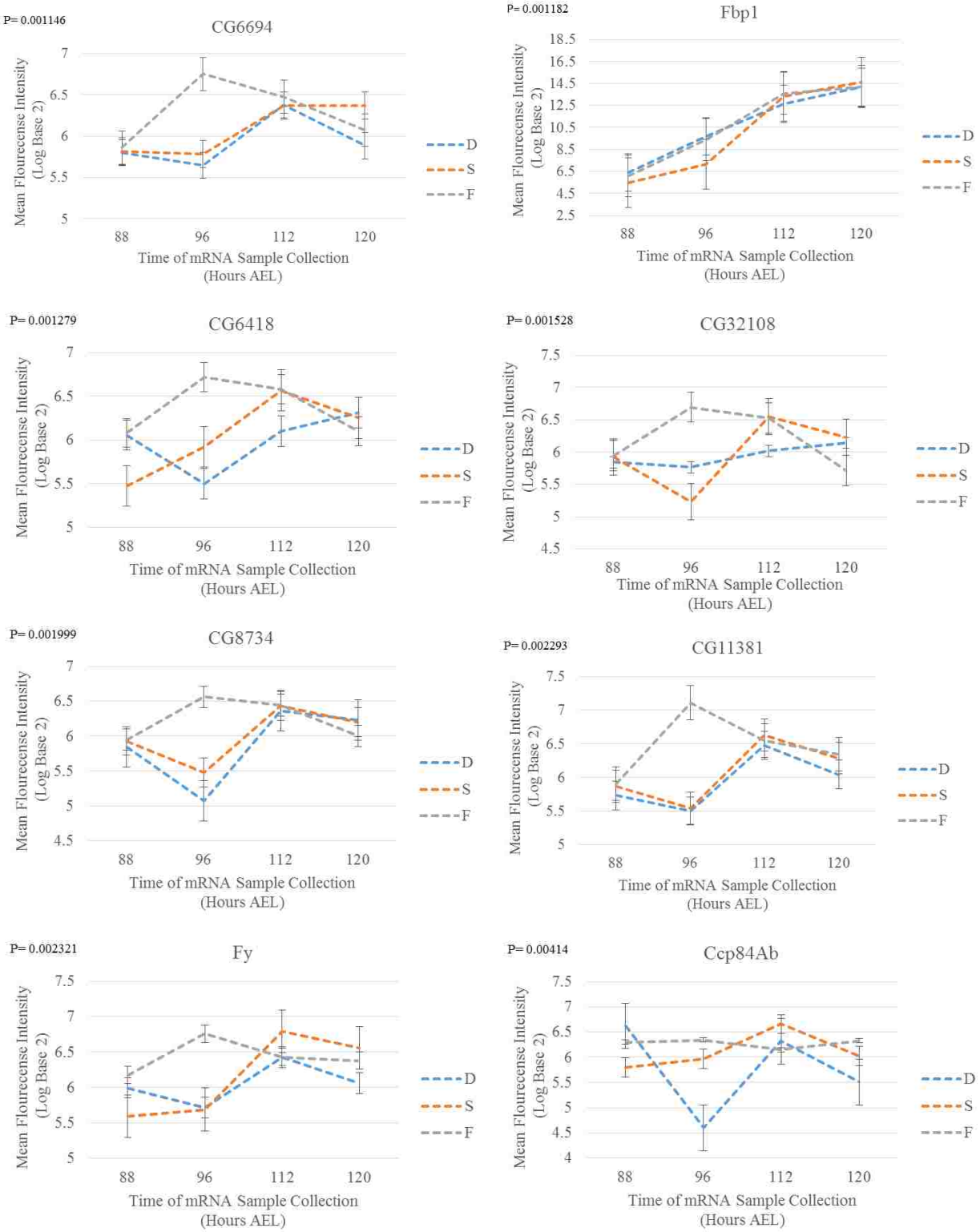

P= 0.004616

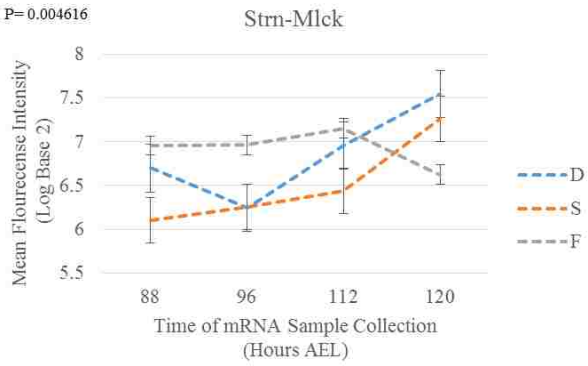

P= 0.004873

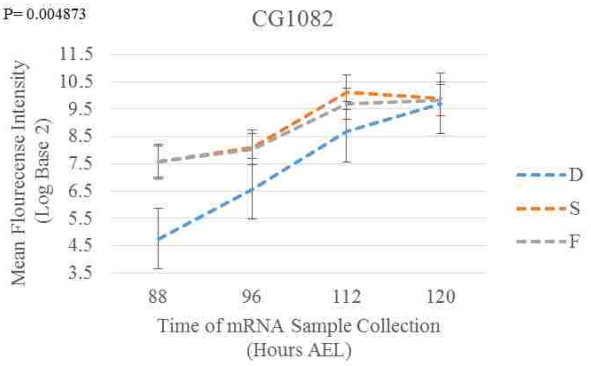

P= 0.012696

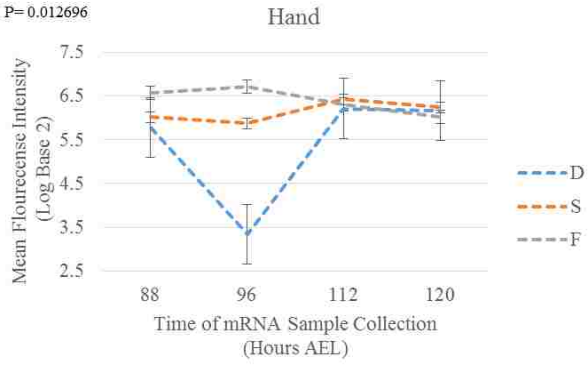

P= 0.01385

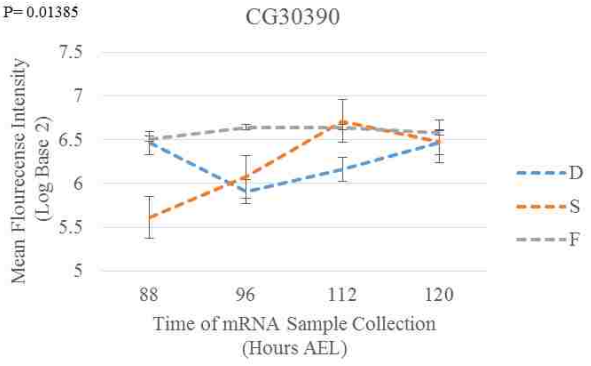

P= 0.015005

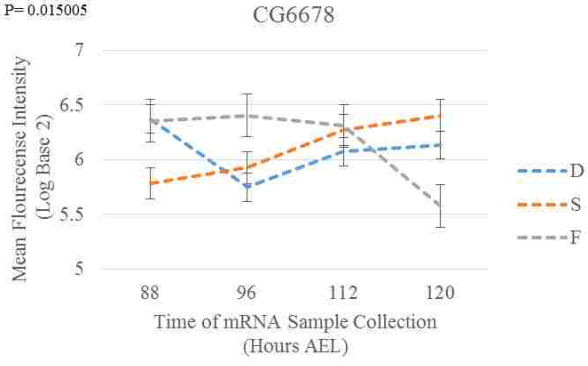

P= 0.016159

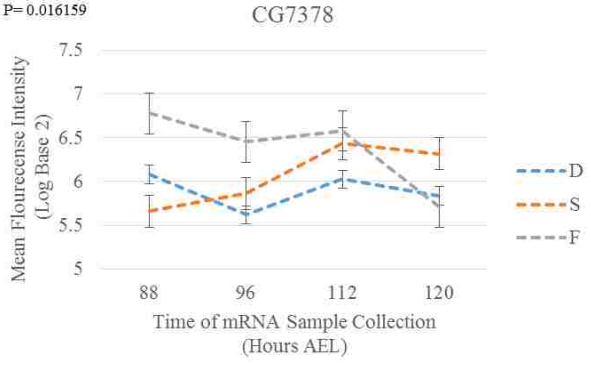

P= 0.017313

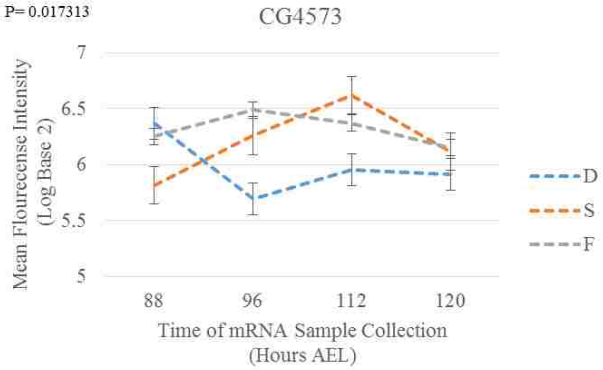

P= 0.006455

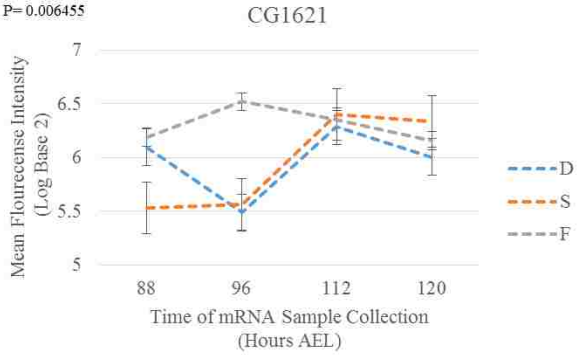

P= 0.006724

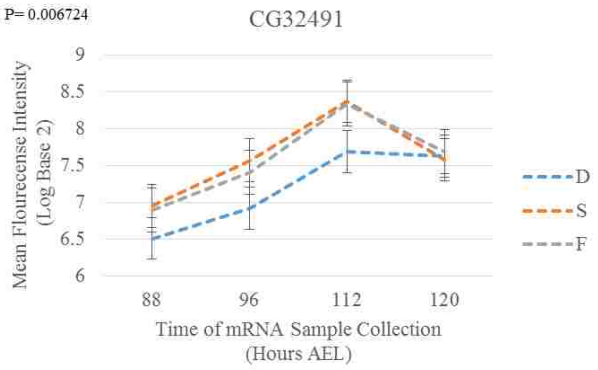

P= 0.007434

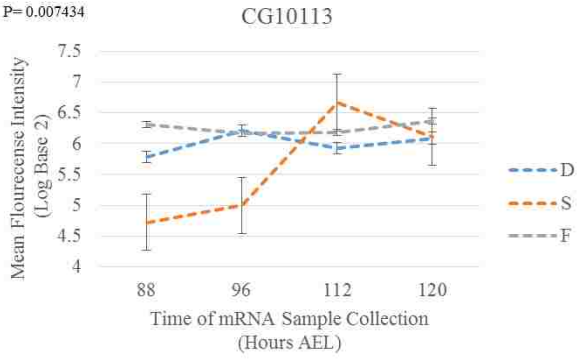

P= 0.007478

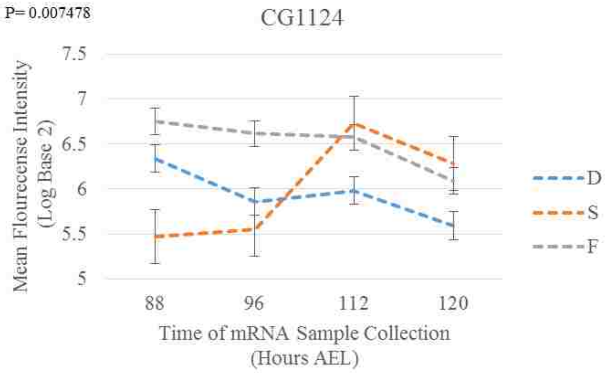

P= 0.012538

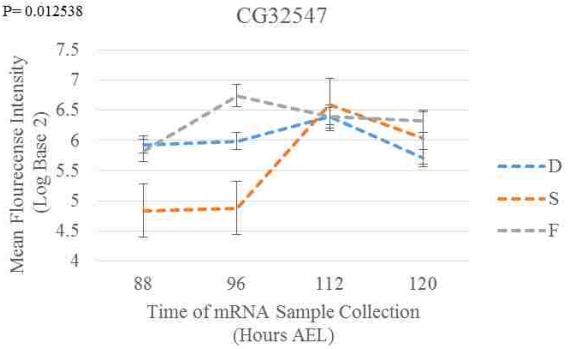

P= 0.012721

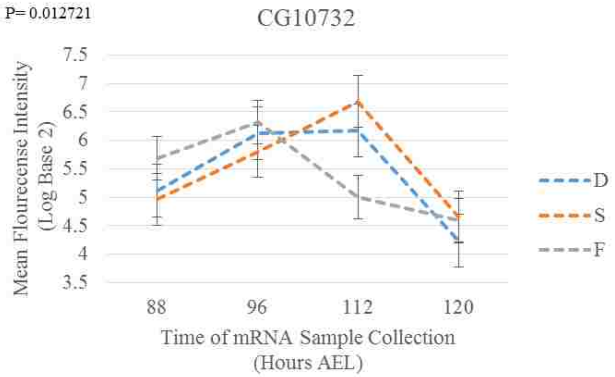

P= 0.013437

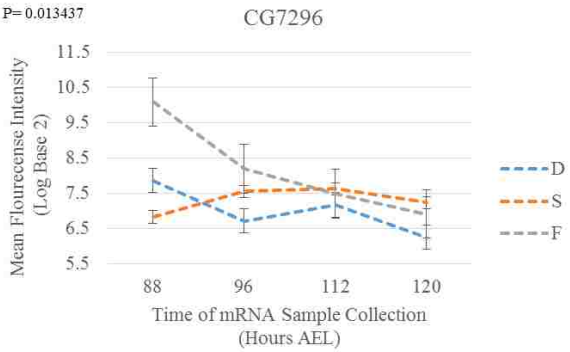

P= 0.013807

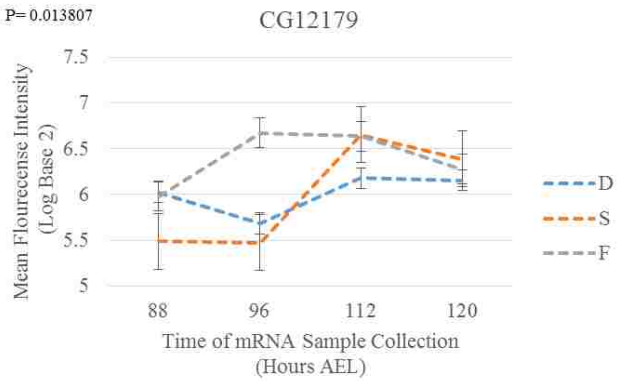

P= 0.014982

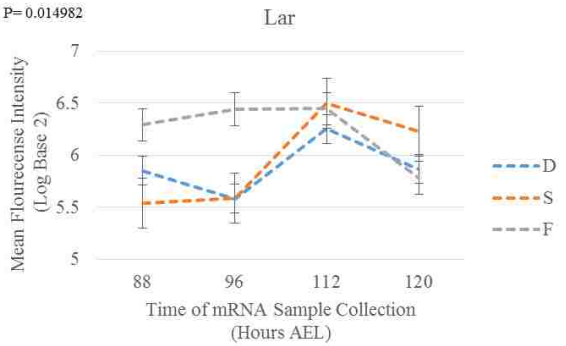

P= 0.009879

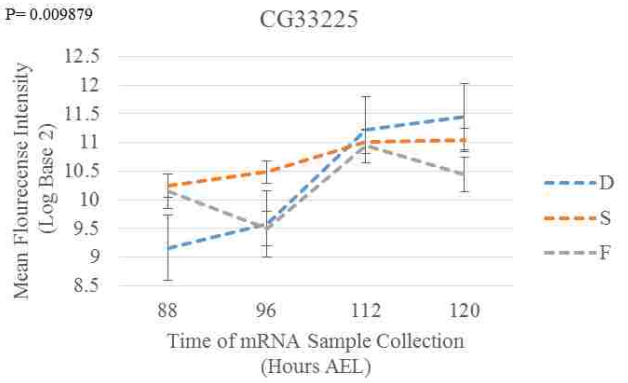

P= 0.01006

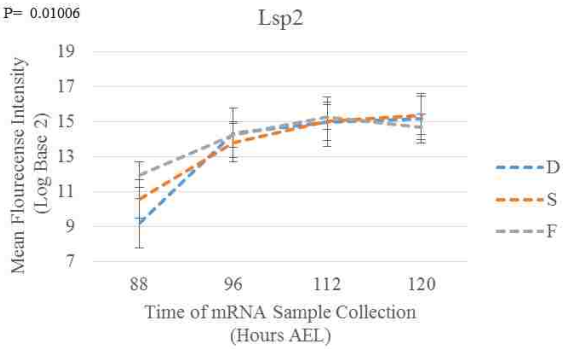

P= 0.015033

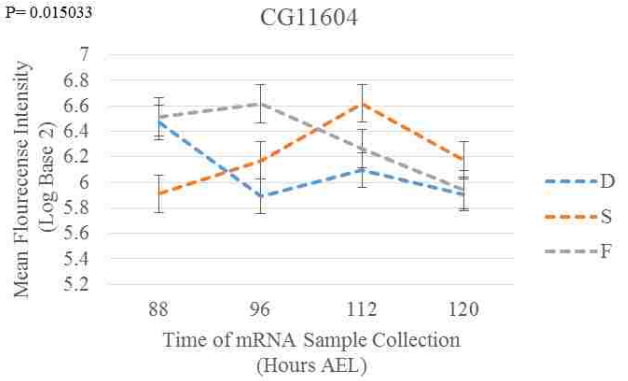

P= 0.010829

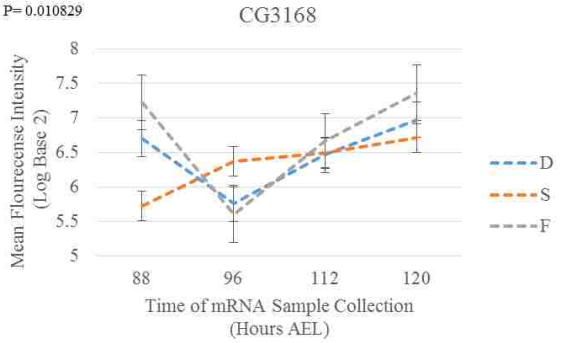

P= 0.015376

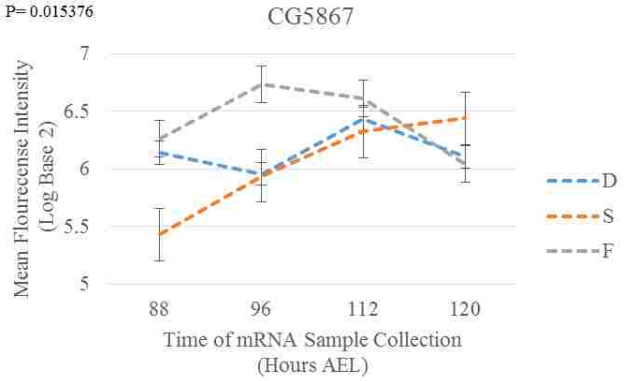

P= 0.011261

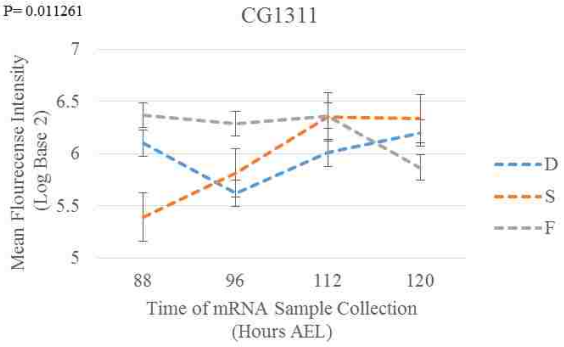

P= 0.015467

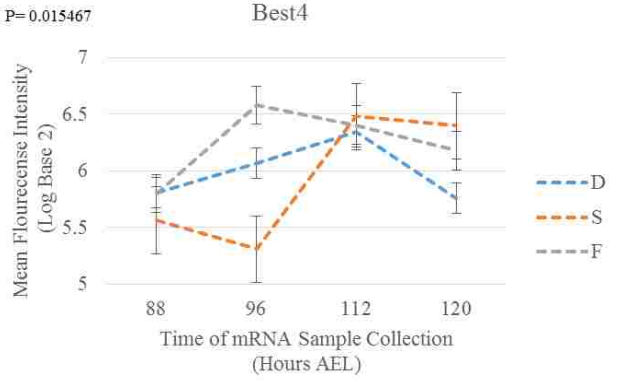

P= 0.011327

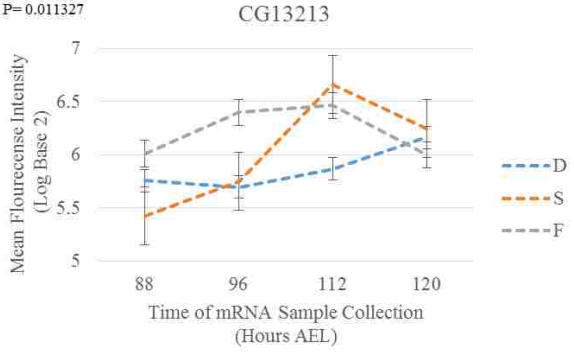

P= 0.015534

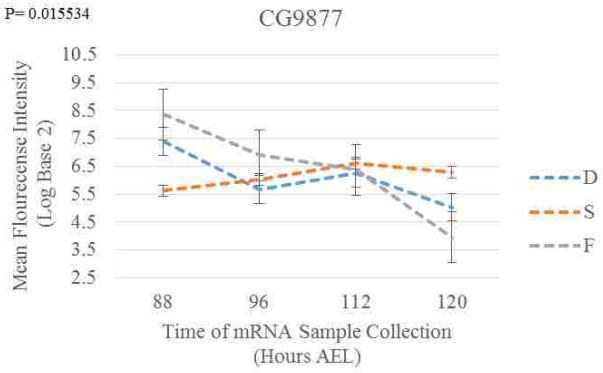

P= 0.011757

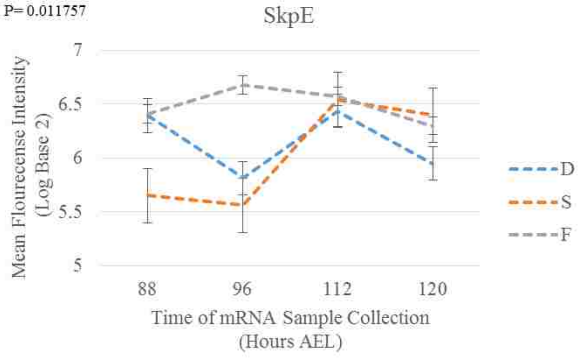

P= 0.015545

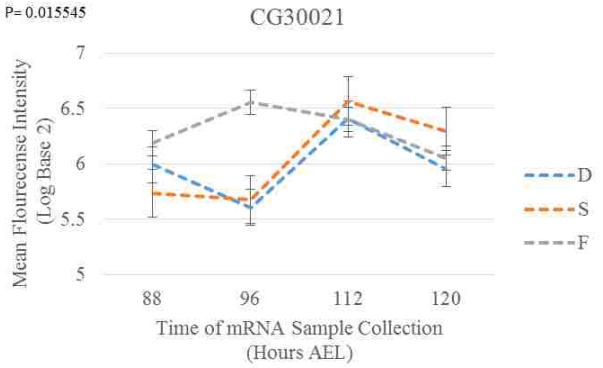

P= 0.018949

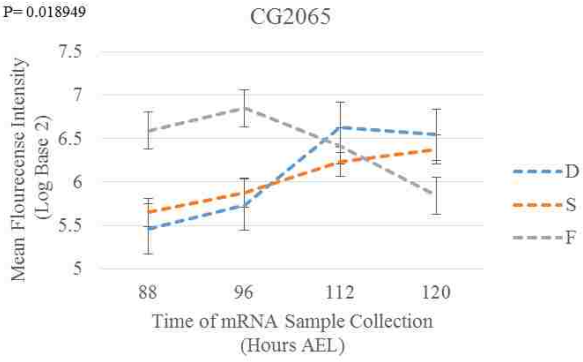

P= 0.021447

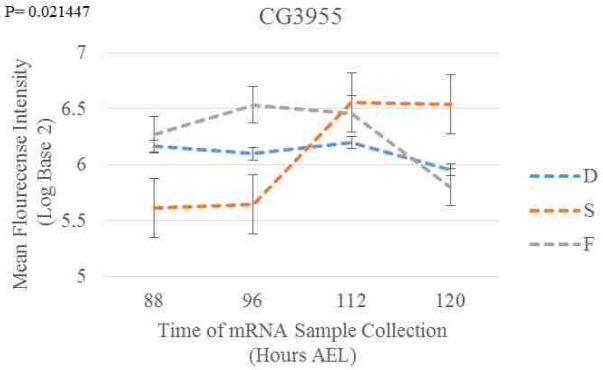

P= 0.018408

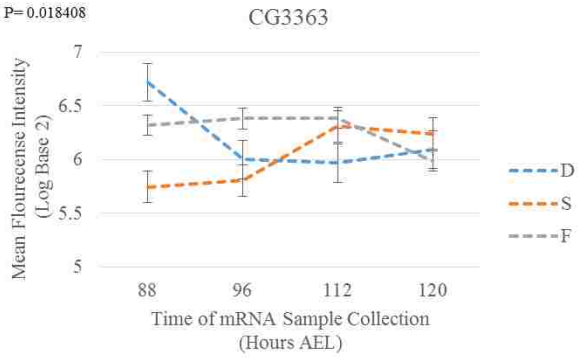

P= 0.021409

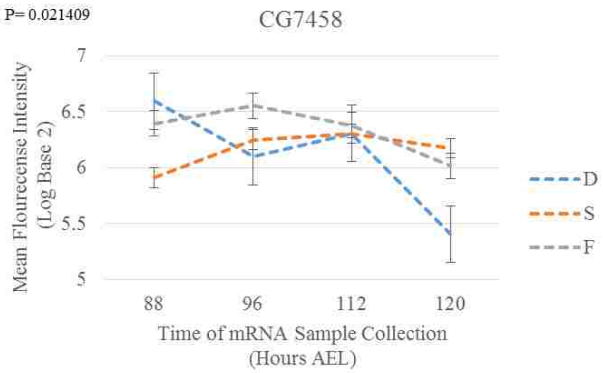

P= 0.018284

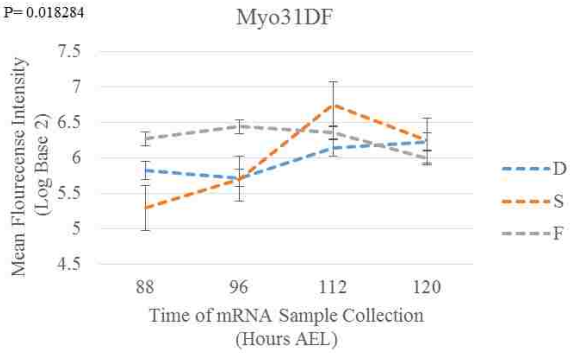

P= 0.021188

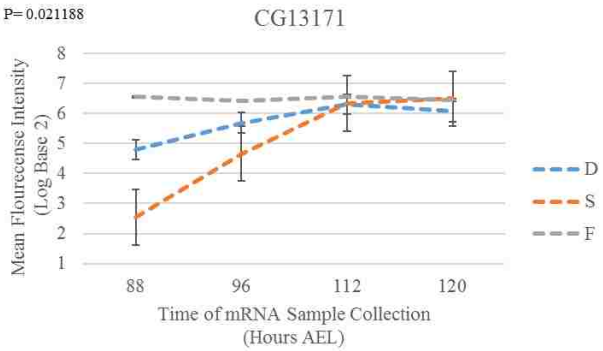

P= 0.018028

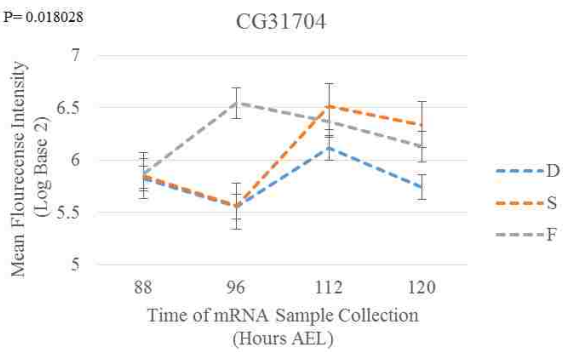

P= 0.021168

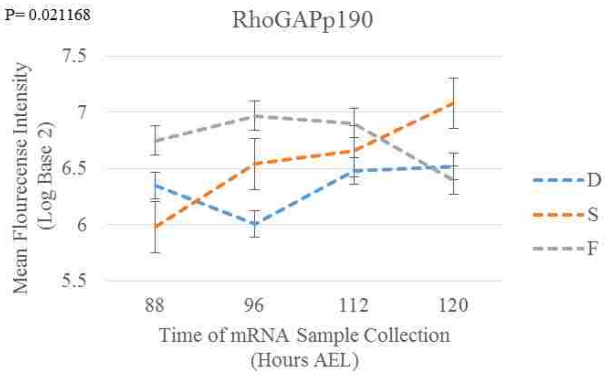

P= 0.01702

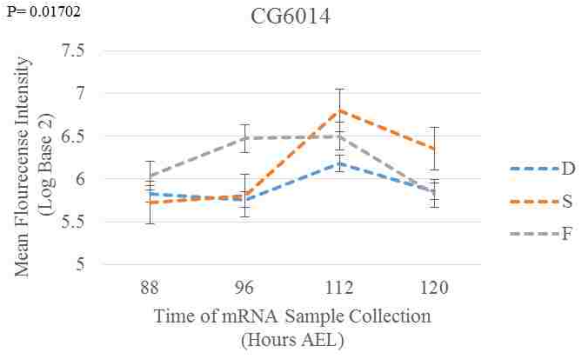

P= 0.020848

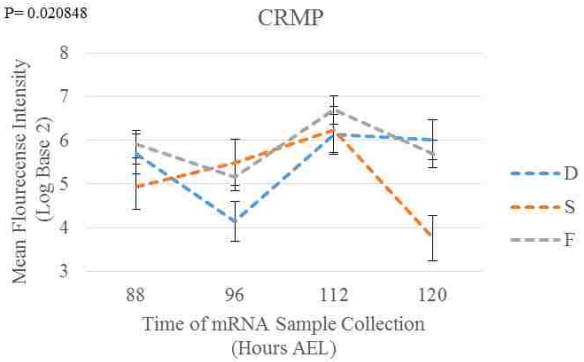

P= 0.016902

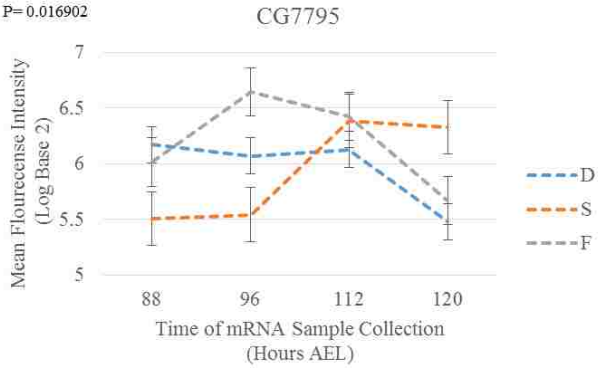

P= 0.020098

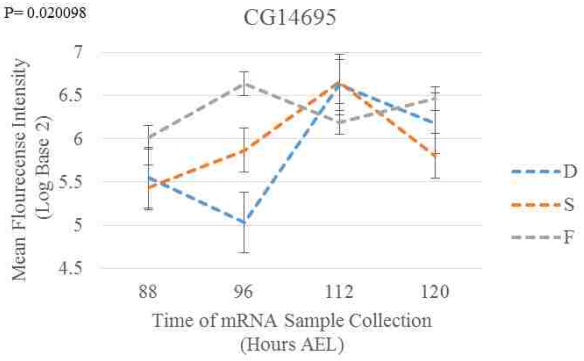

P= 0.016387

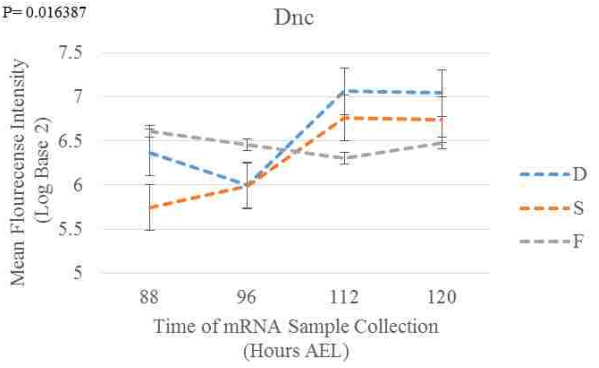

P= 0.019995

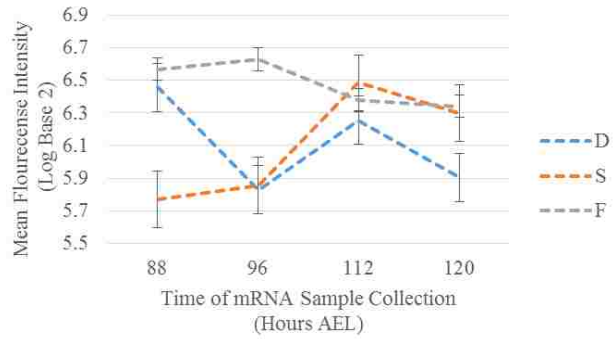

P= 0.01617

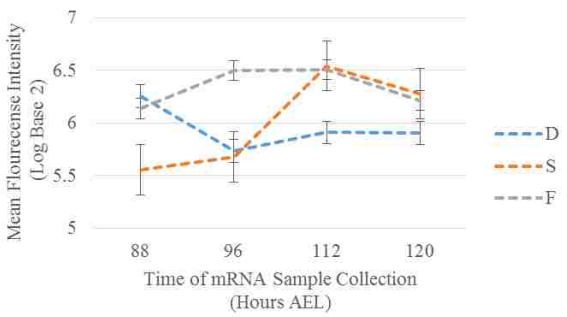

P= 0.019878

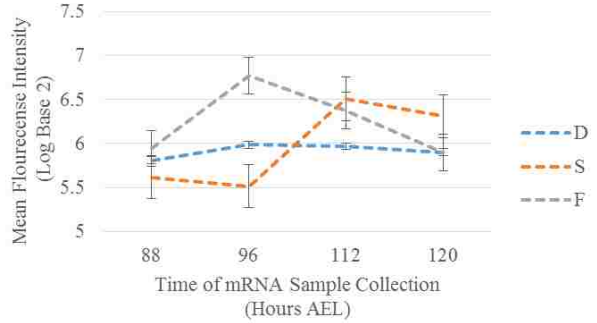

P= 0.016118

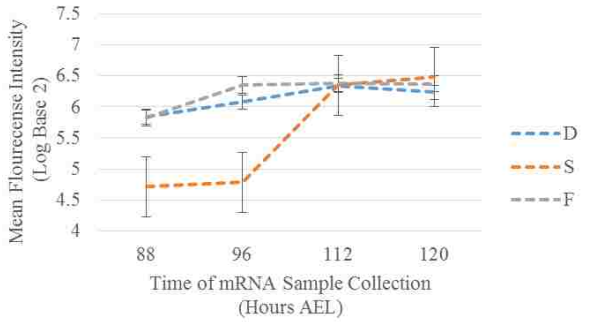

P= 0.019537

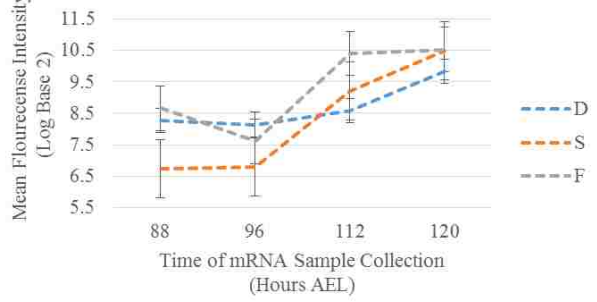

P=0.01906

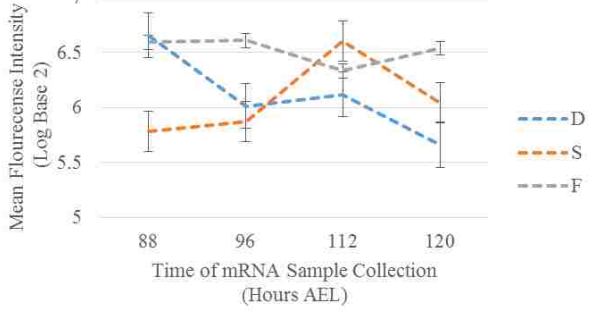

P= 0.021688

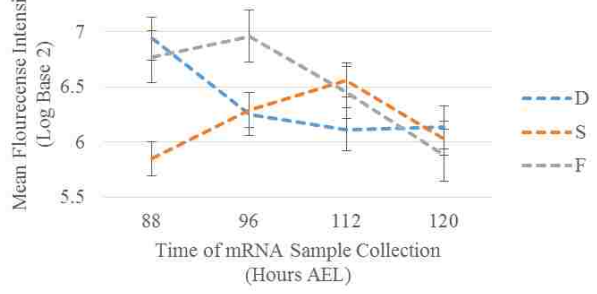

P= 0.02224

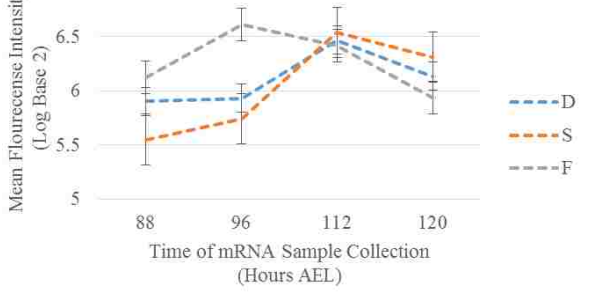

P= 0.024264

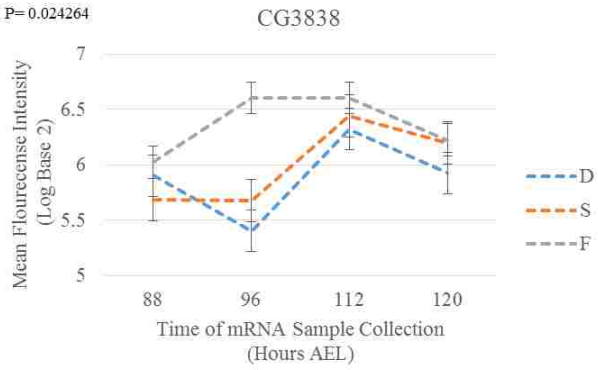

P= 0.027263

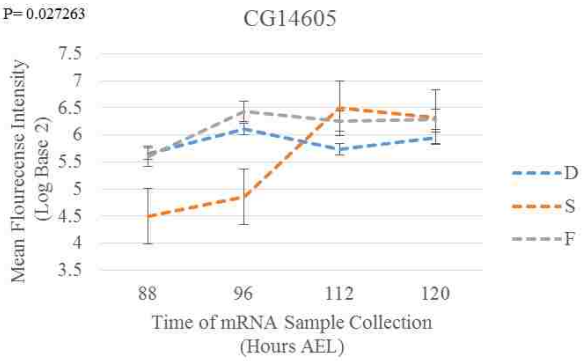

P= 0.028042

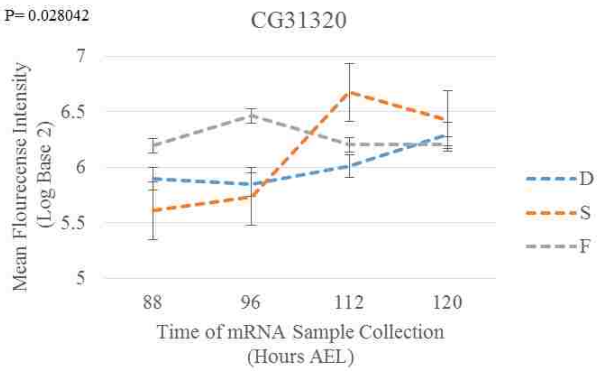

P= 0.028224

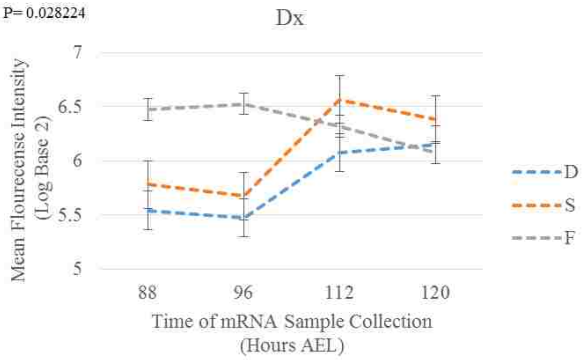

P= 0.031482

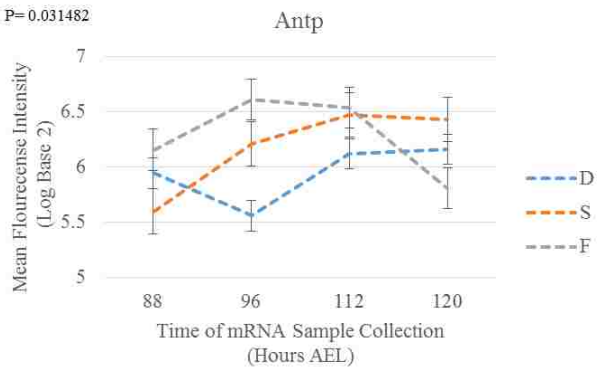

P=0.032293

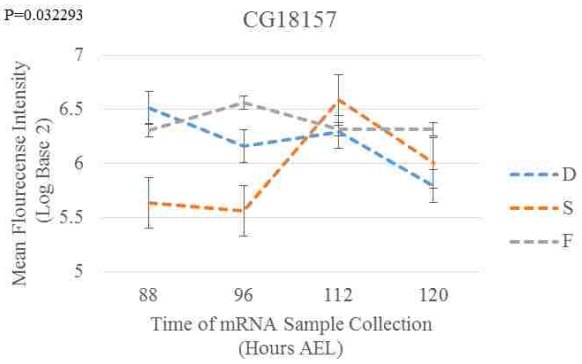

P= 0.024377

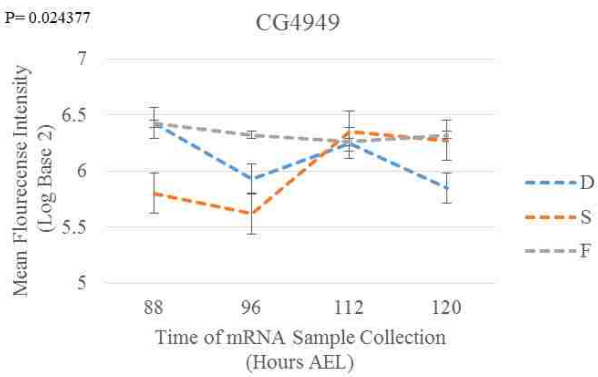

P= 0.028241

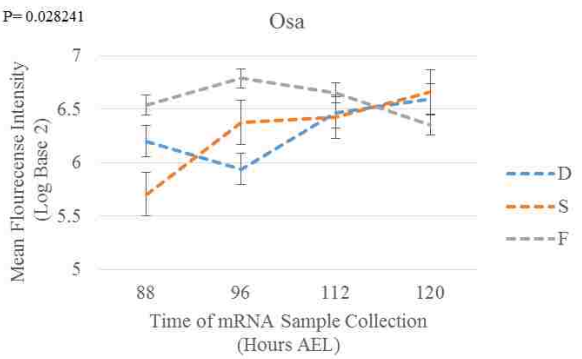

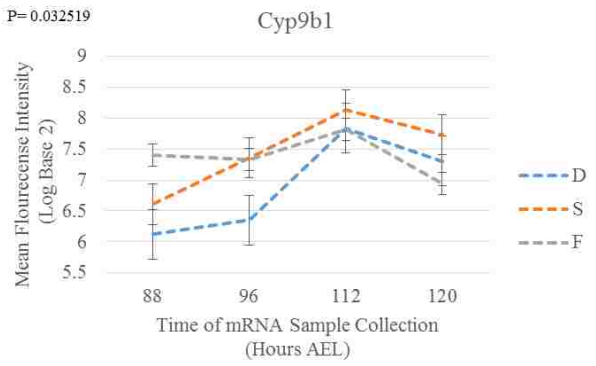
P= 0.032519
Cyp9b1
Mean Flourecense Intensity (Log Base 2)
9
8.5
8
7.5
7
6.5
6
5.5
88
96
112
120
Time of mRNA Sample Collection (Hours AEL)
D
S
F

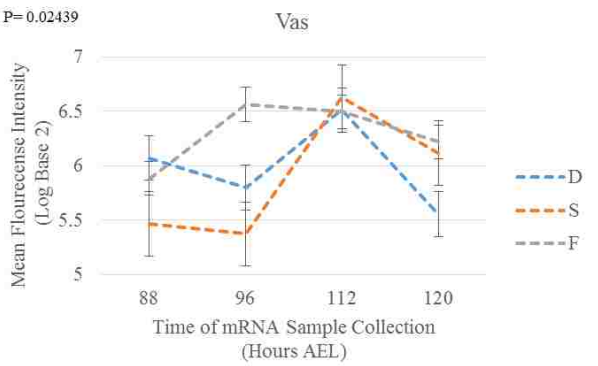
P= 0.02439
Vas
Mean Flourecense Intensity (Log Base 2)
7
6.5
6
5.5
5
88
96
112
120
Time of mRNA Sample Collection (Hours AEL)
D
S
F

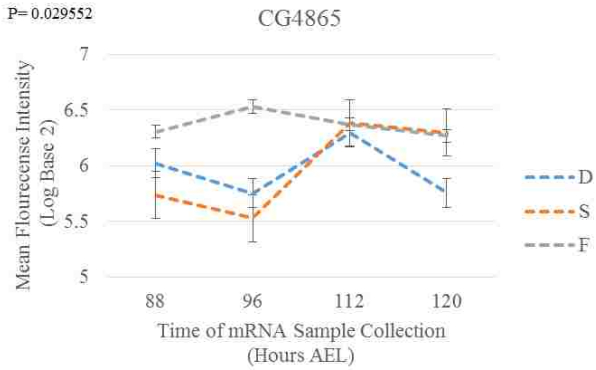
P= 0.029552
CG4865
Mean Flourecense Intensity (Log Base 2)
7
6.5
6
5.5
5
88
96
112
120
Time of mRNA Sample Collection (Hours AEL)
D
S
F

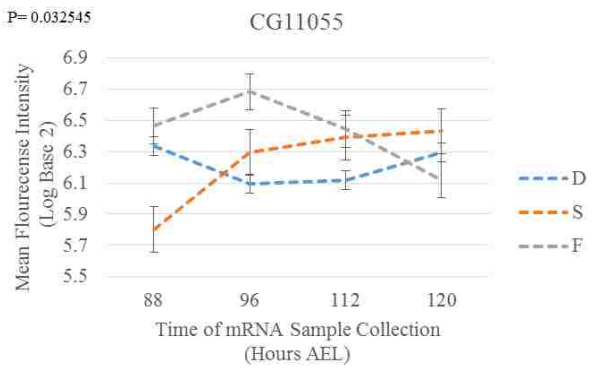
P= 0.032545
CG11055
Mean Flourecense Intensity (Log Base 2)
6.9
6.7
6.5
6.3
6.1
5.9
5.7
5.5
88
96
112
120
Time of mRNA Sample Collection (Hours AEL)
D
S
F

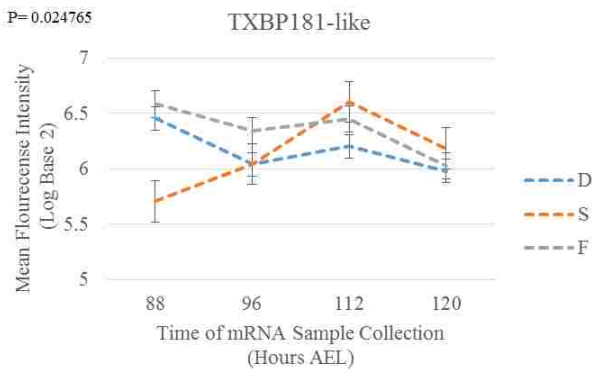
P= 0.024765
TXBP181-like
Mean Flourecense Intensity (Log Base 2)
7
6.5
6
5.5
5
88
96
112
120
Time of mRNA Sample Collection (Hours AEL)
D
S
F

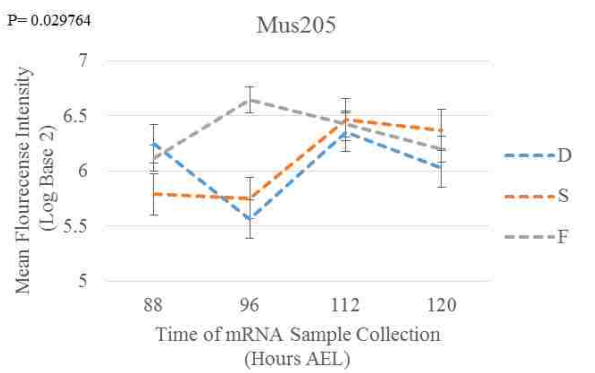
P= 0.029764
Mus205
Mean Flourecense Intensity (Log Base 2)
7
6.5
6
5.5
5
88
96
112
120
Time of mRNA Sample Collection (Hours AEL)
D
S
F

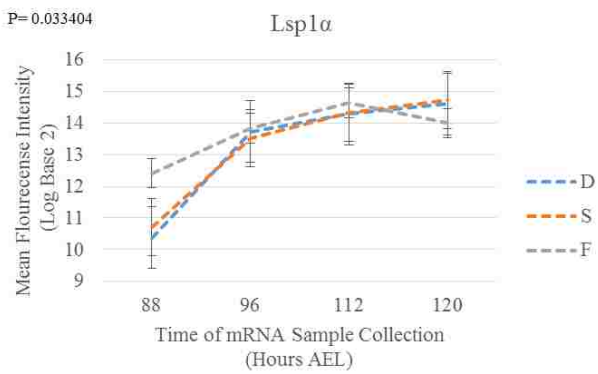
P= 0.033404
Lsp1α
Mean Flourecense Intensity (Log Base 2)
16
15
14
13
12
11
10
9
88
96
112
120
Time of mRNA Sample Collection (Hours AEL)
D
S
F

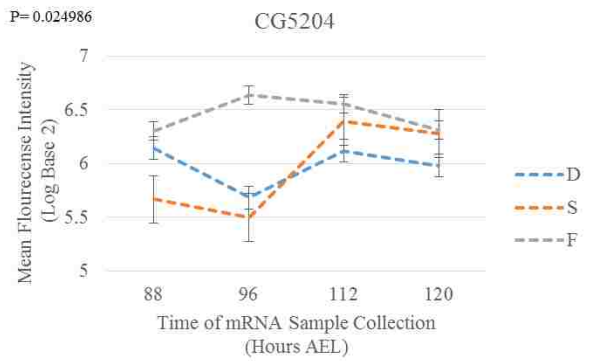
P= 0.024986
CG5204
Mean Flourecense Intensity (Log Base 2)
7
6.5
6
5.5
5
88
96
112
120
Time of mRNA Sample Collection (Hours AEL)
D
S
F

P= 0.02977

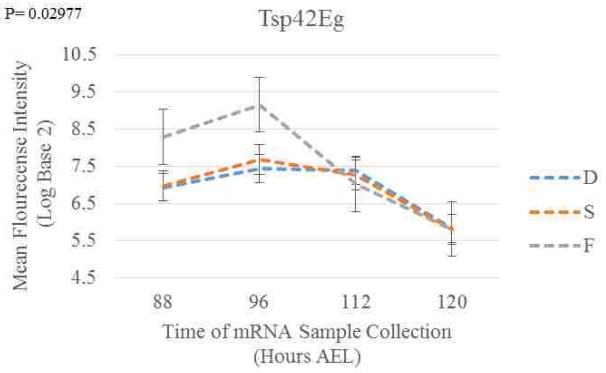

P= 0.033604

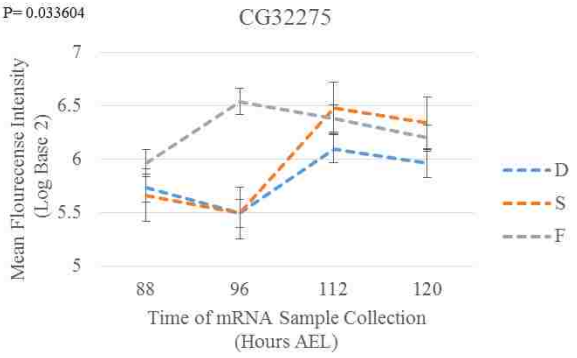

P= 0.025091

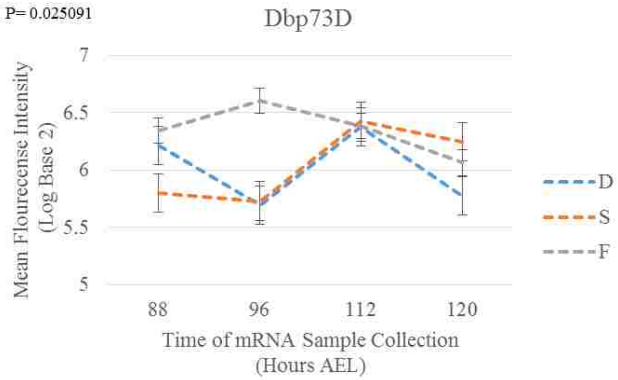

P= 0.030984

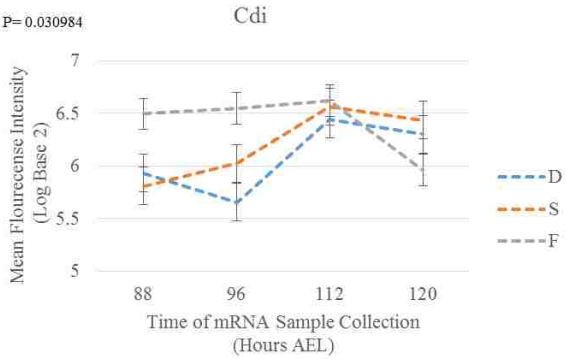

P= 0.031007

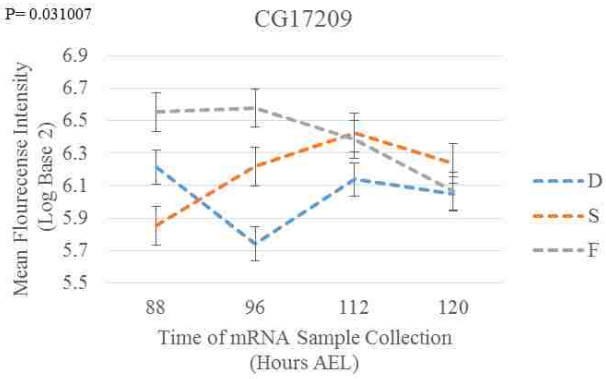

P= 0.025272

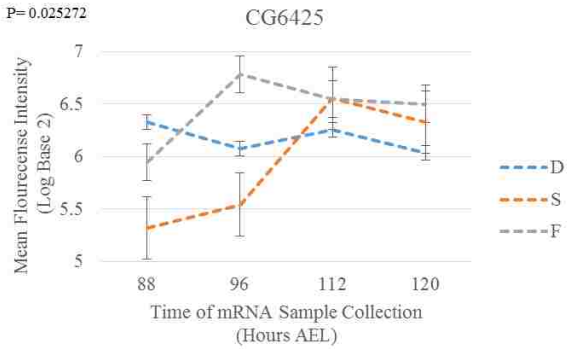

P= 0.034767

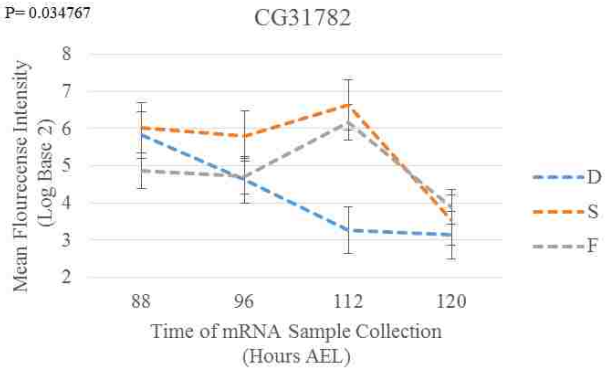

P= 0.02621

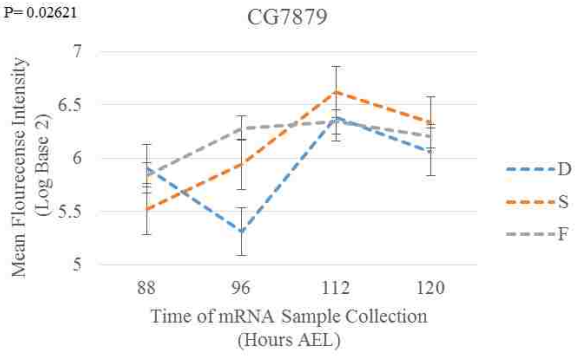

P= 0.031334

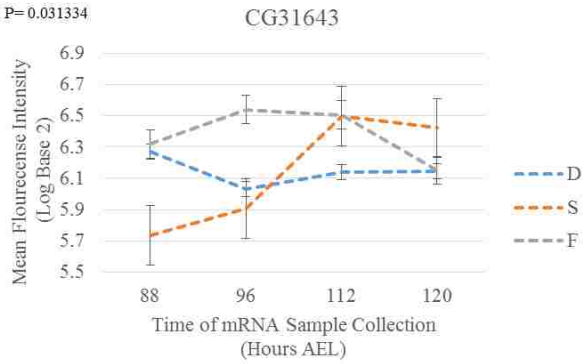

P= 0.035369

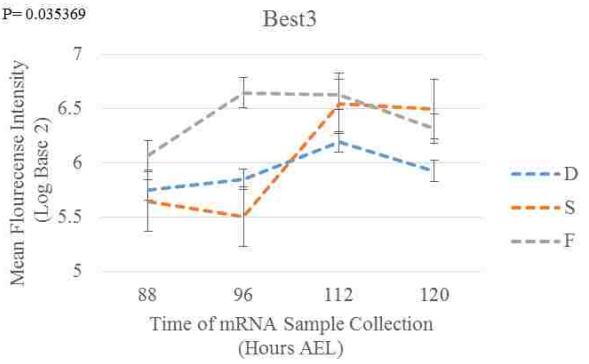

P= 0.034728

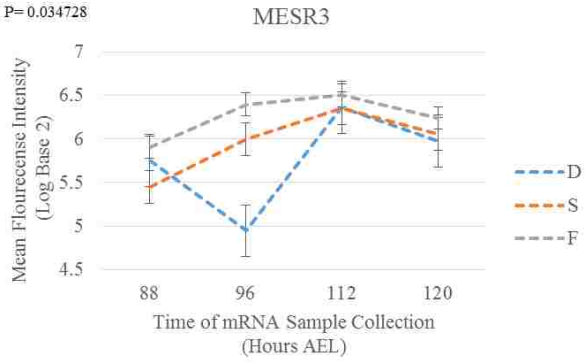

P= 0.03563

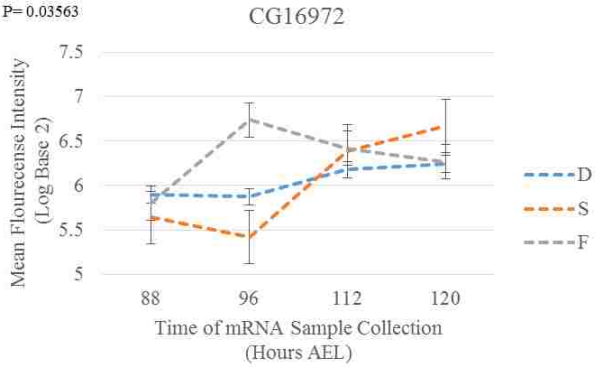

P= 0.035801

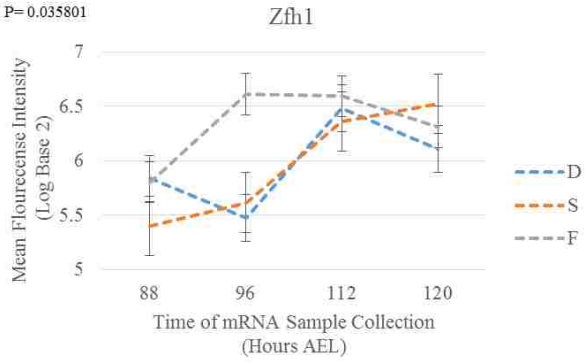

P= 0.036068

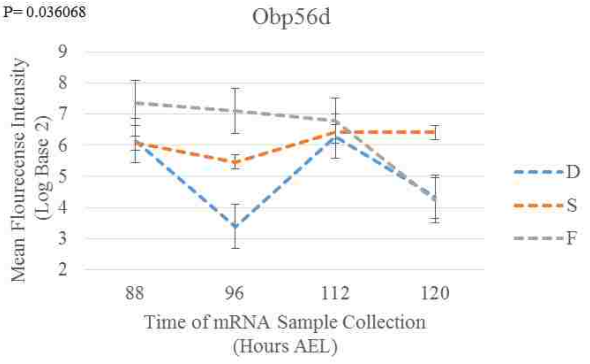

P= 0.039717

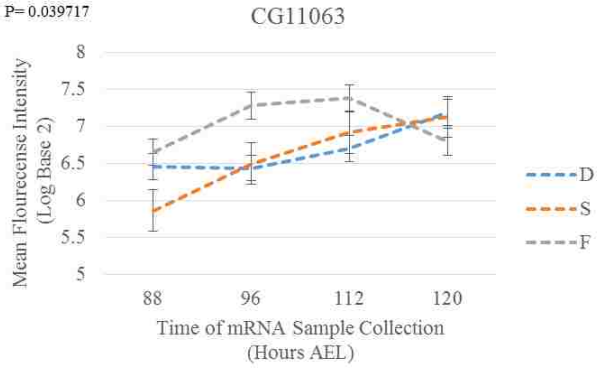

P= 0.039911

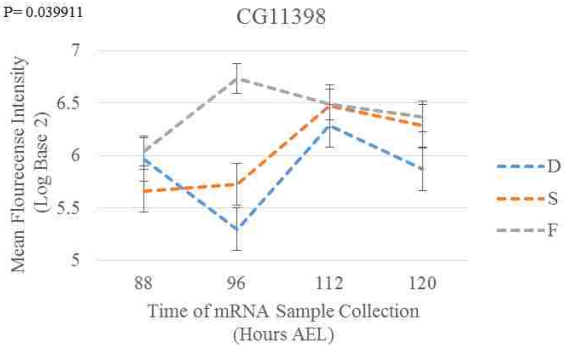

P= 0.040515

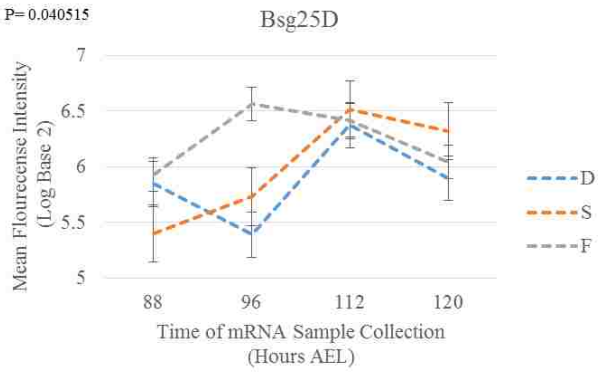

P= 0.036383

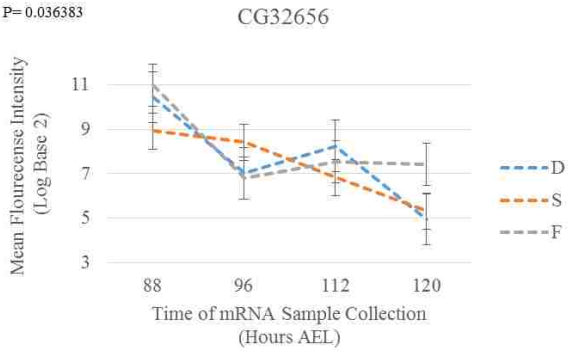

P= 0.036748

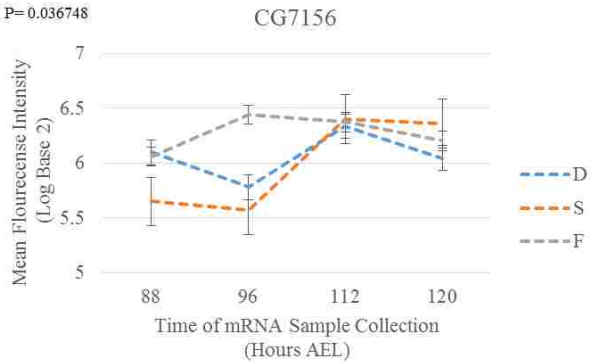

P= 0.041161

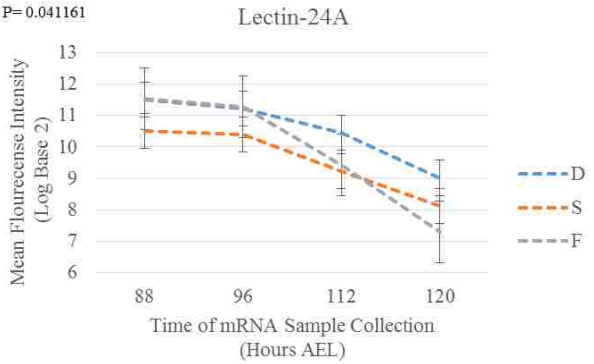

P= 0.042033

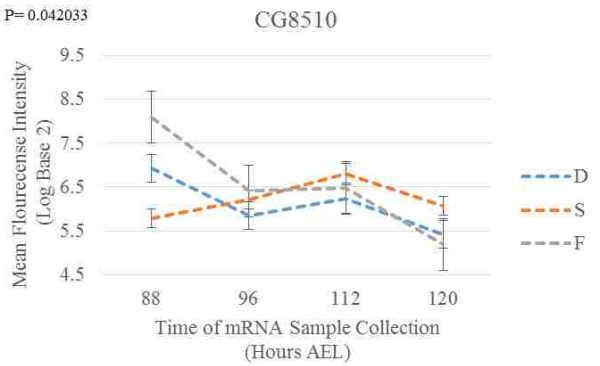

P= 0.037479

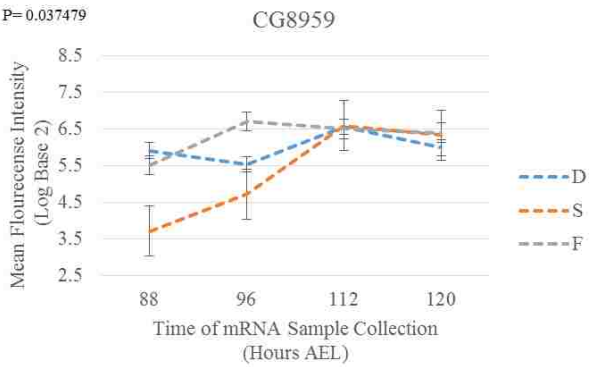

P= 0.037788

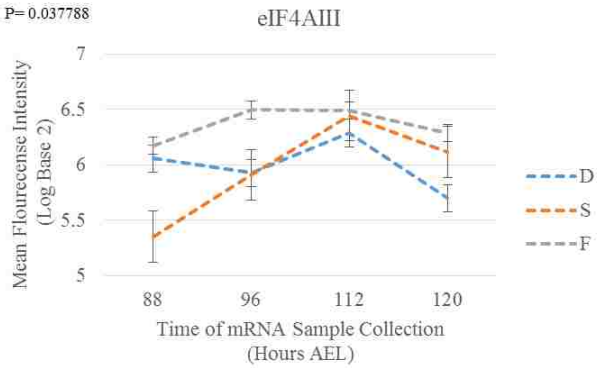

P= 0.038667

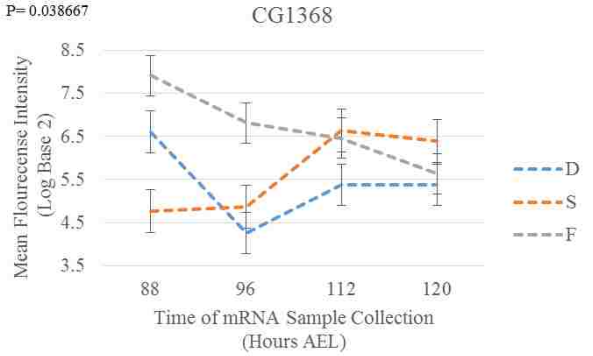

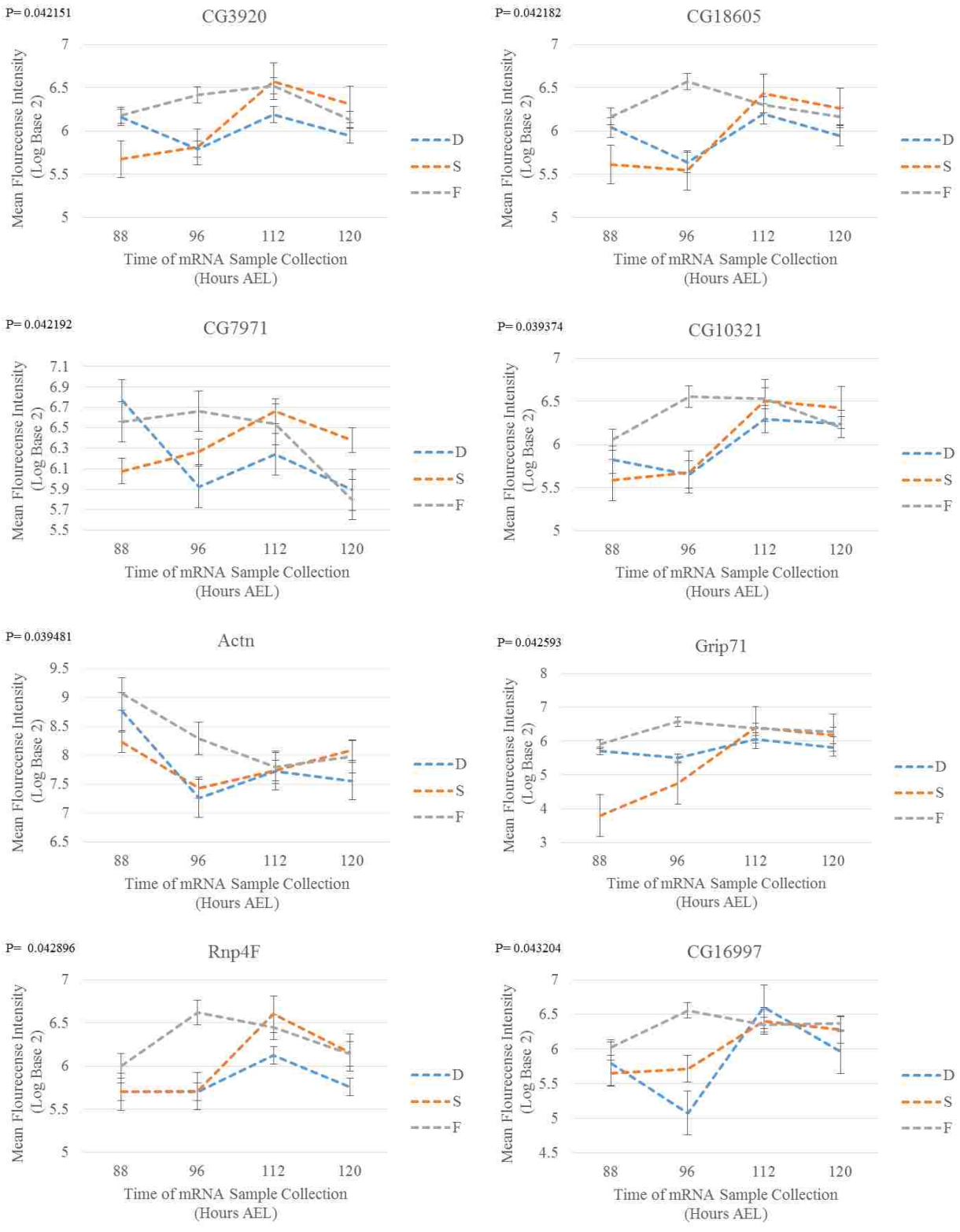
P= 0.042151
CG3920
Mean Flourecense Intensity (Log Base 2)
Time of mRNA Sample Collection (Hours AEL)
D
S
F
P= 0.042182
CG18605
P= 0.042192
CG7971
P= 0.039374
CG10321
P= 0.039481
Actn
P= 0.042593
Grip71
P= 0.042896
Rnp4F
P= 0.043204
CG16997

P= 0.043651

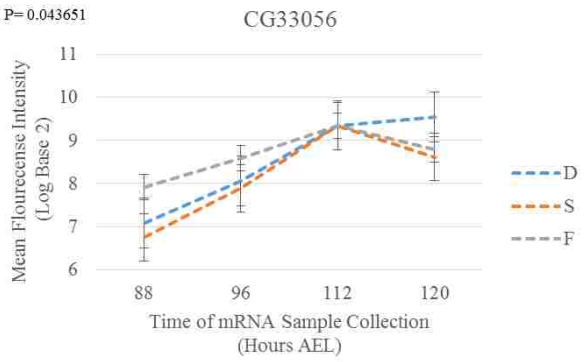

P= 0.043889

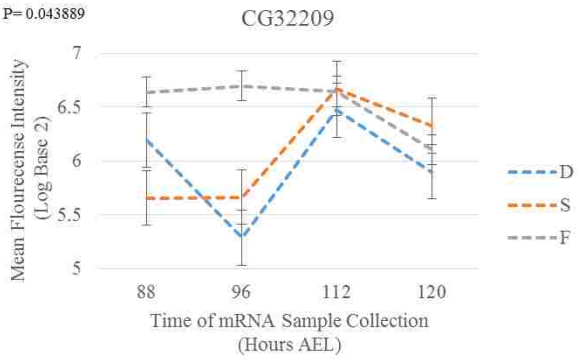

P= 0.046074

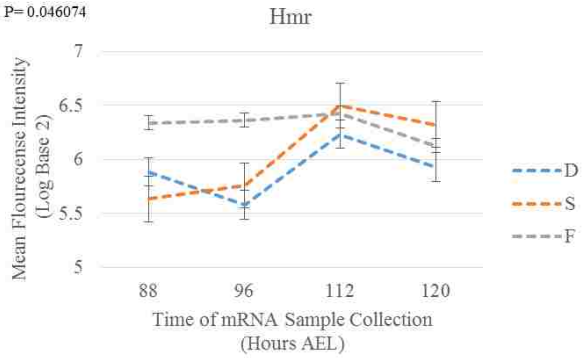

P= 0.046916

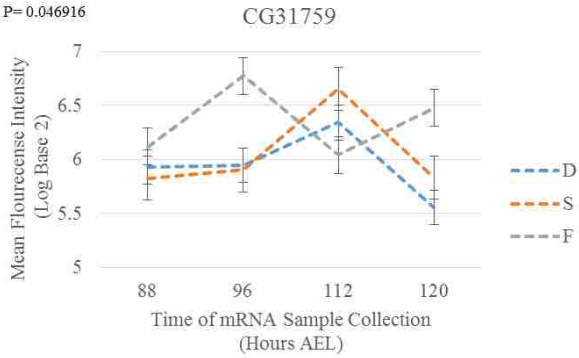

P= 0.047256

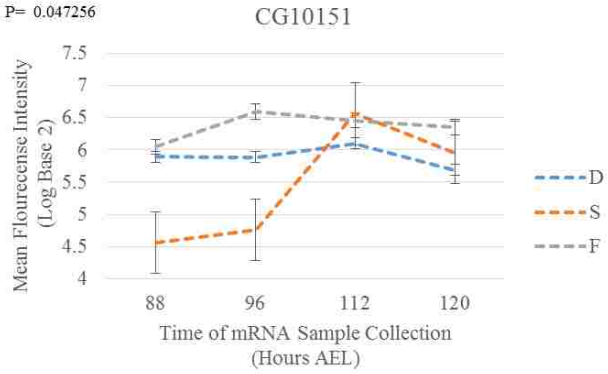

P= 0.044192

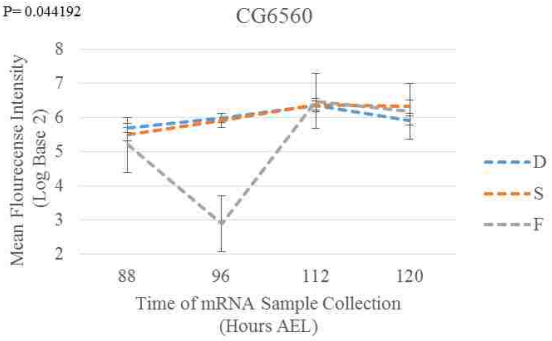

P= 0.044469

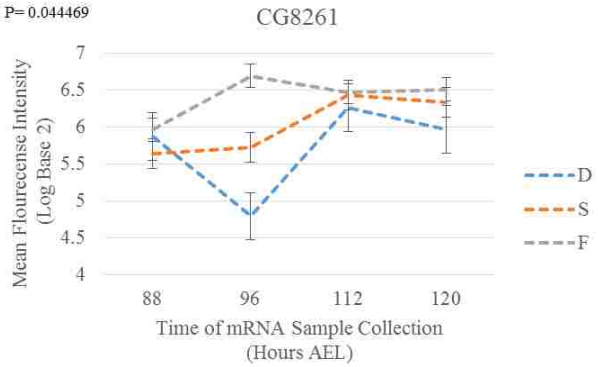

P= 0.0446

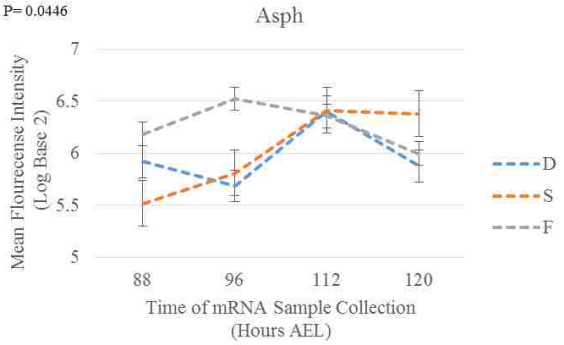

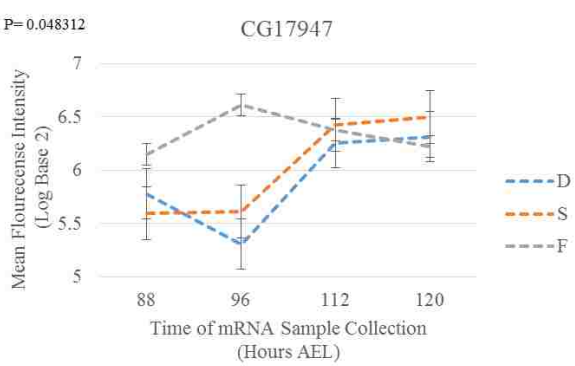
P= 0.048312
CG17947
Mean Flourecense Intensity (Log Base 2)
7
6.5
6
5.5
5
88
96
112
120
Time of mRNA Sample Collection (Hours AEL)
D
S
F

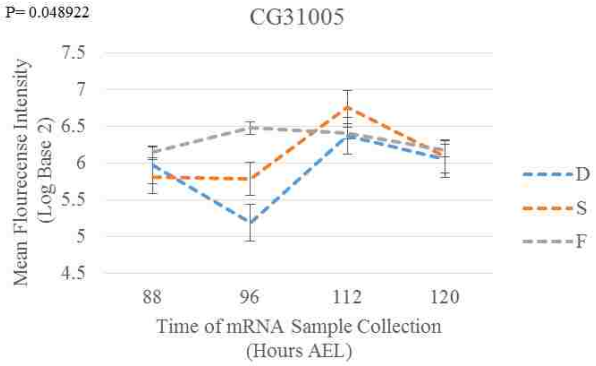
P= 0.048922
CG31005
Mean Flourecense Intensity (Log Base 2)
7.5
7
6.5
6
5.5
5
4.5
88
96
112
120
Time of mRNA Sample Collection (Hours AEL)
D
S
F

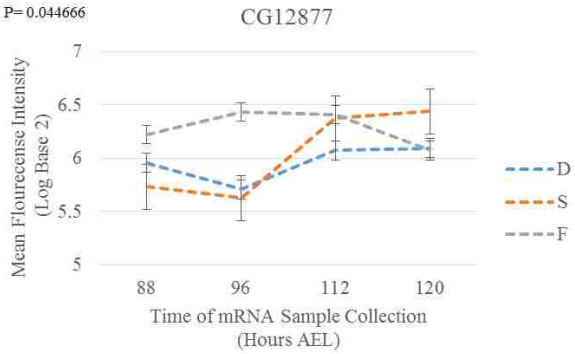
P= 0.044666
CG12877
Mean Flourecense Intensity (Log Base 2)
7
6.5
6
5.5
5
88
96
112
120
Time of mRNA Sample Collection (Hours AEL)
D
S
F

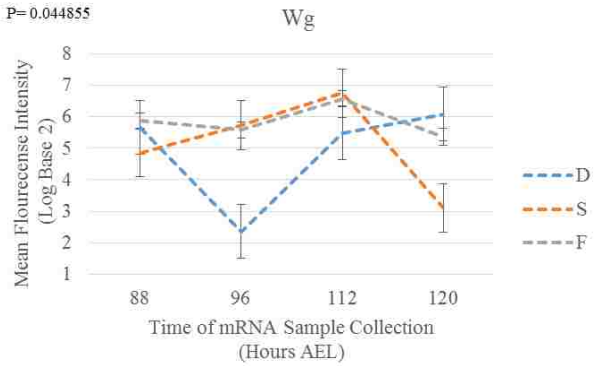
P= 0.044855
Wg
Mean Flourecense Intensity (Log Base 2)
8
7
6
5
4
3
2
1
88
96
112
120
Time of mRNA Sample Collection (Hours AEL)
D
S
F

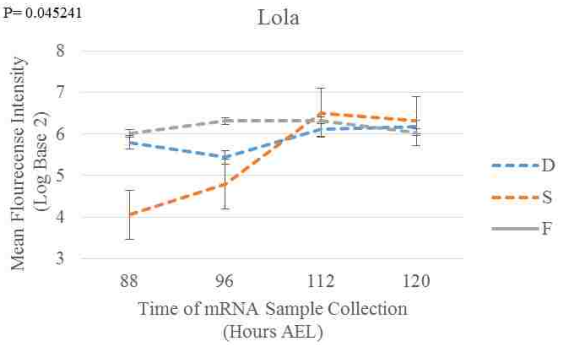
P= 0.045241
Lola
Mean Flourecense Intensity (Log Base 2)
8
7
6
5
4
3
88
96
112
120
Time of mRNA Sample Collection (Hours AEL)
D
S
F

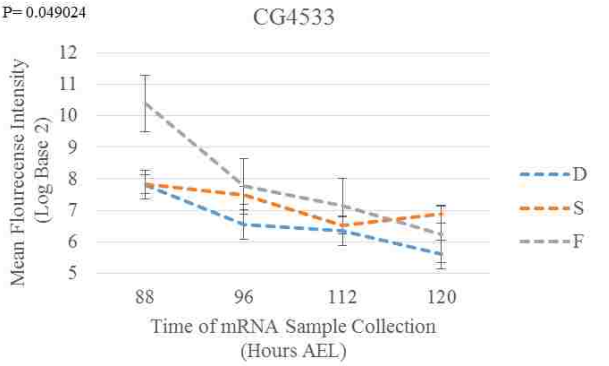
P= 0.049024
CG4533
Mean Flourecense Intensity (Log Base 2)
12
11
10
9
8
7
6
5
88
96
112
120
Time of mRNA Sample Collection (Hours AEL)
D
S
F

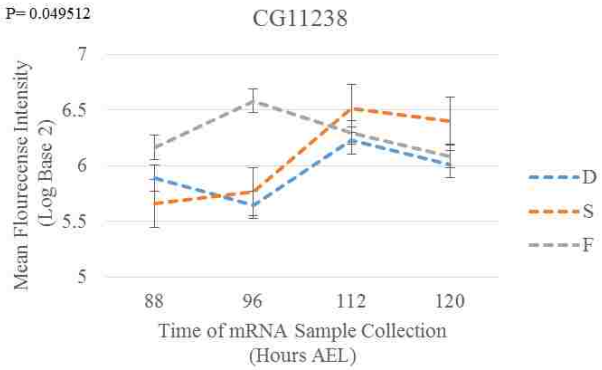
P= 0.049512
CG11238
Mean Flourecense Intensity (Log Base 2)
7
6.5
6
5.5
5
88
96
112
120
Time of mRNA Sample Collection (Hours AEL)
D
S
F

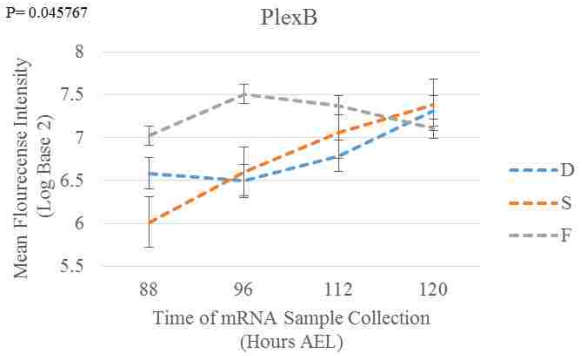
P= 0.045767
PlexB
Mean Flourecense Intensity (Log Base 2)
8
7.5
7
6.5
6
5.5
88
96
112
120
Time of mRNA Sample Collection (Hours AEL)
D
S
F

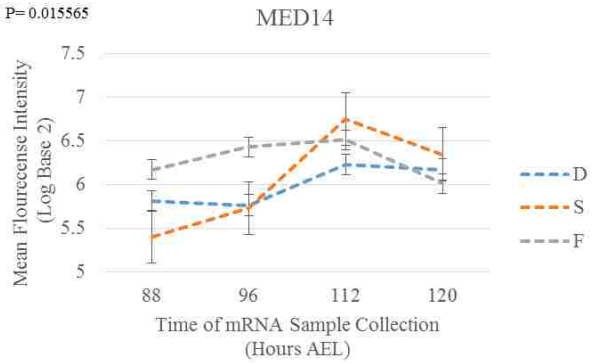
P= 0.015565
MED14
Mean Flourecense Intensity (Log Base 2)
7.5
7
6.5
6
5.5
5
88
96
112
120
Time of mRNA Sample Collection (Hours AEL)
D
S
F

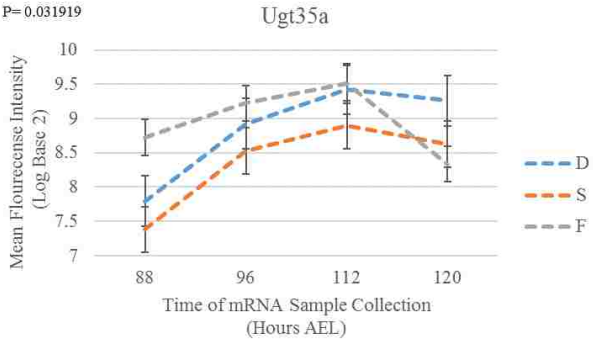
P= 0.031919
Ugt35a
Mean Flourecense Intensity (Log Base 2)
10
9.5
9
8.5
8
7.5
7
88
96
112
120
Time of mRNA Sample Collection (Hours AEL)
D
S
F

Literature Cited

1. Colombani J., Raisin S., Pantalacci S. Radimerski T., Montagne J., and P. Leopold. 2003. A nutrient sensor mechanism controls Drosophila growth. *Cell*. 114: 739-749.

2. De Moed G.H., Kruitwagen C.L.J.J., De Jong G., and W. Scharloo. 1999. Critical weigh for the induction of pupariation in *Drosophila melanogaster*: genetic and environmental variation. *Journal of Evolutionary Biology*. 12: 852-858.

3. Draghici, S. 2012. Data processing and normalization, pp. 693-747. Statistics and Data Analysis for Microarrays Using R and Bioconductor. Taylor and Francis Group, Boca Raton, FL.

4. Ernst J. and Z. Bar-Joseph. 2006. STEM: a tool for the analysis of short time series gene expression data. *BMC Bioinformatics*. 7:191.

5. Gibbs A.G., Chippindale A.K., and M.R. Rose. 1997. Physiological mechanisms of evolved desiccation resistance in *Drosophila melanogaster*. *The Journal of Experimental Biology*. 200: 1821-1832.

6. Gibbs A.G. and E. Gefen. 2009. Physiological Adaptation in Laboratory Environments, pp. 523-550. In T. Garland and M.R. Rose (eds.), *Experimental Evolution*. University of California Press.

7. Gefen E., Marlon A.J., and A.G. Gibbs. 2006. Selection for desiccation resistance in adult *Drosophila melanogaster* affects larval development and metabolic accumulation. The Journal of Experimental Biology. 209: 3293-3300.

8. Hoffmann A.A., and L.G. Harshman. 1999. Desiccation and starvation resistance in Drosophila: patterns of variation at the species, population and intrapopulation levels. *Heredity*. 83: 637-643.

9. Huang D.W., Sherman B.T., and R.A. Lempicki. 2009. Bioinformatics enrichment tools: paths towards the comprehensive functional analysis of large gene lists. *Nucleic* Acids Res. 37: 1-13.

10. Huang D.W., Sherman B.T., and R.A. Lempicki. 2009. Systematic and integrative analysis of large gene lists using DAVID Bioinformatics Resources. *Nature Protoc*. 4: 44-57.

11. Huang J., Yu H., Guan X., Wang G., and R. Guo. 2015. Accelerated dryland expansion under climate change. *Nature Climate Change*. 6: 166-171.

12. Pavlidis P. 2008. Using ANOVA for gene selection from microarray studies of the nervous system. Methods. 31: 282-289.

13. Zhang B., Kirov S.A., and J.R. Snoddy. 2005. WebGestalt: an integrated system for exploring gene sets in various biological contexts. *Nucleic Acids Res* (Web Server issue). 33: W741-748

14. Yang X., Li J., Lee Y., and Y.A. Lussier. 2011. GO-Module: functional synthesis and improved interpretation of Gene Ontology patterns. *Bioinformatics*. 10: 1444-1446.

Curriculum Vitae

EDUCATION

University of Nevada Las Vegas Graduated: May 2017

- M.S. in Biological Sciences
- Concentration: Cell and Molecular Biology
- Thesis: Gene expression profiling in the larval fat body of desiccation selected *Drosophila melanogaster*

University of Nevada Reno Graduated: May 2014

- B.S. in Biology

TEACHING EXPERIENCE

Teaching Assistant- Biology 189- UNLV August 2014- present

- Serve as an instructor leading laboratories for a diverse student body, including international and non-traditional students, at the post-secondary level
- Assist in the design of course materials and evaluation tools to highlight basic biological concepts and experiment designs, reinforcing topics covered in lecture
- Support new instructors by allowing them to shadow in lab and answer any questions
- Navigate online support management system for uploading class material and maintaining records of students' grades
- Hold office hours, attend organization meetings, and proctor examinations

Project Listos! Facilitator- ESL- Las Vegas Urban League September 2016- present

- Develop curriculum as outlined by program goals and provisions for federal funding
- Guide Spanish-speaking adults of various education levels through the English language focusing on pronunciation, grammar, and skills for fluid conversation and writing
- Adapt curriculum to provide individual and group instruction to meet the needs of individuals and subgroups of students
- Maintain communications with other facilitators and supervisors regarding paperwork, training schedules, and the exchange of ideas for classroom implementation.

K-12 Substitute Teacher- Washoe County School District August 2012- June 2014

- Aid students in understanding subject matter coinciding with lessons and assignments left by regular teacher
- Reinforce established classroom procedures and routines to foster a familiar and conductive learning environment
- Ensure safety of students during various drills by implementing steps learned in training and reporting to the principal and office support staff